

PROJECT PERIODIC REPORT

Grant Agreement number: 214402

Project acronym: ANGIOSCAFF

Project title: Angiogenesis inducing bioactive and bioresponsive scaffolds in tissue engineering

Funding Scheme: FP7– NMP-2007-LARGE-1; Activity NMP-2007-2.3-

Date of latest version of Annex I against which the assessment will be made: 10/08/2010

Periodic report: 2nd

Period covered: from 01/12/2009 to 30/11/2010

Name, title and organisation of the scientific representative of the project's coordinator¹:

Professor Jeffrey A. Hubbell, Ecole Polytechnique Federale de Lausanne

Tel: +41 21 693 9681

Fax: +41 21 693 9665

E-mail: jeffrey.hubbell@epfl.ch

Project website² address: www.angioscaff.eu

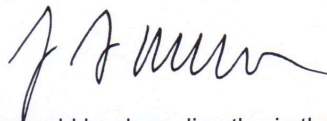
Declaration by the scientific representative of the project coordinator

I, as scientific representative of the coordinator of this project and in line with the obligations as stated in Article II.2.3 of the Grant Agreement declare that:

- The attached periodic report represents an accurate description of the work carried out in this project for this reporting period;
- The project (tick as appropriate) ¹:
 - has fully achieved its objectives and technical goals for the period;
 - has achieved most of its objectives and technical goals for the period with relatively minor deviations.
 - has failed to achieve critical objectives and/or is not at all on schedule.
- The public website, if applicable
 - is up to date
 - is not up to date
- To my best knowledge, the financial statements which are being submitted as part of this report are in line with the actual work carried out and are consistent with the report on the resources used for the project (section 3.4) and if applicable with the certificate on financial statement.
- All beneficiaries, in particular non-profit public bodies, secondary and higher education establishments, research organisations and SMEs, have declared to have verified their legal status. Any changes have been reported under section 3.2.3 (Project Management) in accordance with Article II.3.f of the Grant Agreement.

Name of scientific representative of the Coordinator:Professor Jeffrey Hubbell.....

Date: .13th ./ ..January../ ...2011



For most of the projects, the signature of this declaration could be done directly via the IT reporting tool through an adapted IT mechanism.

¹ If either of these boxes below is ticked, the report should reflect these and any remedial actions taken.

1		PUBLISHABLE SUMMARY	4
	1.1	Project Objectives	4
	1.2	Work Performed Since the Beginning of The Project	5
	1.3	Main Results Achieved So Far	5
	1.4	Expected Final Results and Their Potential Impact and Use.	10
	1.5	Contact Details and Logo	11
2		PROJECT OBJECTIVES FOR THE PERIOD	12
3		WORK PROGRESS AND ACHIEVEMENTS DURING THE PERIOD	13
		WP1 – Engineered Biomaterial Scaffold Development	15
		WP2 – Engineered Bioactives Development	34
		WP3 – Fundamental Characterization: Angiogenesis	45
		WP4 – Translation: Bone Repair	68
		WP5 – Translation: Skin Repair	94
		WP6 – Translation: Neuromuscular Repair	106
		Horizontal Work Package - Imaging	117
4		DELIVERABLES AND MILESTONES TABLES	126
	4.1	Deliverables Table	126
	4.2	Milestones Table	133
5		PROJECT MANAGEMENT	135
	5.1	Consortium Management	135
	5.2	Problems that Have Occurred and how they were Solved or Envisaged Solutions	136
	5.3	Changes in the Consortium	136
	5.4	Project Meetings, Dates and Venues	136
	5.5	Project Planning and Status	137
	5.6	Deviations from the Planned Milestones and Deliverables	159
	5.7	Changes in legal status	162
	5.8	Development of the Project Website	162
	5.9	Use of Foreground and Dissemination Activities During this Period	162
	5.10	Coordination activities	167
6.		EXPLANATION OF THE USE OF RESOURCES	169
7.		CERTIFICATES	181

1. PUBLISHABLE SUMMARY

1.1. Project Objectives

The **overall objective** of ANGIOSCAFF is to create bioresponsive, bioactive and injectable materials capable of carrying therapeutics which can be used for tissue regeneration in humans. The new biomaterials will respond to cell-associated environmental signals, such as extracellular proteases and endoglycosidases and generate bioactivity by virtue of bound peptides or recombinant adhesion molecules and growth factors.

This necessitates:

1. Radical innovations in state-of-the-art biomaterials.
2. The design of high-performance biomaterials inspired by natural processes.
3. Biomaterials that control cell differentiation.
4. Injectable biomaterials that can induce angiogenesis in the body.
5. Bioresorbable, highly porous, and structurally sound tissue-engineered scaffolds.
6. Functionalized biomaterials that have direct influence on cell behavior.
7. Bioactive scaffolds with broad applicability for complex tissues.
8. Advanced bioactive scaffolds enabling internal growth of tissue and site-specific delivery of bioactive signaling factors.
9. Effective delivery devices.

In line with these objectives, the work has been divided into six interlocking but distinct strategic areas. Individual partners bring in specific expertise and resources that are collectively leveraged.

The first area develops novel biomaterials platforms suitable for use in regenerative medicine. These biomaterials will possess *in situ* transformation, biospecific resorption and incorporation of biological ligands (referred to herein as *bioactives*, or *morphogens*) to induce tissue-specific differentiation and morphogenesis, with emphasis on angiogenesis.

The second area develops engineered morphogenetic biomolecules (peptides, proteins and the genes that encode them) to induce angiogenesis and other desirable angiogenesis-associated morphogenetic processes in the target tissues. These engineered morphogens will be combined with the developed biomaterial platforms so that all of the constructs developed will be biofunctionalized to be bioactive.

The third area functionally validates the biomaterials on the blood vessel itself by: (a) *in vitro* and *in vivo* characterization of their intrinsic angio- and lymph-angiogenic potential; (b) using them as a quantitative, designed and controllable platform to probe hypotheses on fundamentals of blood and lymph-angiogenesis.

Thus, AngioScaff's objectives are both translational (induction of blood and lymph-angiogenesis) and fundamental (development of material and molecular tools for the understanding of angiogenesis).

The fourth area assesses the functional activity of the biomaterials in bone repair by: (a) developing practical therapeutic materials for bone repair with materials/biomolecular therapeutics with and without transplanted stem and progenitor cells; (b) using these constructs as a quantitative, designed and controllable platform to probe hypotheses on fundamentals of osteodifferentiation, osteogenesis and bone repair, with an emphasis on the role of angiogenesis in these processes.

The fifth area develops practical therapeutic materials for skin repair with materials/biomolecular therapeutics. These constructs will be used as a quantitative, designed and controllable platform to probe hypotheses on fundamentals of skin (lymph)angiogenesis in normal and pathophysiological models (e.g., in diabetes) and its impact on skin healing in pathophysiological situations such as burns and chronic wounds.

Finally, **the sixth area** addresses a broader application of the materials for neuromuscular tissue by developing practical therapeutic materials for neuromuscular repair with materials/biomolecular therapeutics with and without transplanted cells in the context of skeletal muscle, cardiac muscle, and associated motor and sensory nerve.

1.2 Work performed since beginning of the project

Since the beginning of the project we have developed a set of seven novel biomaterials tuned to combine with bioactives, which possess and transmit various patterns of spatio-temporal biofunctionality. We have selected and compared materials produced during year 1 and the first part of year 2 and have produced biofunctionalised scaffolds containing growth factors, ephrins, adhesion molecules and genes for delivery into specific target areas.

The first stage of characterisation of similar functionalized materials has now been completed and the materials are being assessed for regenerative stimulation in degenerative disease models. We initiated the first series of validation studies *in vitro* in angiogenic, skin, bone, cardiac, neurological and skeletal muscle models to specifically assess their regeneration and repair stimulating capacities. This has enabled us to address the important question as to whether different materials will be able to produce similar angiogenic and regenerative responses *in vivo*.

The first *in vivo* tests have revealed striking and unique results for the repair of skin, bone and skeletal muscle tissues with selected materials, while the more complex neurological and cardiac tissues require further study and optimisation.

The novel material generated so far have demonstrated high impact, thus laying the groundwork for the final two years of the project that aim at the generation of regenerative therapeutics.

1.3 Main results achieved so far

Biomaterials

The results obtained with the first generation materials has created the incentive to **extend the existing biomaterial platform** to better meet the requirements of the other research areas. The results obtained by testing new biomaterials in angiogenesis and tissue engineering in bone, skin and neuromuscular tissues have informed further research, stimulating further development and characterisation to improve **mechanical properties** of injectable matrices, adjust **biofunctionalization**, develop injectable **hyaluronic acid-based** matrixes and conjugate **FN-GBD to starPEG-heparin** hydrogels to produce new generation scaffolds (*Figures 1 and 2*).

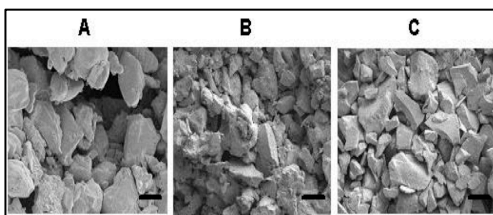


Figure 1. Microstructure of injectable, mechanically stable matrixes.
(A) PLGA/PEG; (B) PLGA/PEG + G5
(B) glass (melt blend);
(C) PLGA/PEG + G5 glass (powder blend)

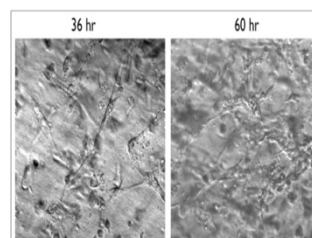
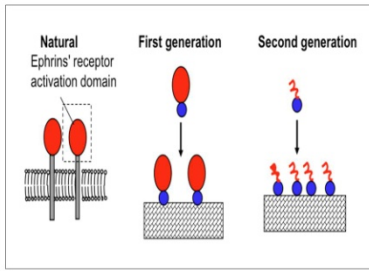


Figure 2. Endothelial cell morphology over time on new generation star-PEG-heparin gel. Cells attach to gels, have no sign of toxicity and start forming tubes.

Engineered Morphogens

To induce angiogenesis and desirable angiogenesis-associated morphogenetic processes in the target tissues we have generated growth factors-containing scaffolds such as: Fibrin-binding and cys-containing VEGF-A and VEGF-C and fibrin-binding PIGF; Fibrin-binding and cys-containing VEGF-syndecan; Wild-type, fibrin-binding and cys-containing TGF- β 1 and TGF- β 3; Fibrin-binding PDGF-AB; Wild-type, fibrin-binding and cys-containing IGF-1; Fibrin-binding BMP-2.



Second generation ephrin-modified scaffolds (TG-EMP peptides, *Figure 3*) were generated by incorporating ephrin peptides into fibrin gels in the presence of serum components and cells. In particular, TG-EMP-A2 peptide activated EphA2 receptor signalling preferentially in fibrin matrix-bound form and TG-EMP-B4 retained inhibitory potential in free form. TG-EMP-A2 could be efficiently incorporated in PEG-based gels and used for EphA2 receptor signalling activation in 2D and 3D cell cultures.

Figure 3. Schematic of ephrin-modified scaffolds. The whole recombinant ephrins activation domain is tagged for scaffold incorporation

in the first generation scaffolds, whereas only small synthetic ephrin peptides are tagged in the second generation scaffolds (A.Zisch et al. *Biomaterials* 2004).

Controlled delivery of VEGF and Ephrin peptides improved the functionality of mesenchymal stem cells and endothelial progenitor cells in 3D culture, where cells also showed changes in gene expression, including chemokine receptor and growth factor genes.

Fibronectin fragments supported the isolation and expansion of human bone marrow-derived mesenchymal stem cells more efficiently compared to the full length protein. The most efficient fragment comprises the CBD and the GBD.

Angiogenesis

We have determined the range of matrix components and the degradation rate of different matrix compositions in vivo to define how hydrogel composition controls the duration of growth factor release to meet the long term goal of delivering VEGF locally by hydrogels. In the context of lymphangiogenesis, we found that fibrin-binding TG-VEGF-C with a matrix metalloproteinase (MMP)-degradable sequence improved lymphatic endothelial cell proliferation and capillary formation compared with wildtype VEGF-C. In vivo, TG-MMP-VEGF-C drove efficient functional lymphatic regeneration.

Low dose growth factors (VEGF-A and PDGF-BB) delivered in FN fragments with appropriate integrin ligands induced enhanced wound healing and angiogenesis in vivo. The signaling through the growth factor receptors was enhanced and prolonged. Thus FN III9-10/12-14 act in synergy with growth factors and the synergy was mostly dependent on the integrin $\alpha_5\beta_1$ (*Figure 4*). Along similar lines, the covalent integration of VE-cadherin in a fibrin matrix increased ring formation of endothelial cell lines.

We have established a powerful Zebrafish model that will allow rapid and minimally invasive screens for different biomaterial/morphogen combinations in vertebrates (*Figure 5*). Furthermore endothelial cell progenitor migration towards SDF-1 was increased by a new starPEG-heparin hydrogel, which resulted in increased cell infiltration, vessel formation, matrix remodelling and angiogenesis in vivo (*Figure 6*). Preliminary results have also shown that TG-VEGF121 activated fibrin matrix at low concentrations of VEGF121 were most effective in reducing tissue necrosis on day 7 post surgery in the rodent epigastric flap model. Finally neovessel formed in vivo upon co-transplantation in mice of clonogenic mesenchymal progenitors from different tissue sources (human postnatal bone marrow, human postnatal muscle, human cord blood) and human endothelial cell lines in mice, whereas the angiogenic potential of the progenitor cells alone was limited. This system revealed that endothelial cells can introduce a specific spatial pattern in an otherwise isotropic distribution of differentiating mesenchymal progenitors.

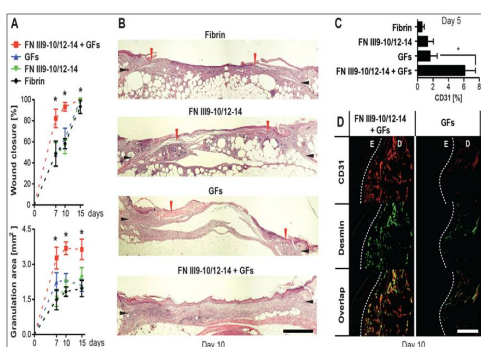


Figure 4. Growth factors synergise with fibronectin fragments to enhance wound healing and angiogenesis.

After wounding, wounds were filed with fibrin matrices functionalized with or without FN III9-10/12-14 and GFs (VEGF-165 and PDGF-BB). **A)** Wounds where GFs have been delivered using FN III9-10/12-14 closed more rapidly ($n=7$) and contained more granulation tissue, compared to fibrin only ($n=7$). **B)** Representative histology of wounds at day 10. Black arrows indicate the wound edges, red arrows indicate the end of the new epithelium (haematoxylin and eosin staining, scale bar = 1mm). **C)** Enhanced recruitment of CD31+ endothelial cells within the wounds when GFs were delivered with FN III9-10/12-14 ($n=6$).

D) Greater blood vessels formation within granulation tissue when GFs were delivered with FN III9-10/12-14 (E = epidermis, D = dermis, scale bar = 0.2mm).

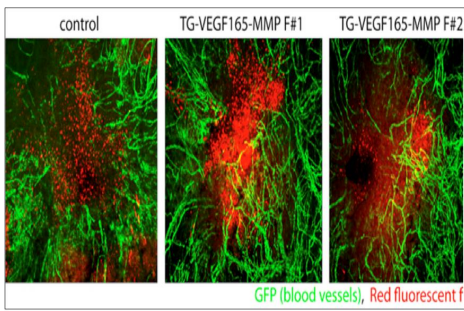


Figure 5. Confocal stacks of control fibrin gel (left panel) and two TG-VEGF165-MMP/fibrin gel implanted fli:GFP fishes (central and right panel). Angiogenesis toward and within the gel (red) can be observed (in green, GFP positive vessels); the presence of VEGF into the gel induces higher levels of angiogenesis compared to control.

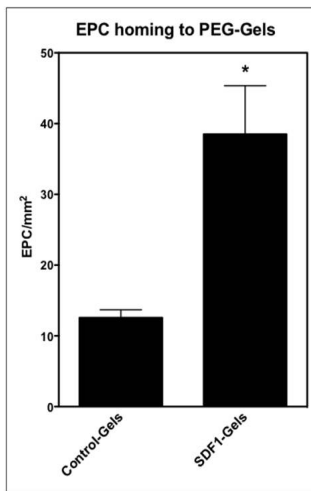


Figure 6. Attraction of progenitor cells to angiogenic sites. Effect of SDF-1-loaded gels on in vivo homing of human early outgrowth EPC

Preliminary results have also obtained from a single donor suggest that a selective medium supports CD133⁺CD34⁺ mesenchymal stem cells from liposuction material. Mature endothelial cells in whole human blood have been detected, magnetically isolated and characterized by flow cytometry.

Bone repair

Using subcutaneous or cranial implantation models of bone formation, we have compared by Micro-CT and by histology various scaffolds produced by AngioScaff laboratories. Below is an example of osteogenesis induced by BMP-2 complexed with PLGA/PEG (Figure 7).

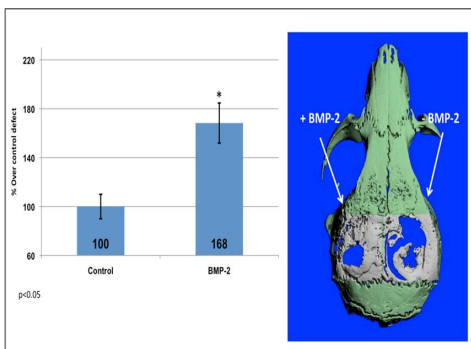


Figure 7. Bone formation induced by BMP-2 complexed with PLGA/PEG in cranial implantation. BMP-2 induced significantly greater bone formation than the empty control.

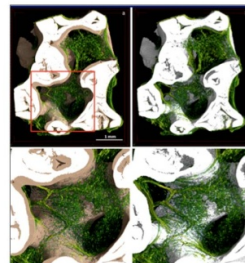


Figure 8. Example of microCT imaging of a bone section

A spinal fusion model in rabbits was used to address whether a limited vascular network in different implants may correlate to lack of bone formation and non-fusion. Osteoprogenitors in combination with fibrin, HA, PLA +/- osteoconductive materials +/- VEGF were evaluated in a heterotopic model aiming to find a novel concept for bone regeneration. We are also testing polylactic acid/glass/calcium phosphate scaffolds in combination with Platelet-derived growth factors and stromal cells to assess cell recruitment patterns for bone regeneration. Imaging, including high resolution, three-dimensional X-ray synchrotron radiation microtomography (microCT) is used to generate 3-D representation of angiogenesis, bone formation and scaffold degradation (Figure 8).

Preliminary results indicate osteogenic potential of purified human bone marrow CD146+ mesenchymal stem cells. Samples of cells transfected with VEGF165 were ectopically transplanted in athymic nude mice for testing their ability to enhance bone and vascularisation. Finally we are currently improving mechanical properties of injectable matrices, adjusting biofunctionalization, developing injectable hyaluronic acid-based matrixes and conjugating FN-GBD to starPEG-heparin hydrogels.

Skin repair

We have tested VEGF-isoforms produced in HEK 293 EBNA for angiogenesis in skin repair in the diabetic mouse model. These VEGF-isoforms are biologically active, promote VEGFR-2 phosphorylation, can be covalently bound to fibrin and are retained for prolonged time periods, promote accelerated wound closure in vivo (Figure 9). Covalently linked isoforms are superior to soluble VEGFmut in regard to the induction of angiogenesis.

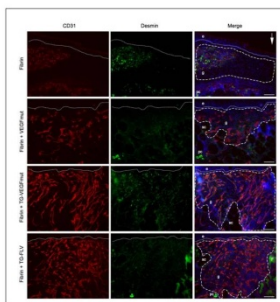


Figure 9. VEGF-isoforms promote angiogenesis in vivo. Day 10 wounds in the diabetic mouse model

Studies on the angiogenic potential of Placenta Growth Factor (PIGF) have progressed. We have mapped the angiogenic capacity of PIGF to its heparin binding site. PIGF is cleaved by plasmin, which induces loss of the heparin binding domain, resulting in reduced chemotaxis, loss of matrix-binding capacity, reduced sprouting capacity and decreased granulation tissue formation after wound treatment in diabetic mice.

Neuromuscular repair

We have established two transgenic mouse lines in which endothelial cell-specific and tamoxifen-inducible expression of Cre-recombinase marks endothelial cells. The effect of soluble and immobilized angiogenic factors is currently analyzed using these reporter mice.

PEG-Fib was able to promote mature well-differentiated myofibers in vitro and also showed well defined skeletal muscle organization and differentiation in vivo. In mouse models of muscle injury TG-PEG and PEG-Fib caused increased survival of transplanted cells and an overall improvement in cell engraftment. Moreover PEG-Fib enhanced skeletal muscle differentiation of engrafted cells (Figure 10).

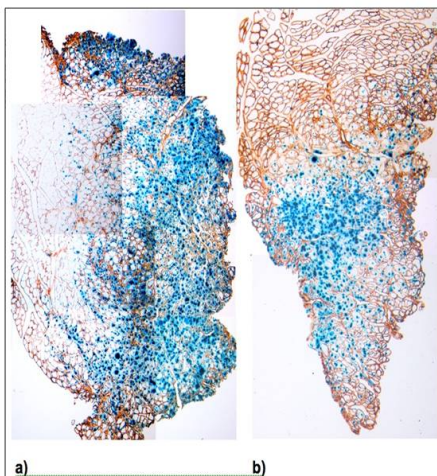


Figure 10. In vivo injection of Mesoangioblast expressing LacZ with (a) or without (b) PEG-Fib. Remarkable amelioration on cell engraftment and retention into host Anterior Tibialis

Neonatal mouse cardiac cells, i.e. CMs, can be reprogrammed and grown in feeder-free conditions to generate iPS cells. CM-derived iPS cells survive, integrate, and differentiate in the host myocardium, significantly improving cardiac function. The results show that iPS cells methodology integrated with tissue

engineering approach can ameliorate cardiac function when introduced into an infarcted myocardium.

FN-910-GBD gel gave superior support for the growth of dorsal root ganglia (DRG) neurites. We are continuing the screening by determining the effect of hyaluronan scaffold on the outgrowth of DRG explants. Neurite extension was significantly enhanced by the presence of BDNF in the gel and reached long distances into gels containing FN-9-10, FN-9-10-GBD and full-length fibronectin. Using MACS[®] Cell Separation System from Miltenyi-Biotec, we are establishing a method to mobilize sufficient amounts of autologous Schwann cell-like cells from rat adipose tissue.

Imaging

We have demonstrated: *i)* in vitro, the dynamic range of reporter expression and its correlation with changes in mRNA expression; *ii)* in vivo bioluminescence of gene expression using the DBM reference biomaterial; *iii)* a fluorescent angiography procedure that has been optimized to analyze vascular structures in implanted scaffolds and their structural relation with seeded stem cells. To monitor vascular growth within biomaterials by micro-CT (Figure 11) we have found that with water soluble contrast agent we can obtain visualization of entire organs, tissues and major vessels. We generated correct values of vascular density in brain tissue, whereas other tissues (i.e. *M. tibialis anterior*) have leakage of contrast, which can nevertheless be used to study dynamic tissue perfusion by micro-CT (Figure 12).

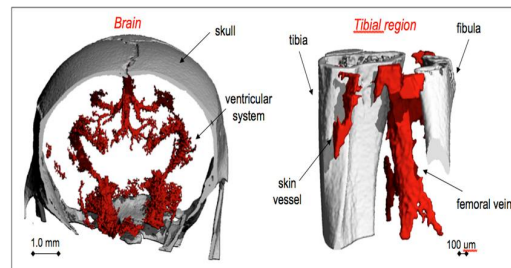
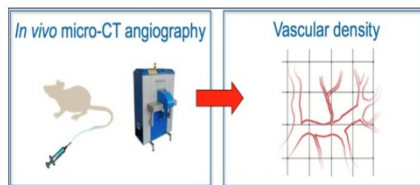


Figure 11. Schematic of in vivo monitoring of angiogenesis

Figure 12. Example of anatomical micro-CT

We have developed a methodology to import synchrotron data, reconstruct in 3D the vascular network and perform a large scale computational fluid dynamic analysis using sample-specific geometries. Results in one network indicates the heterogeneity of fluid flow and shear distribution within the different vessels (Figure 13). Comparison of in silico results with in vivo results on many different samples will be made to determine the functionality of the angiogenic process in tissue regeneration.

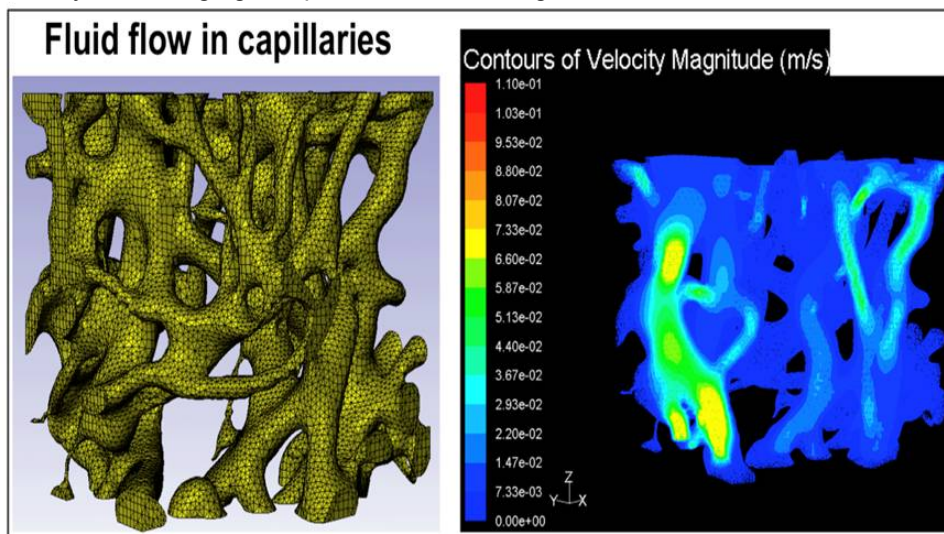


Figure 13. Example of 3D reconstruction of capillary fluid velocity

1.4 Expected final results & their potential impact and use

The proposed projects capitalize on combined expertise in different areas of regenerative medicine and collaborative interactions allow us to merge our unique and complementary expertise in the field. The expected final results will be the generation of new scaffolds that:

- Are 'smart', 'resorbable', can accommodate seeded cells and present correct signals
- Contain factors that stimulate specific cell differentiation *in vivo*
- Provide sufficient vascular supply

Moreover, we will:

- Precisely identify the type and numbers of cells (endogenous and/or exogenous) required to restore biological functions to regenerate tissues.
- Validate these bioactive biomaterials to the first step of pre-clinical development in relevant animal models.

Impact on science

AngioScaff includes teams working on specific areas of tissue engineering that are associated with clinical targets. *The clinical targets were selected because of their high societal and economic impact.* By translating our knowledge in biomaterials and angiogenesis into clinical targets we put our science to the real test of usefulness. *New biofunctional materials and angiogenic molecules with therapeutic application will be introduced to the clinic and to commercial development.*

The impact of AngioScaff is best illustrated by the need for organ transplantation, the major motivation behind regenerative medicine: 25% of patients waiting for an organ donor die before one can be found, and in 2001 there were 12 607 available donors available to help 81 528 patients in need. The stimulation of tissue repair via the use of optimized scaffolds (porous, angiogenic, bioactive and resorbable) that stimulate endogenous cells to regenerate a fully functional tissue should address this problem and decrease related mortality.

Impact on society - socio economic benefits

Degenerative diseases create a life-altering experience for the person with injury, for their partner, parents, siblings, and children. The subsequent diminishment of body functions associated with the diseases can cause depression and loss of self-esteem. It has been considered essential, based on European policy consistent with human rights principles, that people with disabilities should be treated with dignity, encouraged to have independence, be given equality of opportunity, encouraged to have an active participation, a full citizenship and a high quality of life. Given the diversity of degenerative diseases indicated above, pathological manifestation can occur at any age: either as a child, during an individual's most productive years, or as an aged person. The trauma frequently results in morbidity, and as a result, patients typically require continuous physical and medical care depending on the disease, severity of manifestation, degree of disability, and location of injury.

The prevalence of degenerative diseases is on the rise because aging population is increasing and this has created the need for biomaterials. Over the past 50 years, average life expectancy at birth has increased globally by over 20 years, from 46.5 years in 1950-55 to 65.2 years in 2002. Today there are 600 million people in the world aged 60 years or over, and this will double by 2025 and reach 2 billion by 2050. While degenerative diseases are not the exclusive domain of the aged, they do impact this sector of society the highest with subsequent increased social and economic burdens on the health care systems on which they depend.

The direct healthcare costs of organ replacement are about € 240 billion globally (about 8 percent of global healthcare spending) arising from therapies that keep people alive (such as kidney dialysis), implanted replacement devices, and organ transplants. With a € 240 billion global industry already built on first generation tissue and organ therapy products and substitutes, regenerative medicine has a potential to exceed € 600 billion by 2030.

1.5 Project Contact Details and Logo

Project Co-ordinator Contact details:

Professor Jeffrey A. Hubbell, Ecole Polytechnique Federale de Lausanne

Tel: +41 21 693 9681

Fax: +41 21 693 9665

E-mail: jeffrey.hubbell@epfl.ch

Project website² address: www.AngioScaff.eu



2. PROJECT OBJECTIVES FOR THE PERIOD

The objectives of year 2 of AngioScaff involved the initiation of complex testing of the first generation materials in the various tissue systems, the development of second generation materials, maintenance of the network and optimised capacity building matched with the initiation of high level innovation management and exploitation.

Network maintenance, capacity building, innovative development and exploitation are detailed in section 5: in brief these entailed online congresses for theoretical training, enhancement of the exchange scheme, the implementation of a young scientist networking meeting, the initiation of the prototype validation support programme and review of the market in light of the new data for potential commercialisation.

Scientific objectives of this period, as based on the gantt chart from the Annex 1, involved the implementation of scheduled tasks, with the specific focus on ensuring that milestones were reached and deliverables generated.

This was also aligned with the ongoing scientific activities of the research teams to ensure that the data were as disseminated as efficiently and effectively as possible via publications and congresses.

Scientifically we aimed in this period to:

1. Initiate the first series of testing of the first generation bioactive biomaterials in angiogenic, skin, bone, cardiac, neurological and skeletal muscle systems
2. Perform the development of the next generation of composite materials via collaboration between the biomaterials teams
3. Test the first series of morphogens for stimulating angiogenesis and tissue repair.
4. Continue the development of cutting edge imaging techniques to permit accurate and easy measurements of the regenerative capacity of the materials.
5. Refine the approaches utilized to achieve the scientific, materials and medical/application goals of the consortium, thus reducing the number of parallel paths being pursued to achieve the same ends.

3. WORK PROGRESS AND ACHIEVEMENTS DURING THE PERIOD

The first stage of in vitro comparison of functionalized materials across the project has now been completed and *in vivo* work has revealed exciting results for certain combinations of material and tissue. New composite materials are also being developed.

The progress during the second period has created the incentive to extend the existing biomaterial platform to better meet the requirements of the other WPs. For example, informed by the results of the application of the new biomaterials to angiogenesis, we have successfully incorporated several growth factors-containing scaffolds, some of which are now being validated to develop a standardized procedure for the cultivation of human mesenchymal stem cells from human bone marrow (Task 2.4 in WP2).

To induce endothelial cell signalling and angiogenesis we are engineering fibrin matrices with ephrin mimetic peptides (Tasks 3.10 and 3.11 in WP3) and to isolate, characterize and experimentally manipulate rare cell populations relevant to AngioScaff, we are optimizing two new protocols to isolate: *i*) mesenchymal stem cells and endothelial progenitor cells from liposuction material (Task 3.12 in WP3); *ii*) circulating endothelial cells from blood (Tasks 3.14 in WP3).

We have developed a calcium phosphate bioactive glass biomaterial for tissue engineering with pro-angiogenic properties (Tasks 3.13 in WP3) and are currently improving mechanical properties of injectable matrices, adjusting biofunctionalization, developing an injectable hyaluronic acid-based matrix and conjugating FN-GBD to starPEG-heparin hydrogels (Tasks 4.5-8 in WP4).

Below we describe the progress and achievements of all the work packages with specific references to the individual tasks. The biomaterials and the morphogens generated in WP1 and WP2 have now advanced into in vitro and in vivo validation in angiogenesis (WP3) and in specific tissues (WP4-6) and optimised imaging.

Summary of the recommendations from the previous reviews and how these have been taken into account.

Deliverables

Summary of request: Clarification and finalisation of new list of deliverables to be sent by J Hubbell directly to project officer and all deliverables to be sent to the EC.

Response: This was performed as requested.

Number of projects being performed by Angioscaff

Summary of request:

That due to the large number of projects originally indicated in the DoW, and the ongoing parallel initiatives, the coordinator indicated the need to reduce the number of projects by the end of year 2. The project officer agreed to this "I am very much in support of this view and would like to add that, as time will be of the essence, the consortium needs to implement a concrete strategy to select the most promising approaches or applications (and to actually drop less promising ones) during the second year. Otherwise, there is the risk that the consortium will follow too many applications to be able to reach its goals in years 3 and 4." (Direct quote from comments of the project officer).

That patent and regulatory information should also be used in the selection procedure

Response: In line with the comment and the milestone 7.2 we have reduced the number of projects for years 3 and 4, including selection based on translation and commercialisation potential. See page 141 of this report. On page 10 of the DoW, we indicated that we would perform a screening process, such that some of the parallel approaches to achieve our initiatives would be abandoned, but that we would not abandon the initiatives themselves. Quoting from the DoW,

"As the AngioScaff team proceeds along its project, it will thoughtfully select the most appropriate material/morphogen combinations (referred to as a BDP herein, a Biomaterials Development Project) to

proceed in animal testing and moreover in what particular animal models. To be clear, the selection process will not involve abandoning pathways shown on the Project Maps, i.e. developing materials to probe scientific questions about angiogenesis or to develop practical therapeutic approaches in the tissues targeted for translation. Rather, selection entailed finding our way through the several possibilities that exist to reach those ends.”

The consortium has, in the first two years, developed sufficient understanding to be able to select the most promising pathways to reach the originally proposed ends, and in doing so in Years 3 and 4 the resources of the project will be focused on these most promising paths.

IPR issues

Summary of request:

The project officers opinion was that there is no comprehensive picture of the patent situation that affects future exploitation. Several participants mentioned their own patents or patent applications on materials or morphogens within the scope of ANGIOSCAFF. The program officer felt that no systematic overview of relevant patents owned inside or outside the consortium exists and that given the high patent activity in regenerative medicine and biomaterials, this could mean some projects work towards applications for which patent protection will be difficult or impossible to obtain. The consortium was encouraged to obtain a clear picture of the relevant patent situation, including engaging younger scientists in IPR discussions and to organise a ESS seminar during next year's consortium meeting.

(http://ec.europa.eu/research/industrial_technologies/lists/list_402_en.html)

Response:

The IP management and exploitation approach for Angioscaff is based mainly on leveraging the existing inventions of the partners and possibly combining IP approaches of the different teams of the consortium. This was referred to as pre-investment in the DoW, and this is why there was so much preliminary data presented in the DoW. During Year 3, the relevant partners will assess the situation of their IP, both existing and potential, and will present and discuss this during the Year 3 annual meeting, including their activities in exploitation.

We agree with the necessity to train younger scientists in intellectual property, which is an optional training that institutes in Europe offer to their staff. The suggested ESS seminars no longer seem to exist as no relevant links could be found on the internet, and the one provided was non functional. In preparation for the Year 3 annual meeting, we will determine if there exists adequate demand among the young scientists for an addition session, just before or just after the main meeting, to provide training on this topic. Several of the consortium partners have extensive experience both in IP generation and protection, and in IP exploitation through licenses and entrepreneurship, and thus the consortium members are well positioned to undertake such training. If demand is adequate, such training will be provided.

Work package number	1	Start date or starting event:					Month 1					
Work package title	Engineered Biomaterial Scaffold Development											
Activity Type	RTD			Workpackage Leader				Carsten Werner				
Participant number	1	2	3	4	5	6	10	15	21	25	29	
Principal Investigator	JAH/ ML	JH	JP	DS	KS	CW	ME	HR	JA	CD	IB	
Planned Person-months for whole WP duration	51	24	24	78	40	52	12	0	48	16	2	
Actual Person-months so far	13.2	19.2	30.17	58.4 8	35	54	0	1	24	5	0.02	

REPORT OVERVIEW : WP1 - Engineered Biomaterial Scaffold Development

1.1-1.3 and 1.5. Within this WP we (**JAH, DS, JH, BioHyos, KS, JP**) have completed tasks concerned with the initial development of biomaterials that are currently being tested in tissue specific models: *i*) fibrin with bound morphogens; *ii*) fibrinogen-polymer hybrids; *iii*) hyaluronic acid (HA) hybrids; *iv*) porous scaffolds; *v*) calcium phosphate scaffolds.

1.3 Combination Injectable HA matrix was dually functionalized with hydrazide and thiol and covalently bound to FN fragments. The HA-FN hybrid hydrogel formulated with BMP-2 was implanted subcutaneously in rats to evaluate the role of FN in bone regeneration. CT scans revealed higher bone volume as compared with the control group that were implanted with HA hydrogel + BMP-2 w/o FN.

1.4. Moreover, to produce soft tissue-like biomaterials with PEG-peptide hybrids that would promote angiogenesis by enhanced cell binding specificity we (**CW, JAH**) absorbed Fibronectin (FN) fragments to starPEG heparin hydrogels. Heparin is a key component of these biomaterials because of its high affinity to growth factors and to extracellular matrix. In a proof of principle experiment endothelial cells did attach to the FN-containing hydrogels and formed elongated structures, although the fragments detached over time (>22 hours). Protocols are being tested and optimized that will covalently bind the fragments to the starPEG heparin hydrogels. To biofunctionalize soft tissue-like hydrogels with constant biomechanics we (**CW, ML, DS**) compared physical, chemical and biological properties of PEG-fibrinogen, starPEG gels and TG-PEG gels. Frequency sweep measurements determined the degree of stiffness in the range of G 100-1000 Pa. Degradation kinetics were assessed independently of stiffness by enzymatic digestion. Newly designed hybrid starPEG/heparin hydrogels were also assessed for degradation kinetics.

1.6 To generate second generation composite and flexible scaffolds for bone regeneration we (**KS**) combined CaP glass fibers with PLGA/PEG particles. Compression strength, elasticity and flexibility were assessed and quantified in specific assays at various concentration of CaP fibres. Scaffold microstructure was studied by scanning electron microscopy and micro-computerized tomography. These scaffolds are injectable, mechanically stable matrixes that harden at 37 C. They are being optimized for applications in craniofacial defects studies (**TE**) and for promoting angiogenesis and osteogenesis in vitro (**JP**).

Beneath we tabulate the progress towards our original objectives with details for each project that has been initiated & highlighting significant results:

No.	Title	Lead Scientists	Start Month	End Month
Task 1.1	Fibrin with bound morphogens			
Checkpoint	1.1-1.2	JAH, Kuros (CD)	1	12
Deliverables	1.1-1. Optimized morphogen incorporation conditions in fibrin. 1.1-2. Fibrin-binding aprotinin.			
Task update	Biomaterials have been developed and are currently being validated. Further development will be performed based on information generation from tissue testing.			

Publications	None
Patents	None
Other	None
Work to be performed in year 3	No further development tasks will be performed on the material itself in year 3. The only biomaterial work will involve optimising conjugating morphogens with them as part of the tissue specific validation tasks. These tasks include following validation in basic angiogenesis studies, chronic wound models, in bone repair models, in nerve repair models, and perhaps also in muscle repair models.

No.	Title	Lead Scientists	Start Month	End Month
Task 1.2	Fibrinogen-polymer hybrids			
Checkpoint	1.3-1.4	DS	1	12
Deliverables	1.2-1. Control gel biomechanical properties 1.2-2. Control of gel resorption rate 1.2-3. Entrapment and release wild type morphogens. 1.2-4. Control incorporation cys modified morphogens			
Task update	Biomaterials have been produced and are currently being validated. Further development will be performed based on information generation from tissue testing.			
Publications	None			
Patents	None			
Other	None			
Work to be performed in year 3	No further development tasks will be performed on the material itself in year 3. The only biomaterial work will involve optimising conjugating morphogens with them as part of the tissue specific validation tasks. These tasks include following validation in bone repair models.			

No.	Title	Lead Scientists	Start Month	End Month
Task 1.3	Hyaluronic Acid hybrids			
Checkpoint	1.5-1.6	JH, Bio-Hyos (JA)	1	24
Deliverables	1.3-1. Click chemistry for HA crosslinking 1.3-2. Entrapment and release of wild type morphogens from HA hybrids 1.3-3. Biomolecule functionalization for click chemistry 1.3-4. Control of gel biomechanical properties			
Task update	BioHyos has worked to produce Hyaluronic acid of very high Mw (15 million Dalton Hya) but also to develop a new method to produce extremely low Mw, i.e. lower than 300.000 Dalton Hya. This involved the development of a new method regarding the purifying the Hya product from nucleic acids. They have succeeded in developing a new sterilization method. It is well known that in a normal steam sterilization program degradation of the molecular weight can be up to 50%. I have succeeded in developing a system where the breakdown of molecular weight is only about 25%. In working with this development/enhancement it was			

necessary to fill the high Mw Hya in syringes of very high concentration. Both steps entailed difficult work, due to their very high zero shear viscosity (> 300 million mPa s, for comparison the viscosity of water is approx. 1 mPa s).

Throughout this period, they have been involved in two separate special selection and breeding of our roosters in order to reach the required very high molecular weight and very low molecular weight of Hya. This work has involved conducting biopsies ($n > 220$), the processing of each sample, analysis, calculation and finally genetic selection from the different groups to the breeding of the roosters.

Additionally, Hyaluronic acid (HA) has been functionalized in one-pot procedure with two sets of orthogonally reactive chemoselective groups, hydrazide and thiol, basing on our previously reported disulfide protecting group strategy. The ability of the dually functionalized HA-hydrazide-thiol derivative to participate in a sequential assembly of HA hydrogel with covalently integrated fibronectin FNIII9-10 fragment was examined (Figure 1). The *N*-terminal cysteine of the fibronectin fragment has been modified with excess of divinyl sulfone to provide further coupling to the thiol groups of the HA-hydrazide-thiol. Incubation of the HA-hydrazide-thiol derivative with vinyl sulfone-modified FN fragment resulted in the attachment of fibronectin fragments to the HA backbone as was judged from SDS-PAGE analysis. During the second step of our modular approach, FN-HA conjugate was further cross-linked with the HA derivative carrying aldehyde groups to prepare HA-fibronectin hybrid hydrogel.

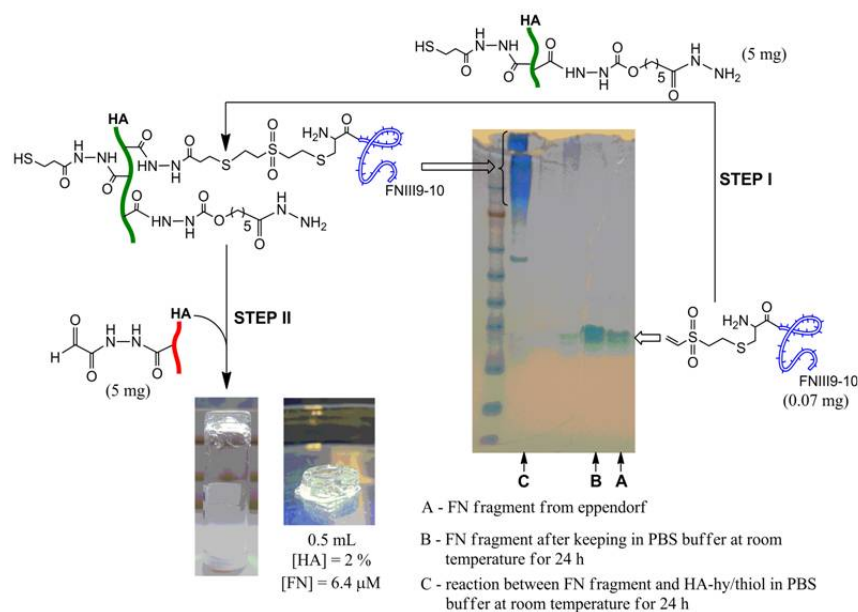


Figure 1: Modular synthesis of HA-FN hybrid hydrogel.

To evaluate the role of fibronectin for the process of bone regeneration, the obtained hybrid hydrogel was formulated with bone morphogenetic protein (BMP-2, Wyeth Europe) at a concentration of 20 μ g/ml. Two groups of hydrogels were evaluated: (HA-al + HA-hydrazide-thiol + BMP-2), (HA-al + HA-FN + BMP-2). Male Sprague-Dawley rats ($n=6$) were injected subcutaneously on the back with 0.2 ml of treatment. Hydrogels were premixed 1 hour before the injection. No sign of infection or other complication was visible. After 8 weeks animals were euthanatized and bone ossicles were harvested. The specimen was evaluated by X-ray and pQCT and processed for histology and histometrical analysis.

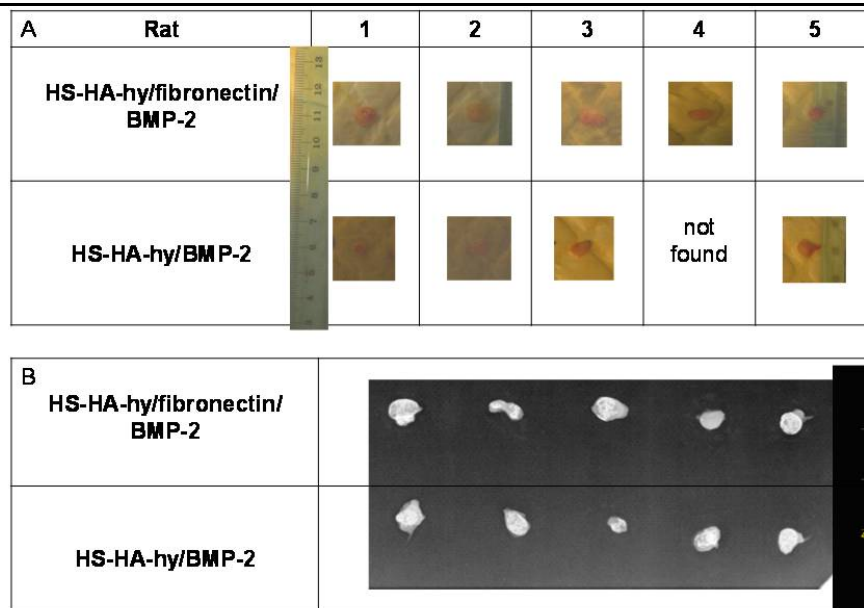
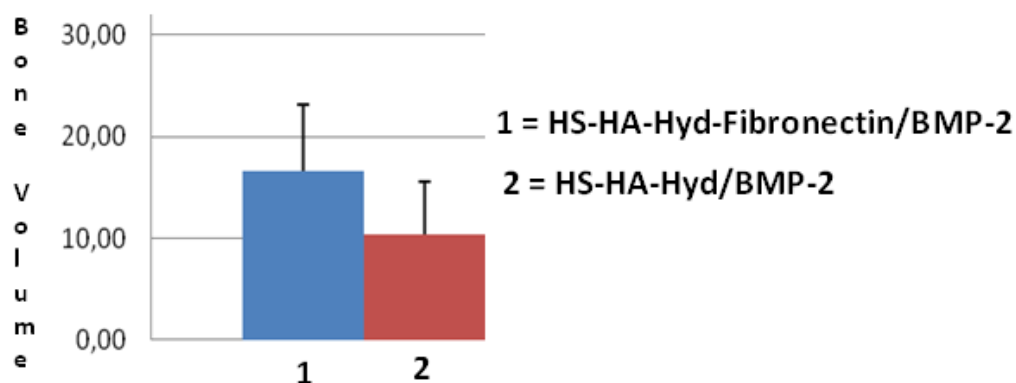


Figure 2: A: Eight weeks after implantation of 0.2 ml volume of hydrogel with 20µg/ml BMP-2 bone ossicles were harvested. B: X- ray of treatment groups: 1: HS-HA/fibronectin/BMP-2 and 2:HS-HA-hy/BMP-2.

Figure 3: Peripheral CT scan (pQCT) showed higher bone volume in the group.



In vitro experiments with human dermal fibroblasts have been preliminary examined.

Publications	None
Patents	None
Other	None
Work to be performed in year 3	No further development tasks will be performed on the material itself in year 3. The only biomaterial work will involve optimising conjugating morphogens with them as part of the tissue specific validation tasks. These tasks include following validation in bone repair models, especially with entrapped or bound BMP-2.

No.	Title	Lead Scientists	Start Month	End Month
Task 1.4	PEG-peptide hybrids			

Checkpoint	1.7-1.8	CW, JAH	1	21
Deliverables	1.4-1. Control of gel biomechanical properties 1.4-2. Control of incorporation of cys modified morphogens 1.4-3. Incorporation of bound heparin sites 1.4-4. Incorporation and release wild type heparin binding morphogens			
Task update	<p>The aim of this task is to develop a soft tissue-like biomaterial for tissue regeneration with enhanced cell binding specificity. In this direction, we have developed starPEG-heparin hydrogels in which the physical properties of the material can be tuned independently of the heparin concentration. Key to this approach is the high affinity of heparin to many natural biomolecules (e.g. soluble growth factors and insoluble extracellular matrix molecules). Furthermore, the carboxylic acid groups located with the polysaccharide chain allow for subsequent conjugation with a variety of biomolecules through various approaches. By tuning the physical properties of the hydrogel independently of biofunctionalization, we are able to more precisely direct cell fate decisions.</p> <p>Along these lines, we are using integrin-binding domains isolated from fibronectin (FN) to better control specific cell adhesion. Previously, it was found that the RGD-containing FN III10 domain has a low affinity for integrin $\alpha 5\beta 1$ which is critical for angiogenesis. Moreover, the specificity for integrin $\alpha 5\beta 1$ binding can be adjusted by including the FN III9 domain in the recombinant fragments. Furthermore, a high affinity binding site for $\alpha 5\beta 1$ integrin can be engineered through a simple Leu¹⁰⁴⁵>Pro mutation of the FN III9 domain (termed FN III9*-10). It is in this direction, that the scope of this project is directed. By functionalizing starPEG-heparin hydrogels with recombinant fibronectin fragments which have a variety of affinities to integrin $\alpha 5\beta 1$, we hope to enhance the angiogenic properties of the starPEG-heparin hydrogel system.</p> <p>In a proof of principle experiment, we utilized recombinant FN III9-10-GBD and FN III9*-10-GBD fragments which contains the C-terminal heparin-binding domain of FN to functionalize starPEG-heparin hydrogels via simple adsorption. Figure 1 shows that at low concentrations of FN fragments, FN III9*-10 enhances initial endothelial cell attachment to the hydrogels over pure starPEG-heparin hydrogels to which the cells cannot attach. At higher concentrations of both fragments, the cells can attach to the gels equally well. This trend is further illustrated by an increase in elongated (tubular) morphology of the endothelial cells after 8 hour on the gels (Fig 2). Cells on hydrogels with only low concentrations of the FN domains (10μg/mL) spread more and adopted a better morphology on hydrogels functionalized with FN III9*-10. On hydrogels with higher concentrations of FN domains (100μg/mL), cell morphology appeared similar.</p> <p>Although these adsorption experiments show that in principle the recombinant fragment can adsorb to starPEG-heparin hydrogels and endothelial cell attachment can be modulated, the simple adsorption of the fragments to the heparin component appeared to be too weak to support long-term cell attachment and survival (Fig 3). Along these lines, work in the Werner lab to optimize the covalent attachment of the recombinant FN fragments to the starPEG-heparin hydrogels via a Michael-type addition reaction is ongoing. In this direction, we are developing a protocol to functionalize starPEG-heparin hydrogels through the covalent attachment of the Cys-terminated fragments to maleimide-functionalized heparin. With this protocol completed, we hope to further characterize the endothelial response of incorporating integrin-specific extracellular matrix fragments in combination with the natural binding and release of cytokines and growth factors from the heparin component to determine ideal conditions for promoting angiogenesis.</p>			

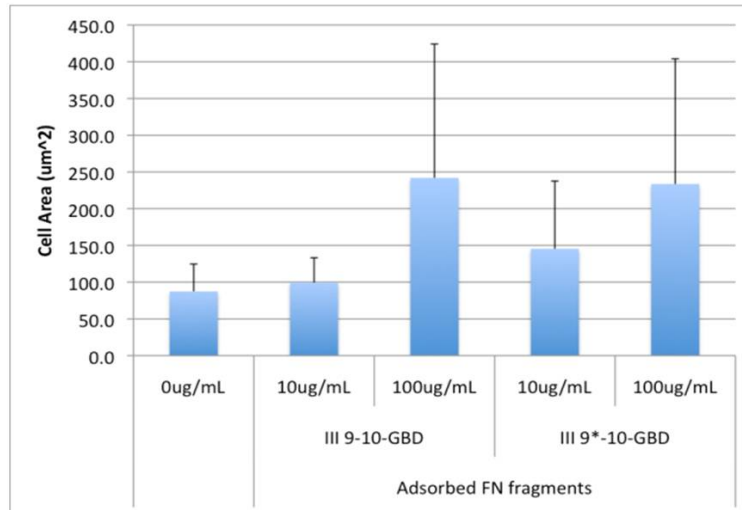


Figure 1. FN III9-10-GBD and FN III9-10-GBD fragments were adsorbed to starPEG-heparin hydrogels. The initial attachment of endothelial cells to the functionalized hydrogels was determined by analysis of their cell spreading at 30 minutes after plating (n>4 for all conditions).*

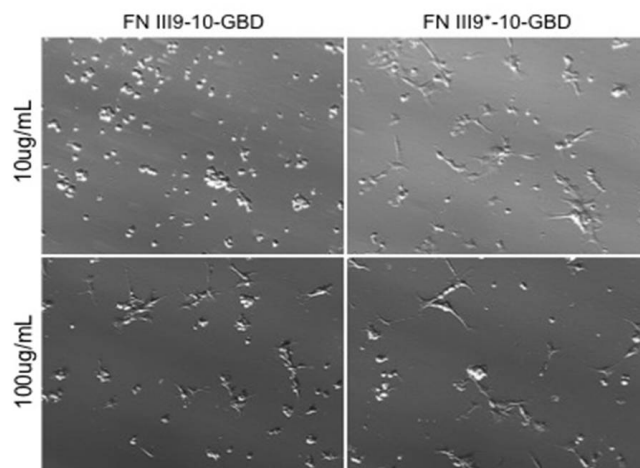


Figure 2. Endothelial cells attach and form elongated, tubular-like structures on adsorbed FN fragments (100µg/mL). At low concentrations (10µg/mL), cell attachment and morphology was enhanced on FN III9-10-functionalized hydrogels.*

We also aimed to investigate the various physical, chemical, and biological characteristics of three “soft tissue-like” PEG-based hydrogels (starPEG-heparin hydrogels, Werner lab; PEG-fibrinogen hydrogels, Seliktar lab; TG-PEG-peptide hydrogels; Lutolf lab) with the goal of defining a system, which has a definable biofunctionalization with constant biomechanics. To identify gels with constant biomechanics, the mechanical properties of three gel variants from each lab (with a range of rigidity surrounding $G'=1000\text{Pa}$) were initially tested through rheological measurements. By performing frequency sweep measurements with a constant 2.0% strain, we found variants within the three different material systems which satisfy the initial proposed ideal properties (e.g gels surrounding $G'=1000\text{Pa}$, Fig 1) with the PEG-Fibrinogen gels falling on the softer side and starPEG-heparin gels on the stiffer. Work in the Werner laboratory is ongoing in which the goal is to produce materials which have the capability of being in the 500-1000Pa range.

Furthermore, the enzymatic degradation of each hydrogel variant within each material system was systematically determined by spectroscopic measurements of the supernatant surrounding the material as it was incubated in collagenase IV solution (1.0U/mL) at 37°C over time. By comparing materials with similar mechanical properties, we could determine the degradation of the materials independently of their stiffness. These results showed that the PEG-Fibrinogen materials degrade substantially faster than the other materials (compare to the TG-PEG gels at 500-1000Pa, Fig 2A). The TG-PEG hydrogels degrade the slowest of the three materials, although the difference between the starPEG-heparin and TG-PEG hydrogels (1000-2000Pa, Fig 2B) is not great. Complications with the handling of PEG-Fibrinogen system prevented the direct comparison of all materials in the 1000-2000Pa range, however these experiments are planned as a follow up. Within both the TG-PEG and starPEG-heparin gel systems, there is a possibility of tunable degradation rate while keeping mechanical properties constant. (Ehrbar et al. *Biomacromolecules*, 2007; Bott et al. *Biomaterials*, 2010; Chwalek et al, in preparation).

Currently, work is ongoing in the Werner laboratory to optimize a gelation chemistry which allows for 3D cell embedding as the other two materials do. With this work, we aim to produce hydrogels which allow for a more complete comparison of all gel types through the initial screening process through the final comparative analysis. Here we present results from a MMP-cleavable starPEG-heparin hydrogel system which is crosslinked through a Michael-type reaction (via maleimide-functionalized heparin and Cysteine-containing starPEG). Fig 3 shows the results from this initial screen in which softer gels ($G' = 100\text{-}1000\text{Pa}$, which are in the range of this work package proposal) can be produced. Additionally, the degradation profile of these materials is similar to the TG-PEG gels and original starPEG-heparin hydrogels (compared Fig 4 with Fig 2). Additionally, through this work package, the Werner and Lutolf groups are working to engineer a hybrid system in which starPEG and heparin moieties are covalently crosslinked via a Factor XIII-mediated transglutaminase reaction.

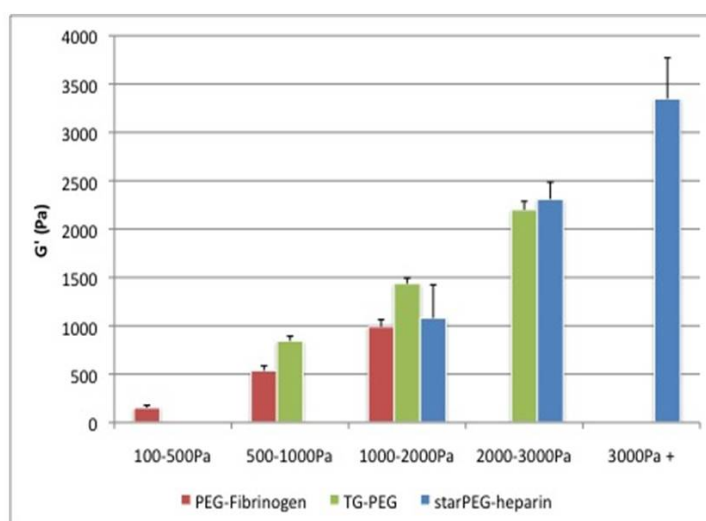


Figure 3. Storage moduli (Pa) of PEG-Fibrinogen, TG-PEG, and starPEG-heparin hydrogels determined through a standardized frequency sweep at constant strain protocol. (n = 3)

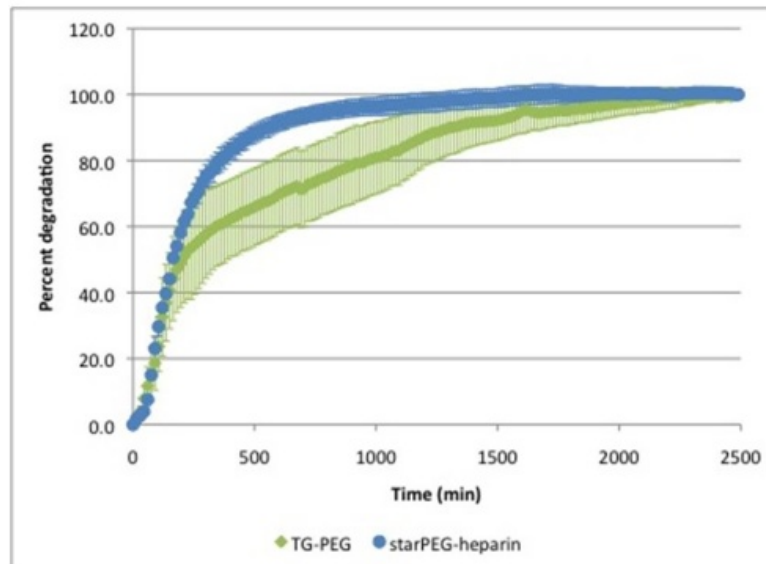
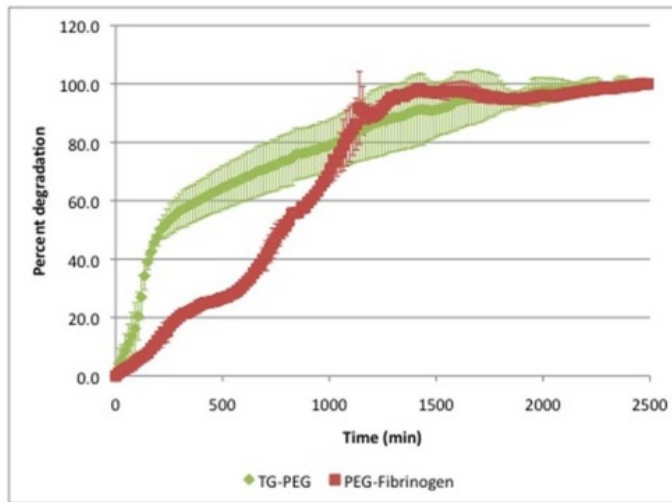


Figure 4. Degradation kinetics of materials incubated in 1.0U/mL collagenase IV solution at 37°C over indicated time. Results shown are the average percent degradation of measurements collected via spectroscopic analysis with an absorption at 278nm. A (left) TG-PEG and PEG-Fibrinogen gels in the 500-1000Pa range and B (right) TG-PEG and starPEG-heparin gels in the 1000-2000Pa range are shown as a comparison at constant biomechanics. (n=3)

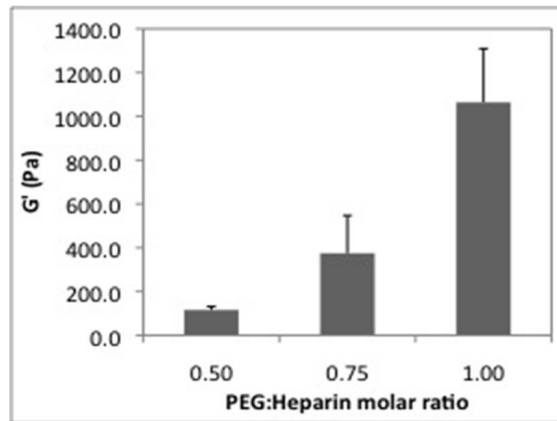


Figure 5. Rheology measurements of newly designed in situ gelling starPEG-heparin hydrogels (n=3)

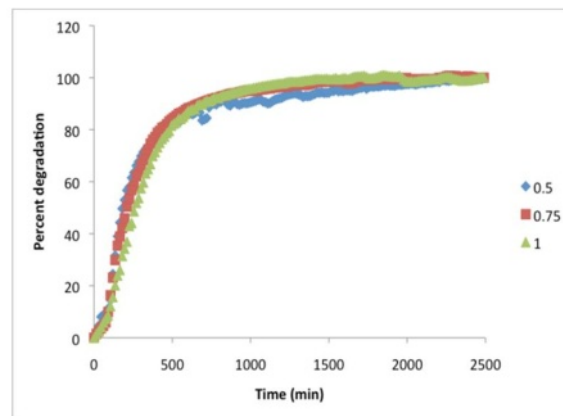


Figure 6. Degradation kinetics of newly designed in situ gelling starPEG-heparin hydrogels performed as in Figure 2 above.

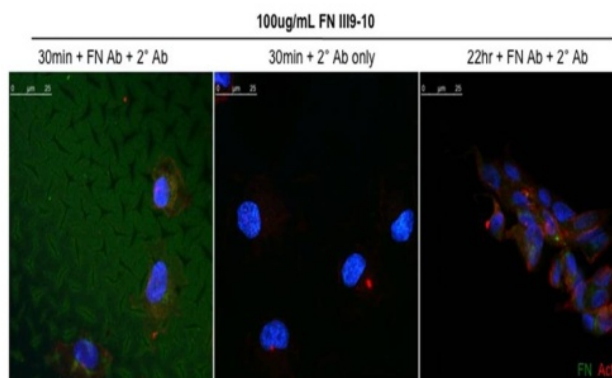


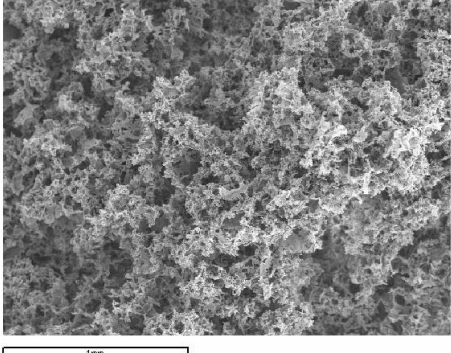
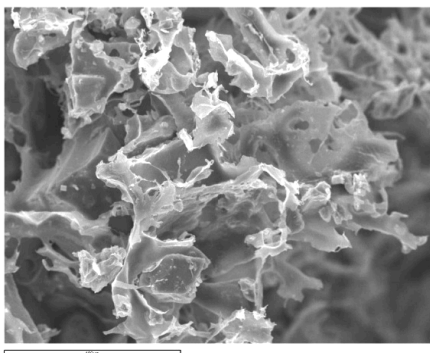
Figure 7. FN specific staining is prominent on hydrogels after incubation with cells for only 30 minutes (green); however, this staining is lost after incubation with cells for 22 hour suggesting that the adsorbed FN fragments might be displaced over time, thus leading to cell detachment and death after 24 hours in culture.

Publications	<p>Tsurkan, M.; Levental, K. R.; Freudenberg, U.; Werner, C. Enzymatically degradable heparin–polyethylene glycol gels with controlled mechanical properties. <i>Chemical Communications</i> (46) 2010, 1141-1143.</p> <p>Tsurkan, M.; Chwalek, C.; Levental, K.R.; Freudenberg, U.; Werner, C.: Modular starPEG-heparin gels with bifunctional peptide linkers. <i>Macromolecular Rapid Communications</i> 31 (2010) 1529-1533.</p> <p>Zieris, A.; Prokoph, S.; Levental, K.R.; Welzel, P.B.; Grimmer, M.; Freudenberg, U.; Werner, C.: FGF-2 and VEGF functionalization of starPEG-heparin hydrogels to modulate biomolecular and physical cues of angiogenesis. <i>Biomaterials</i> 31 (2010) 7985-7994.</p>
Patents	None
Other	<p>Work Presented at following events:</p> <p>Platform Presentation: Werner, C.; Freudenberg, U.; Welzel, P.; Levental, K. R.; Tsurkan, M.; Zieris, A.; Panyanuwat, W.; Grimmer, M.: (invited) A biohybrid hydrogel platform to support regenerative therapies. Annual Scandinavian Society for Biomaterials, Copenhagen, 29.–30.4.2009</p> <p>Platform Presentation: Werner, C.; Freudenberg, U.; Welzel, P.; Levental, K. R.; Tsurkan, M.; Zieris, A.; Panyanuwat, W.; Grimmer, M.: (invited keynote) Biohybrid hydrogels for regenerative therapies. 73rd Prague Meeting on Macromolecules (PMM 2009)Prague, Czech Republic, 9.7.2009</p> <p>Platform Presentation: Werner, C.; Freudenberg, U.; Welzel, P.; Levental, K. R.; Zieris, A.; Tsurkan, M.; Chwalek, K.; Prokoph, S.: (invited keynote) Heparin-star PEG hydrogels to enable cell replacement therapies for neurodegenerative diseases. <i>Biotechnología Habana</i> 2009, Havana, Cuba, 2.–5.11.2009</p> <p>Platform Presentation: Werner, C.; Freudenberg, U.; Welzel, P.; Levental, K. R.; Tsurkan, M.; Zieris, A.; Panyanuwat, W.; Grimmer, M.: (invited keynote) Heparin-starPEG-hydrogels for tissue engineering. 6th Singapore International Chemical Conference (SICC 6), Singapore, 15.–18.12.2009</p> <p>Platform Presentation: Freudenberg, U.; Welzel, P.; Levental, K.R.; Tsurkan, M.; Zieris, A.; Panyanuwat, W.; Sommer, J.-U.; Werner, C.: (invited) Biohybrid polymer networks for regenerative therapies. <i>Makromolekulares Kolloquium</i> 2010, Freiburg, 25.-27.2.2010</p> <p>Platform Presentation: Freudenberg, U.; Hermann, A.; Welzel, P.; Schwarz, S.; Grimmer, M.; Zieris, A.; Panyanuwat, W.; Storch, A.; Werner, C.: Modular biohybrid hydrogels for cell replacement therapies of neurodegenerative diseases. 6th Symposium on Biologic Scaffolds for Regenerative Medicine. Silverado Resort, Napa Valley, CA, USA, 25.–27.04.2010</p> <p>Platform Presentation: Werner, C.; Freudenberg, U.; Welzel, P.; Levental, K. R.; Zieris, A.; Tsurkan, M.; Chwalek, K.; Prokoph, S.: (invited) Polymeric polymer gels in regenerative medicine. Ludwig Boltzmann Institute for Experimental and Clinical Traumatology, Austrian Cluster for Tissue Regeneration Vienna, 28.04.2010</p> <p>Platform presentation: Kandice Levental, Karolina Chwalek, Mikhail Tsurkan, Andrea Zieris, Uwe Freudenberg, Carsten Werner. “The angiogenic potential of starPEG-heparin hydrogels.” Center for Regenerative Therapies Dresden (CRTD) Symposium: Biomaterials for Regenerative Therapies. Dresden, Germany. June 2010.</p> <p>Platform presentation: Kandice Levental, Karolina Chwalek, Mikhail Tsurkan, Andrea Zieris, Uwe Freudenberg, Carsten Werner. “StarPEG-Heparin Hydrogels for Tissue Regeneration.” Tissue Engineering and Regenerative Medicine International Society –</p>

	<p>EU Annual Conference. Galway, Ireland. June 2010.</p> <p>Poster Presentation: Karolina Chwalek, Kandice Levental, Mikhail Tsurkan, Uwe Freudenberg, Carsten Werner. "VEGF-decorated enzymatically cleavable starPEG-heparin hydrogels to promote angiogenesis." 4th CRTD Summer Conference on Regenerative Medicine. Dresden, Germany. June 2010.</p> <p>Platform presentation: Kandice Levental, Karolina Chwalek, Mikhail Tsurkan, Andrea Zieris, Uwe Freudenberg, Carsten Werner. "Optimization of starPEG-heparin hydrogels for inducing angiogenesis." TOPEA Meeting. Barcelona, Spain. July 2010.</p> <p>Platform presentation: Katarzyna Mosiewicz, Adrian Ranga, Matthias Lutolf, "Modulating the physicochemical properties of the PEG-TG hydrogel" TOPEA Meeting. Barcelona, Spain. July 2010.</p> <p>Platform presentation: Karolina Chwalek, Kandice Levental, Mikhail Tsurkan, Uwe Freudenberg, Carsten Werner. "Enzymatically cleavable peptides promote angiogenesis in starPEG-heparin hydrogels." 3rd International Congress on Stem Cells and Tissue Formation. Dresden, Germany. July 2010.</p> <p>Platform Presentation: Welzel, P.B.; Freudenberg, U.; Zieris, A.; Prokoph, S.; Werner, C.: Modulating physical properties of biohybrid hydrogels with constant biomolecular composition. 23rd European Society for Biomaterials Conference 2010, Tampere, Finland, 11.-15.9.2010</p> <p>Platform Presentation: Werner, C.; Freudenberg, U.; Welzel, P.; Levental, K. R.; Zieris, A.; Tsurkan, M.; Chwalek, K.: (invited keynote) Engineered polymer matrices to aid stem cell based therapies. 2nd Materials Science and Engineering Tagung: Materials Surfaces and Cell Interactions. Darmstadt, 24.-26. 8.2010</p> <p>Platform Presentation: Werner, C.; Freudenberg, U.; Welzel, P.; Levental, K. R.; Zieris, A.; Tsurkan, M.; Chwalek, K.; Prokoph, S.: (invited keynote) Multi-biofunctional polymer gels to aid regenerative therapies. TERMIS-AP 2010 Annual Conference, Sydney, Australia, 15.-17.9.2010</p> <p>Platform Presentation: Werner, C.; Freudenberg, U.; Welzel, P.; Levental, K. R.; Zieris, A.; Tsurkan, M.; Chwalek, K.; Prokoph, S.: (invited): Biofunctional polymer materials for regenerative therapies. University of Auckland, Auckland, New Zealand, 20.-21. 9.2010</p>
--	--

<p>Work to be performed in year 3</p>	<p>Some final optimization of materials issues and characteristic will be performed, including optimization of the gelation chemistry that allows for 3D cell embedding, and engineering of a hybrid system in which starPEG and heparin moieties are covalently crosslinked via a Factor XIII-mediated transglutaminase reaction. Tasks in validation include combination of the PEG-peptide materials with VEGF-A or the ephrin domains for investigation in angiogenesis models.</p>
--	---

No.	Title	Lead Scientists	Start Month	End Month
Task 1.5	Porous biomaterial scaffolds			
Checkpoint	1.9-1.10	KS	1	12
Deliverables	1.5-1. Control of slurry to solid transition. 1.5-2. Incorporation of releasable morphogens.			

	1.5-3. Incorporation of bound morphogens.			
Task update	Biomaterials have been produced and are currently being validated. Further development will be performed based on information generation from tissue testing.			
Publications	None			
Patents	None			
Other	None			
Work to be performed in year 3	No further development tasks will be performed on the material itself in year 3. The only biomaterial work will involve optimising conjugating morphogens with them as part of the tissue specific validation tasks. These tasks include following validation in bone repair models.			
No.	Title	Lead Scientists	Start Month	End Month
Task 1.6	Calcium Phosphate Scaffolds			
Checkpoint	1.11-1.13	JP, KS, TE	1	24
Deliverables	1.6-1. Scaffold fabrication, scaffold microstructure and seeding/invasion/nutrient transport properties 1.6-2. Control scaffold biomechanical properties 1.6-3. Incorporation and release of adsorptively bound morphogens 1.6-5. Incorporation of cation stabilized plasmid DNA			
Task update	<p>PLA/CaP glass scaffolds have been fabricated using the solvent-casting and particle leaching technique. Scanning electron microscopy (SEM) has been carried out to study the microstructure of the scaffolds as well as pore size and distribution. Glass particles distribution was also observed by SEM analysis (See Figure 1)</p> <div style="display: flex; justify-content: space-around;">   </div> <p><i>Figure .1 a and b. SEM images showing the microstructure of the scaffolds.</i></p> <p>Scaffold porosity was measured (n=5) by mercury immersion. The calculated porosity resulted in a mean porosity of 95.7 % with a standard deviation of 0.3 % for the five samples.</p>			

m_{sample} [g]	m_{Hg} [g]	V_{Hg} [cm ³]	$\rho_{apparent}$ [g/cm ³]	P [%]
0.014	2.364	0.17	0.080	95.3
0.013	2.443	0.18	0.072	95.8
0.017	3.091	0.23	0.075	95.6
0.020	3.980	0.29	0.068	96.0
0.021	4.101	0.30	0.069	95.9

The ability of these scaffolds to support homogeneous cell seeding and nutrient transport was also assessed. To this end, a custom developed perfusion bioreactor has been designed and fabricated to evaluate the perfusion to enhance cell seeding inside the scaffolds. Parameters such as fluid flow rate and cycle frequency were optimized.

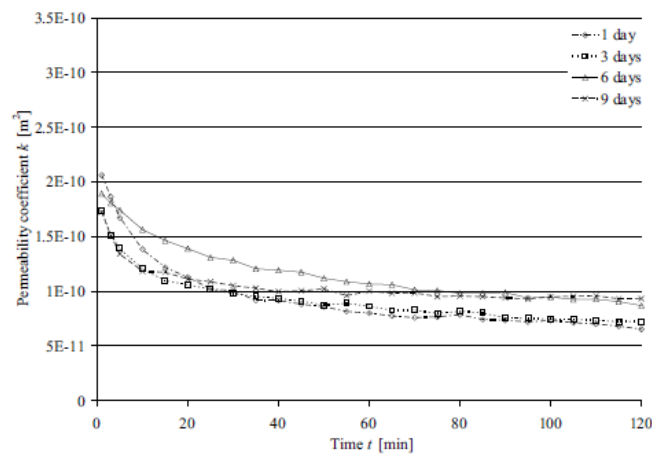


Figure 2. Permeability results (n=20). Preliminary test had shown that the permeability of the soft PLA/glass scaffold dropped during two hours of continuous perfusion to a stable value. Hence the measurement of fluid flow on the scaffold was conducted over two hours, measuring after 1, 3, 6 and 9 days prewetting, five samples for each group

Static cell seeding and perfusion cell seeding were carried out using MG63 osteoblastic like cells. In the former case, cells were injected in the scaffolds and samples were left in complete medium at 37°C for 4 h to allow cell adhesion. Four samples were washed with PBS and frozen in serum-reduced medium and used for the determination of the cell number. Two samples were used for the determination of the cell distribution in the interior by acridine orange staining. In the latter case, cell seeding was conducted under oscillating perfusion of the scaffolds with different values for cycle number and fluid flow velocity.

Three cycle numbers were studied: 50, 100, and 500 cycles. Four fluid flow velocities were studied: 1, 5, 10, and 15 mm/s. Consequently, experiments (**n = 12**) were conducted with six scaffolds for every condition. When perfusing, the system displaced per cycle a fixed volume, resulting in frequencies of up to 0.09 Hz (see table below). The total seeding time depending on velocity and cycle number ranged from 9 min to 23 h.

Total seeding time for every perfusion flow velocity and perfusion cycle number.

Perfusion Flow Velocity [mm/s]	Frequency [Hz]	Perfusion Cycle Number		
		50	100	500
1	0.006	2 h 19 min	4 h 36 min	23 h 09 min
5	0.03	28 min	55 min	4 h 36 min
10	0.06	14 min	28 min	2 h 19 min
15	0.09	9 min	19 min	1 h 33 min

Cell distribution and cell number were assessed after 4 h. Scaffolds were stained with Acridine Orange to identify living cells. The samples for 50 cycles and 100 cycles were additionally stained with ethidium bromide. The scaffolds were then washed twice with sterile PBS and observed under fluorescence stereoscope (Leica MZ16F) with DSR filter for EB and GFP-3 filter for AO.

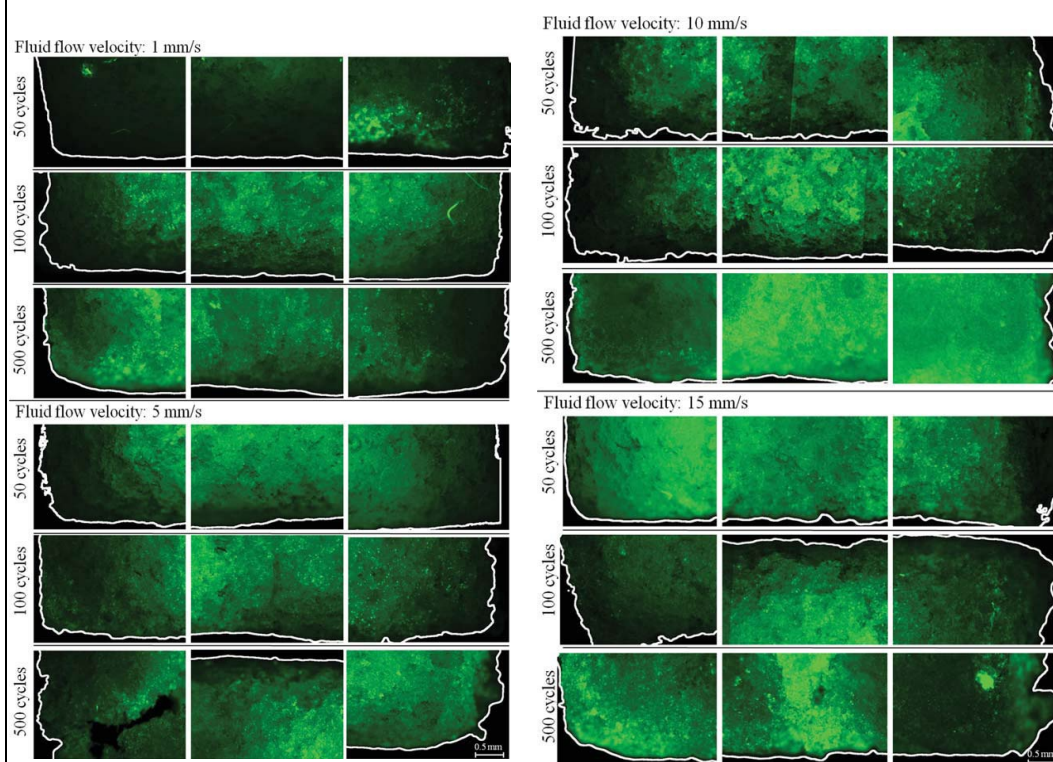


Figure 3. Cell staining with AO, distribution of living cells inside the scaffold (in green) Cells seeded at 1, 5, 10 and 15 mm/s fluid flow velocities and 50, 100, and 500 cycles.

The images suggested that the cell density inside of the scaffolds increased with cycle number, showing higher densities at 100 and 500 cycle seedings. Likewise, the increase of cycle number seemed to improve the distribution throughout the scaffolds. Similarly, an increase in fluid flow velocity improved the cell distribution on inside the scaffold. This showed that a minimum fluid flow velocity and cycle number had to be applied to achieve an uniform cell distribution and high cell density.

The amount of cells located in the scaffolds after perfusion seeding was observed by release of the LDH. It was found that the uniformity of seeding efficiencies between individual samples increased with an increasing number of perfusion seeding oscillations which is represented by the narrowing standard deviations (Fig. 4). At the same time, higher cell seeding cycles did lower the efficiency of the seeding from about 50% to about 20%. Changes of fluid flow velocity did not influence the cell seeding

efficiency significantly at constant perfusion cycle numbers. In the case of the 15 mm/s perfusion fluid flow velocity at 500 perfusion cycles, the seeding efficiency was statistically significantly higher than the efficiencies found at the same number of perfusion cycles and varying velocities.

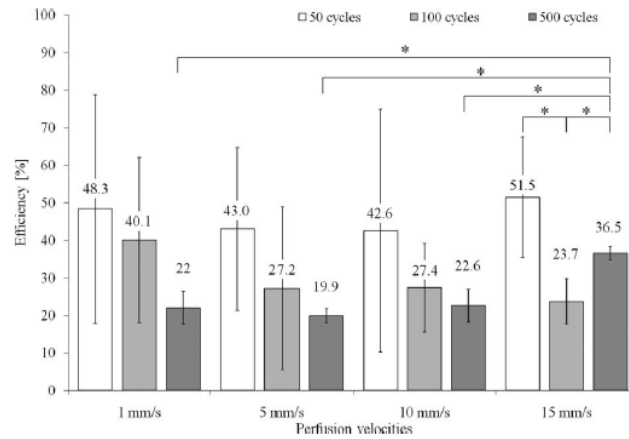


Figure 4. Cell seeding efficiencies achieved with different fluid flow velocities and varying cycle number with initially 106 MG63 cells per scaffold in the perfusion bioreactor system (n = 4). Marked groups (*) are statistically significantly different (Student's t-test, p < 0.05).

Overall, it is concluded that PLA/Glass composites are optimal scaffolds to be used in a bioreactor due to the excellent properties of permeability and porosity, can be produced under controlled and reproducible conditions and provides a good environment for proliferation of various cell types. However, their mechanical behavior is very poor.

We have also aimed therefore to produce scaffolds for bone regeneration, that are flexible and not brittle. To achieve this, CaP glass fibres were combined with PLGA/PEG particles to produce composite scaffolds.

PLGA/PEG-G5 composite scaffolds have successfully been prepared by blending G5 glass particles with (a) melted PLGA/PEG prior to grinding particles (b) PLGA/PEG particles after grinding. The compressive strength of the composite scaffolds was assessed (see figure 5). Scaffold microstructure was assessed using SEM and micro-CT (see figure 6 and 7).

Composite scaffolds prepared using both blending methods are now going to be used for in vitro angiogenesis and osteogenesis assays.

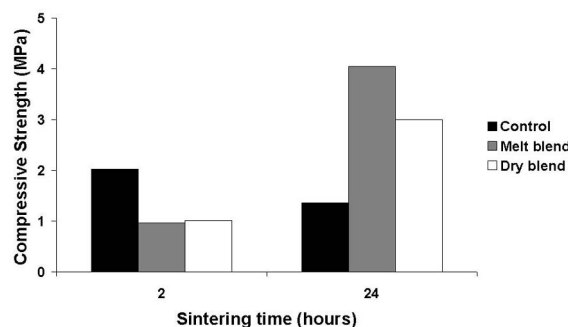


Figure 5: Compressive strength of PLGA/PEG-CaP glass composite scaffolds.

Scaffolds were prepared using a 1:1 ratio of PLGA/PEG to CaP glass by mixing CaP glass particles with melted PLGA/PEG (melt blend) or by mixing CaP glass particles with PLGA/PEG particles (dry blend). A 1:0.6 ratio of particles to saline was used to prepare scaffolds that were sintered for 2 and 24 hours at 37°C. Control scaffolds contain only PLGA/PEG (no CaP glass).

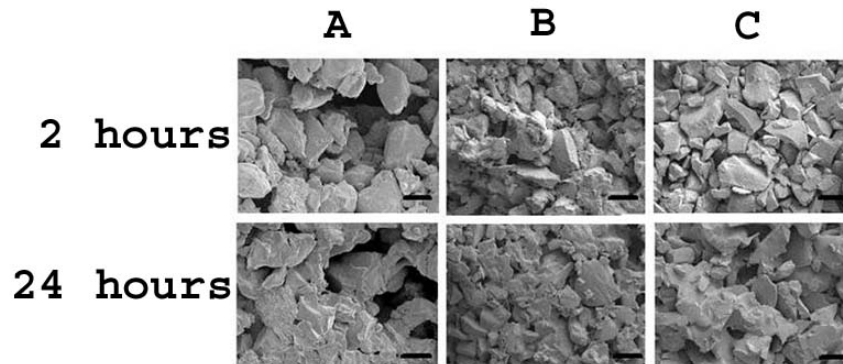


Figure 6 Microstructure of PLGA/PEG-CaP glass composite scaffolds. A 1:0.6 ratio of particles to saline was used to prepare scaffolds that were sintered for 2 and 24 hours at 37°C. (A) Control scaffolds containing only PLGA/PEG (no CaP glass) (B) 1:1 ratio of PLGA/PEG to CaP glass (CaP glass particles mixed with melted PLGA/PEG) (C) 1:1 ratio of PLGA/PEG to CaP glass (CaP glass particles mixed with PLGA/PEG particles). Size bar = 100µm.

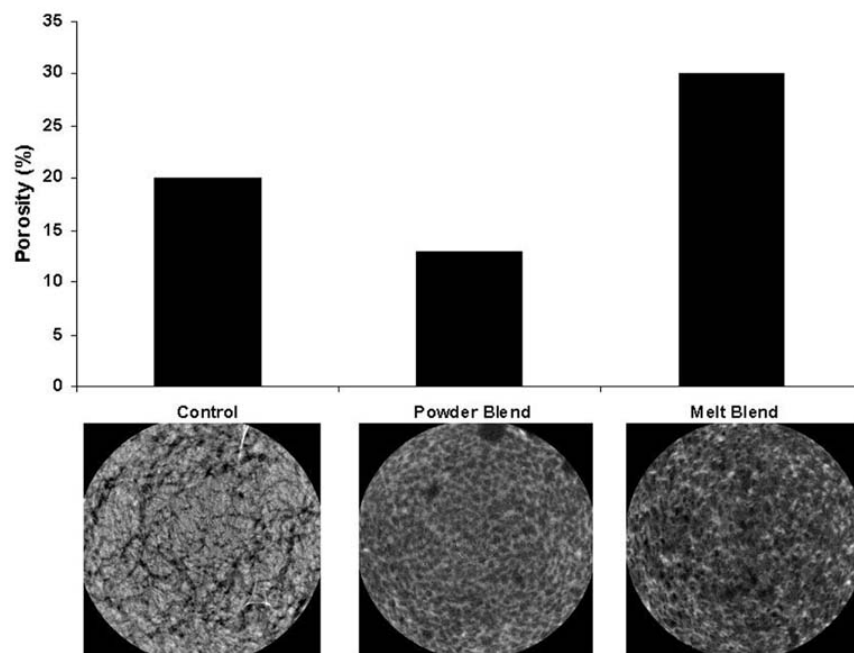


Figure 7: Microstructure of PLGA/PEG-CaP glass composite scaffolds. Scaffolds produced using a ratio of 1:0.6 (particles:saline) and sintered at 37°C for 2 hours were analysed using a SkyScan microCT. (A) Control PLGA/PEG scaffold (B) Composite scaffold produced by mixing PLGA/PEG particles with CaP glass particles (C) Composite scaffold produced by mixing CaP glass into melted PLGA/PEG.

Flexible scaffolds have successfully been prepared. The mechanical properties of the PLGA/PEG-CaP fibre composite scaffolds were assessed, including compressive strength (see Figure 8), Young's Modulus of Elasticity (see Figure 9), and flexibility (see Figure 10). The microstructure of the scaffolds was analysed using SEM. Further

analysis will be performed to assess the flexibility of the scaffolds using cyclic 3-point bend testing. The composite scaffolds will be used in cranial defect studies with Thomas Engstrand early in 2011.

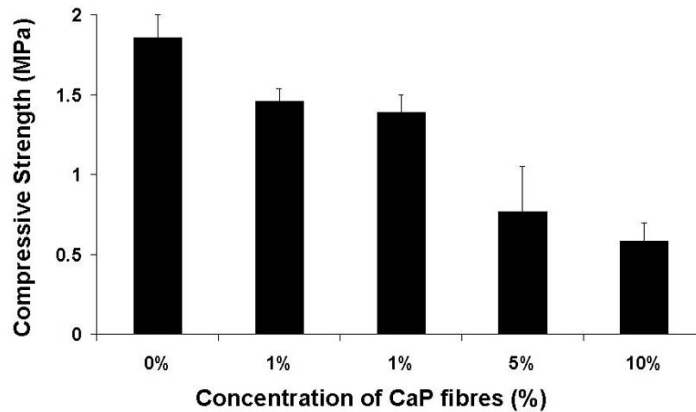


Figure 8: Compressive strength of PLGA/PEG-fibre composite scaffolds. Scaffolds were prepared using increasing amounts of CaP fibres mixed with PLGA/PEG particles. A ratio of 1:0.6 was used for particles-fibres to saline. Scaffolds were sintered at 37°C for 2 hours (n=3).

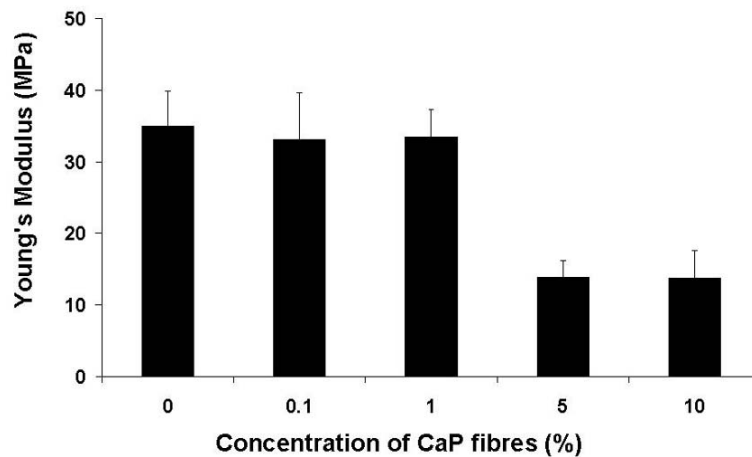
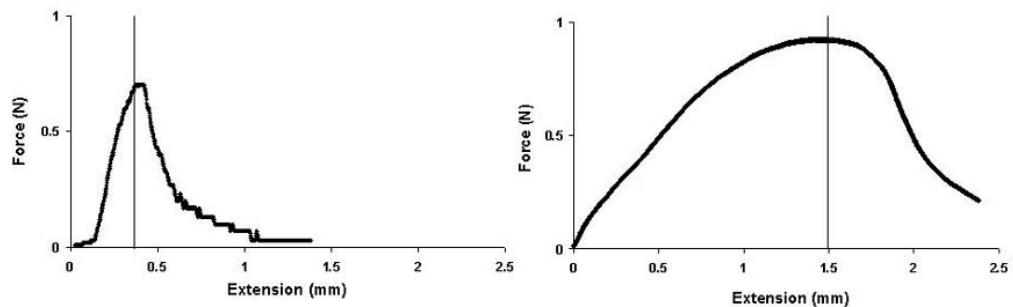
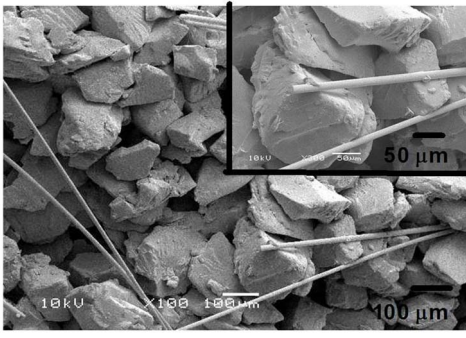


Figure 9: Young's Modulus of PLGA/PEG-fibre composite scaffolds. Scaffolds were prepared using increasing amounts of CaP fibres mixed with PLGA/PEG particles. A ratio of 1:0.6 was used for particles-fibres to saline. Scaffolds were sintered at 37°C for 2 hours (n=3).



	<p><i>Figure 10: Flexibility of PLGA/PEG-CaP fibre composite scaffolds. Scaffolds were prepared using a 1:0.6 ratio of particles/fibres to saline and were sintered for 2 hours at 37°C. (A) Control PLGA/PEG scaffolds (B) PLGA/PEG-fibre scaffolds containing 0.5% fibres. The elongation to break is shown by the extension of the scaffolds under strain (force).</i></p>  <p><i>Figure 11: Microstructure of PLGA/PEG-CaP fibre composite scaffolds. SEM images of scaffolds prepared using a 1:0.6 ratio of PLGA/PEG-CaP fibres (0.5%) to saline and sintered for 2 or 24 hours at 37°C.</i></p>
Publications	Following completion of mechanical testing a publication will be prepared on the development of the flexible scaffold
Patents	EP10382121.1 "Nanostructured Material, Process for its preparation and uses thereof"
Other	None
Work to be performed in year 3	No further development tasks will be performed on the material itself in year 3. The only biomaterial work will involve optimising conjugating morphogens with them as part of the tissue specific validation tasks. These tasks include following validation in bone repair models, especially combined with BMP-2.

No.	Title	Lead Scientists	Start Month	End Month
Task 1.7	Fibrous Silica scaffolds			
Checkpoint	1.14 and 1.15	Bayer	1	24
Deliverables	D 1.7.-1			
Task update	Biomaterials have been developed and are available for validation. Further development will be performed based on information generation from tissue testing.			
Publications	None			
Patents	None			
Other	None			
Work to be performed in year 3	No activities are planned with this biomaterial platform. The corporate partner Bayer has ceased development of the material. This being recognized, the consortium management does not wish to invest resources in investigating the material, when there is no possibility for future exploitation in the case of favourable results.			

WP1 has produced 3 peer-reviewed publications in this period.

During the reporting period we have completed 5/8 tasks for year 2 and task 1.6-5, is on schedule to be delivered during year 3. We have also completed 3 tasks that had not been delivered during year 1 (1.2-4, 1.5-3, 1.7-1).

Collaborations within the work package were as follows.

Exchanges of staff
<ul style="list-style-type: none">• Thomas Engstrand visited Shakesheff lab to discuss scaffold requirements
Exchanges of reagents
<ul style="list-style-type: none">• Dror Seliktar's group (Technion, Israel) supplied PEG-Fibrinogen solutions, supplies, and equipment for gel preparation and Phase I characterization at IPF (Dresden, Germany)• Matthias Lutolf's group (EPFL, Switzerland) supplied TG-PEG-peptide hydrogels for Phase I characterization at IPF (Dresden, Germany)• Prof. Hubbell's group (EPFL, Switzerland) provided FNIII9-10-GBD, FNIII9*-10-GBD, Cys-FNIII9-10, and Cys-FNIII9*-10 to the Werner group• Prof. Hubbel group (EPFL, Switzerland) supplied the thiol-reactive integrin-binding fibronectin domain to the Ossipov group

Work package number	2	Start date or starting event:			Month 1	
Work package title	Engineered Bioactives Development					
Activity Type	RTD	Workpackage Leader			Martin Ehrbar	
Participant number	1	5	7	8	10	13
Principal Investigator	JAH/MS	KS	AB	ED	ME	SE
Planned Person-months for whole WP duration	45	8	12	6	0	15
Actual Person-months so far	24.5	0	3	0	23	0

REPORT OVERVIEW: WP2 - Engineered Bioactives Development

The task of **incorporating growth factors into scaffolds** has been completed (**JAH, MS, AZ**) by generating several growth factors-containing scaffolds such as: Fibrin-binding and cys-containing VEGF-A and VEGF-C and fibrin-binding PIGF; Fibrin-binding and cys-containing VEGF-syndecan; Wild-type, fibrin-binding and cys-containing TGF- β 1 and TGF- β 3; Fibrin-binding PDGF-AB; Wild-type, fibrin-binding and cys-containing IGF-1; Fibrin-binding BMP-2.

2.1 To induce endothelial cell signalling and angiogenesis we (**ME, DO**) are engineering fibrin matrices with ephrin mimetic peptides. The Eph receptor/ephrin system has been shown to direct the positioning, adhesion and migration of cells and cell layers during development and tissue homeostasis, including the formation of tissue boundaries, assembly of intricate neuronal circuits, remodelling of blood vessels and organ size. In order to mimic Eph/ephrin interactions, we developed TG-tagged ephrin mimetic peptides (TG-EMP) to target specific Eph receptors. By varying the amount of Factor XIII TG, we were able to incorporate very efficiently various amounts of TG-EMPs into fibrin gels and provide cells with gradients of stimulating peptides that elicited prolonged EphA2 receptor tyrosine phosphorylation. We are now developing a strategy to cluster peptides using star-shaped PEGs before presenting them to cells in 2D or 3D cultures. Our preliminary data indicates that such multimerized TG-EMP-A2 peptides might be more efficient in inducing EphA2 tyrosine phosphorylation compared to the monomeric peptide. Additionally, we are seeking to incorporate ephrin-Fc proteins into synthetic matrices by affinity-based interactions with the material. This approach will allow the use of commercially available Ephrin ligands to compare the impact of soluble versus matrix-bound ligands on Eph signaling in 2D and 3D environments.

Additionally to develop a standardized procedure for the cultivation of human mesenchymal stem cells (MSCs) from human bone marrow we (**KP, JAH**) evaluated Fibronectin fragments for the attachment and expansion of human MSC in a three-phase project. First we tested the effect of FN fragments FNIII CBD and FNIII CBD-GBD on the clonogenic properties of bone marrow mononuclear cells (BM MNC) in comparison to the full-length fibronectin in serum-free medium or in presence of serum. Secondly, the fragments were incubated with and without calcium containing buffer. Human BM MSCs proliferated best after coating with FNIII CBD-GBD in serum-free medium and under calcium-free conditions. A CFU-F assay revealed the superior supportive properties of FN CBD-GBD on the growth of MSC cells, compared to FN CBD and FN CBD-GBD-CS1. Finally, we will evaluate which FN fragment supports best MSC attachment and proliferation.

Finally to complement this we have designed, cloned and produced engineered recombinant proteins that can be provided to AngioScaff partners we (**JAH**) have developed and produced several TG-morphogens, such as Fibronectin fragments TG-FN910-1214V15 and TG-FNIIIV; Growth factors TG-VEGF-121-AG (VEGF-121 fused with laminin fragment), TG-MMP-VEGF121, and TG-MMP-AG. All the recombinant proteins have been verified as >95% pure by SDS-PAGE and MALDI-TOF analysis. Moreover, proteins have been produced with very low amount of endotoxin. Recombinant protein activities and functions have been confirmed by various assays, such as cell adhesion, receptor phosphorylation and fibrin gel release assay.

2.2 (**JH, DO**). To incorporate adhesion proteins into scaffolds, we (**DO**) have synthesized new aldehyde derivative of heparin (HP-al) and hyaluronic acid (HA-al). These functionalized glucosaminoglycans (GAGs) formed strong hydrogels within half a minute upon mixing with an aqueous solution of poly(vinyl alcohol)-based cross-linker bearing carbazate groups (PVA-carb). To evaluate the role of heparin in sequestering bone inducing growth factor (BMP-2) in a hydrogel matrix we tested the efficiency of four permutations of HA-al + PVA-card hydrogels +/- HP-al and BMP-2 in a mouse model. The hydrogels were implanted subcutaneously and histological examination revealed formation of new bone only in the group of mice that had received the (HP-al + HA-al + PVA-carb+ BMP-2)-hydrogel and not in other three groups.

2.3. We (**JAH, MS, AB**) have recently developed new micelles based on Poly(ethyleneglycol)-Poly(propylenesulfide)-Poly(ethyleneimine) (PEG-b-PPS-b-PEI) block copolymer to deliver nucleic acid. Delivery of plasmids carrying Runx2 (master gene of osteoblast differentiation) and HIF-1 (responses to hypoxia) into bone lesions by using these micelles should significantly help bone regeneration by enhancing osteoblast differentiation and increasing bone vascularization. HIF-1 α and HIF-1 α Δ ODD (HIF-1 α lacking the oxygen-sensitive degradation domain) cDNAs were successfully transfected in HEK293T cells by using PEG-b-PPS-b-PEI micelles, thus confirming the potential of the new vector to mediate in vitro cell transfection. However the micelles failed to mediate in vivo transfection of GFP and Luciferase reporter genes in a rat model of calvarial bone lesion. We therefore developed novel micelles, which are more easily internalizable by cells and with a high capacity to cross cell membranes, based on the use of FN, an extracellular matrix glycoprotein that binds to different integrins, thus promoting integrin endocytosis and recycling. Fluorophore-labeled PEG-PPS (AB) micelles were functionalized with recombinant FNIII9-10/12-14 FN fragment and efficiently internalised into NIH3T3 cells, thus confirming the potential of integrin targeting to increase micelle uptake. Endocytosis was demonstrated by the inhibition of uptake at 4°C and, directly, by confocal microscopy.

Beneath we tabulate the progress towards our original objectives with details for each project that has been initiated & highlighting significant results:

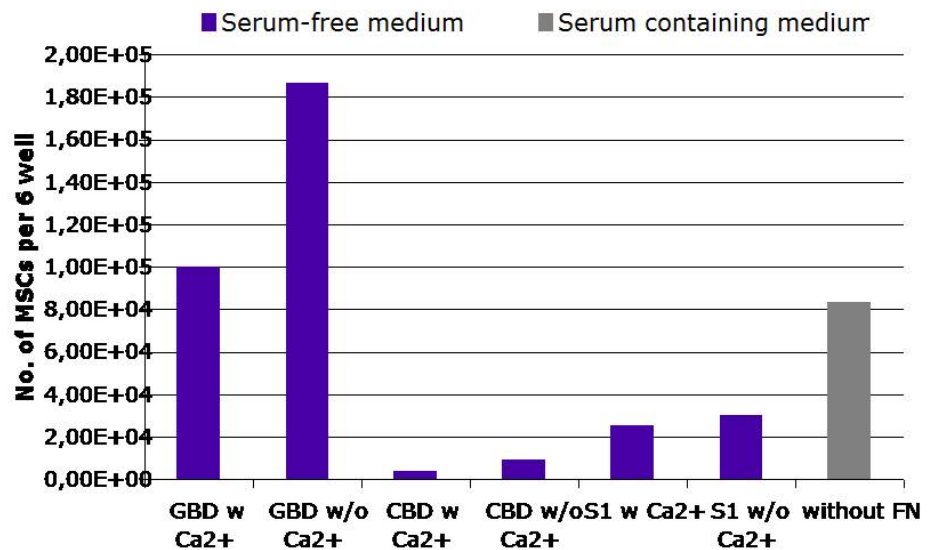
No.	Title	Lead Scientists	Start Month	End Month																							
Task 2.1	Adhesion proteins for incorporation into scaffolds																										
Checkpoint	2.1-2.2	JAH, ME	1	18																							
Deliverables	2.1-1. Wild type, fibrin binding and cys containing fibronectin fragments 2.1-2. Fibrin-binding and cys-containing peptide mimetics of ephrins 2.1-3. Recombinant fibrin binding VE cadherin																										
Task update	<p>To analyze the supportive effect of the fibronectin fragments regarding attachment and expansion of the cells human mesenchymal stromal cells (MSCs) were cultivated with and without fibronectin fragment (FNIII 9-10 and FNIII 9-10-12-14) and serum-free medium. The goal was to develop a standardized procedure for the cultivation of MSCs from human bone marrow using these material+morphogen combinations so that for validation experiments there is an internal control. This was to be reached in three Phases:</p> <div style="text-align: center;"> <p>CFU-F assay with different coating strategies</p> <table border="1"> <caption>CFU-F assay with different coating strategies</caption> <thead> <tr> <th>Coating Strategy</th> <th>Medium</th> <th>Number of CFU-F</th> </tr> </thead> <tbody> <tr> <td rowspan="2">FNIII CBD-GBD</td> <td>Serum-free Medium</td> <td>~55</td> </tr> <tr> <td>FCS containing medium</td> <td>~30</td> </tr> <tr> <td rowspan="2">FNIII CBD</td> <td>Serum-free Medium</td> <td>~20</td> </tr> <tr> <td>FCS containing medium</td> <td>~25</td> </tr> <tr> <td rowspan="2">FN (full-length)</td> <td>Serum-free Medium</td> <td>~58</td> </tr> <tr> <td>FCS containing medium</td> <td>~35</td> </tr> <tr> <td rowspan="2">without FN</td> <td>Serum-free Medium</td> <td>~55</td> </tr> <tr> <td>FCS containing medium</td> <td>~55</td> </tr> </tbody> </table> </div>				Coating Strategy	Medium	Number of CFU-F	FNIII CBD-GBD	Serum-free Medium	~55	FCS containing medium	~30	FNIII CBD	Serum-free Medium	~20	FCS containing medium	~25	FN (full-length)	Serum-free Medium	~58	FCS containing medium	~35	without FN	Serum-free Medium	~55	FCS containing medium	~55
Coating Strategy	Medium	Number of CFU-F																									
FNIII CBD-GBD	Serum-free Medium	~55																									
	FCS containing medium	~30																									
FNIII CBD	Serum-free Medium	~20																									
	FCS containing medium	~25																									
FN (full-length)	Serum-free Medium	~58																									
	FCS containing medium	~35																									
without FN	Serum-free Medium	~55																									
	FCS containing medium	~55																									

Phase 1

The initial testing of the cultivation effect of the fibronectin fragments (FNIII CBD and FNIII CBD-GBD) on MSCs was performed in a CFU-F assay in comparison to the full-length fibronectin. The clonogenic properties of bone marrow mononuclear cells (BM MNC) after cultivation in serum-free medium (purple) were comparable to FCS containing medium only with a coating of full-length fibronectin or FNIII CBD-GBD ($n>3$ for all conditions tested).

Phase 2

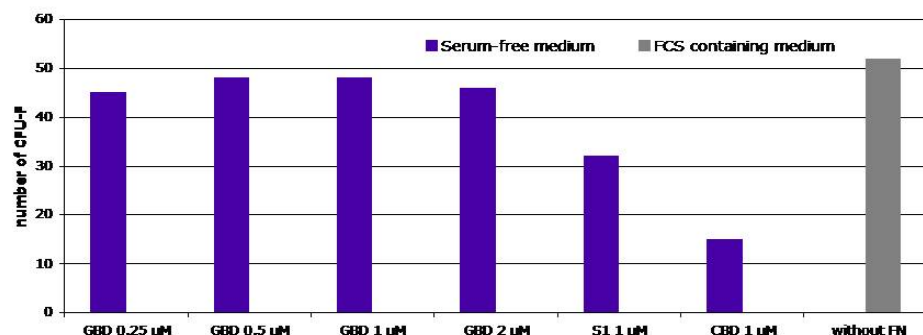
Expansion potential of MSCs after cultivation on coating strategies



To optimize the coating conditions the fragments were incubated with and without calcium containing buffer. The proliferation potential of human bone marrow (BM) MSCs shows best results after coating with FNIII CBD-GBD in serum-free medium compared to serum containing medium. Furthermore the coating under calcium-free conditions nearly doubles the proliferation potential with all fragments

To evaluate the optimized coating concentration for the FN CBD-GBD a CFU-F assay was performed. After 14 days of cultivation FN CBD-GBD reveals again the best supportive effect for MSC growth compared to FN CBD and FN CBD-GBD-CS1. Although the titration effect is not distinct a coating concentration of 1 μM is comparable to FCS-containing medium without coating with regard to number of colonies.

CFU-F assay with different concentrations of FN-fragments



Phase 3

Evaluation of which fibronectin fragment has got the most supportive effect for MSC attachment and proliferation.

To ensure provision of a comprehensive material+morphogen to the partnership we cloned and produced engineered recombinant proteins and provide to Angioscaff partners, as well as to share information (technical and scientific) with other partners such as Eming's lab and Ehrbar's lab who produce engineered proteins.

Most of morphogens have been modified with a transglutaminase sensitive sequence (TG) in order to be covalently incorporated into fibrin matrices by the transglutaminase factor XIII. For the fibronectin fragments, a single cysteine (Cys) at the N-terminus has been added, in order to functionalize other biomaterials such as PEG by thiol coupling.

This year, we produced new protein as following and continue to provide proteins to Angioscaff partners as described below at Collaboration part.

Fibronectin fragments:

TG-FN910-1214V15, TG-FNIIV

Growth factors:

TG-VEGF-121-AG (VEGF-121 fused with laminin fragment), TG-MMP-VEGF121, TG-MMP-AG

All the recombinant proteins have been verified as <95% pure by SDS-PAGE and MALDI-TOF analysis. Moreover, proteins have been produced with very low amount of endotoxin (<0.001EU/ug). Recombinant protein activities and functions have been confirmed by various assays, such as cell adhesion, receptor phosphorylation and fibrin gel release assay.

Eph receptors (erythropoietin-producing human hepatocellular carcinoma) comprise the largest family of vertebrate receptor tyrosine kinases that are crucial for development and tissue homeostasis, including the formation of tissue boundaries, assembly of intricate neuronal circuits, remodelling of blood vessels and organ size. In concert with their ephrin ligands (Eph family receptor interacting proteins), they form an essential cell-cell communication system capable of bi-directional signaling, where receptor signaling is designated "forward" and ephrin signaling is "reverse." Ephs and ephrins are thought to act as graded molecular tags which translate the density of their cognate partner on opposing membranes into precisely graded cellular responses, resulting in cell contact repulsion or cell-cell adhesion. Through this mechanism, the Eph receptor/ephrin system has been shown to direct the positioning, adhesion and migration of cells and cell layers during development. In order to mimic Eph/ephrin interactions, we developed transglutaminase sequence (TG)-tagged ephrin mimetic peptides (TG-EMPs), TG-EMP-A2 (YSA), TG-EMP-B2 (SNEW) and TG-EMP-B4 (TNYL-RAW) targeting accordingly EphA2, EphB2 and EphB4 receptors. By varying the amount of Factor XIII, we were able to incorporate various amounts of TG-EMPs into fibrin gels and provide cells with gradients of stimulating peptides. We demonstrated that peptide incorporation into fibrin gels is very efficient up to 70% and occurs in the presence of both serum components and cells. We focused our study on functionality of the TG-EMPs in comparison to the published non-modified peptides by studying the degree of their ability to stimulate or inhibit receptor tyrosine phosphorylation. TG-EMP-A2 peptide stimulated EphA2 receptor tyrosine phosphorylation in its TG fibrin bound form. The prolonged activation of EphA2 (up to 48 hours in HUVE cell 2D cultures) indicates that matrix-immobilized TG-EMPs might have long-lasting stimulatory effects. We also demonstrate that soluble TG-EMP-B4 peptide inhibited ephrin-B2-induced EphB4 receptor activation in HUVE cells, also indicating that the N-terminal modification did not compromise the peptide's functionality. However, we are currently unable to convert soluble inhibitory peptides to stimulatory peptides after tethering them to fibrin matrices. From our preliminary data, we cannot conclude whether or not the effects are too subtle to be detected by our biochemical assays or the fibrin-bound TG-EMPs at this concentration are unable to cluster multiple receptors. We are developing a strategy to cluster peptides using star-shaped PEGs before presenting them to cells in 2D or 3D cultures. Our preliminary data indicates that such multimerized TG-EMP-A2 peptides

might more efficiently induce the tyrosine phosphorylation of EphA2 compared to the monomeric peptide when presented to HUVE cells. Additionally, we are seeking to incorporate ephrin-Fc proteins into synthetic matrices by affinity based interactions with the material. This approach will allow the use of commercially available Ephrin ligands to compare the impact of soluble versus matrix-bound ligands on Eph signaling in 2D and 3D environments.

Vascular endothelial cadherin (VE-cadherin) has been shown to be an integral protein for proper blood vessel organization and stability. VE-cadherin also regulates cell-cell adherens junctions in the endothelium, which is necessary for proper vessel function. Because VE-cadherin performs such an important role in the stabilization of endothelial cells it is hypothesized that the covalent integration of VE-cadherin in a fibrin matrix will aid in the proper formation of blood vessels.

To covalently bind VE-cadherin in a fibrin matrix a chimeric protein was designed that consists of the first 4 extracellular domains of VE-cadherin, fused to the N-terminus of a FC domain, which is then fused to a transglutaminase substrate sequence (TG) (NQEQVSPL). The 4 extracellular domains are known to cause the high affinity homophilic interaction between intermolecular cadherin molecules. The FC domain causes the VE-cadherin to dimerize which increases the homophilic interaction with cells and increases the solubility of VE-cadherin. The TG sequence causes the covalent linkage to the fibrin matrix when transglutaminase, Factor XIIIa, is present (Figure 1).

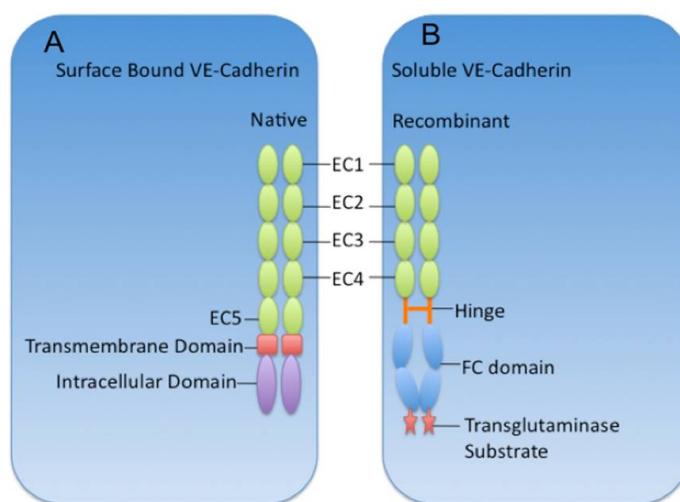


Figure 1: (A) Native VE-cadherin has five extracellular domains (EC1-5), a transmembrane domain, and an intracellular domain that transmits the external signals to intracellular proteins. (B) The recombinant VE-cadherin is expressed as a soluble fusion to the FC region of hlgG1, which has a transglutaminase substrate on the C-terminus for covalent attachment to a fibrin matrix.

The VE-cadherin chimera has been cloned into a mammalian expression system and expressed in HEK293 cells.

Publications	A manuscript is under preparation and is planned to be submitted within the next year.
Patents	None
Other	None
Work to be performed in year 3	Extensive work is planned for Year 3. The FN fragment technology for immobilization of adhesion domains adjacent to morphogen-binding domains appears very promising, and this technology will be examined in validation projects in angiogenesis/skin repair models, bone repair models, and nerve repair models in the context of VEGF-A, PDGF, BMP-2, and NT-3/BDNF biomimetic presentation. Approaches for conjugation of the ephrins to fibrin and the PEG-peptide materials will be focused on read-out validations in angiogenesis. The fibrin-binding VE-cadherin will be investigated in validations of angiogenesis. The VEGF-Syndecan-binding domain fusion will be investigated in validations of angiogenesis.

No.	Title	Lead Scientists	Start Month	End Month
Task 2.2	Growth factor proteins for incorporation into scaffolds			
Checkpoint	2.3-2.8	JAH, MS, AZ,	1	18
Deliverables	2.2-1. Fibrin-binding and cys-containing VEGF-A and VEGF-C and fibrin-binding PIGF. 2.2-2. Fibrin-binding and cys-containing VEGF-syndecan. 2.2-3. Wild-type, fibrin-binding and cys-containing TGF- β 1 and TGF- β 3 2.2-4. Fibrin-binding PDGF-AB. 2.2-5. Wild-type, fibrin-binding and cys-containing IGF-1. 2.2-6. Fibrin-binding BMP-2. 2.2-7. Wild type, fibrin binding, cys containing β NGF, NT 3 and BDNF			
Task update	Bioactive materials have been produced and are currently being validated. Further development will be performed based on information generation from tissue testing.			
Publications	None			
Patents	None			
Other	None			
Work to be performed in year 3	These materials have been developed as planned, and no new molecule development work from the list above is needed or planned in Years 3 and 4. (With regard to 2.2-1) Fibrin-binding VEGF-A and VEGF-C have been developed. A novel mechanism for binding PIGF-2 into fibrin has been developed, and this mechanism is being explored as a novel and generalizable technology for binding of other growth factors into fibrin; this is being characterized in the example of VEGF-A121, which is not fibrin-binding. These molecules will be validated in angiogenesis/skin repair models and in bone repair models. (With regard to 2.2-2) The fibrin-binding VEGF-syndecan has been developed, and this molecule will be validated in fibrin in angiogenesis models. (With regard to 2.2-3) A novel approach for TGF- β 1 in fibrin matrices, a novel method will be developed that enables this, and this method will be characterized. (With regard to 2.2-4) The fibrin-binding PDGF has been developed, and it is currently in clinical trials in chronic wound repair. (With regard to 2.2-5) The fibrin-binding IGF-1 has been developed, and a novel method for delivery of wild-type IGF-1 from fibrin matrices will be developed. The bound IGF-1 forms will be validated in muscle repair models. (With regard to 2.2-6) The fibrin-binding BMP-2 has been developed, and the novel method for binding of wild-type BMP-2 in fibrin matrices will be validated in bone repair models. (With regard to 2-2-7) A novel method for binding of wild-type NT-3 and BDNF is being developed, and these fibrin-bound morphogens will be validated in nerve repair models.			
No.	Title	Lead Scientists	Start Month	End Month
Task 2.3	Genes for morphoregulators and transcriptional morphoregulators			
Checkpoint	2.9-2.11	JAH, MS, AB	1	9
Deliverables	2.3-1. Plasmid DNA for HIF-1 α 2.3-2. Matrix-based nonviral transfection vectors. 2.3-3. Plasmid DNA for wild-type Runx2. 2.3-4. Develop, refine characterization and supply stable transducing VEGF producing and secreting cells.			
Task update	One of the most important challenges in the field of bone tissue engineering is the enhancement of bone graft vascularization. This is not only essential to ensure a good			

diffusion of both oxygen and nutrients through the newly-formed bone but also to regenerate the physiological environment of the tissue.

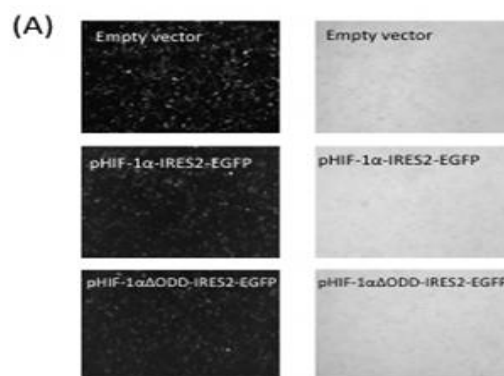
Hypoxia-inducible factor 1 (HIF-1) is a transcription factor that has an essential role in cellular and systemic homeostatic responses to hypoxia while Runt-related Transcription Factor-2 (Runx2) is the master gene of osteoblast differentiation. Recently, our laboratory developed new micelles based on Poly(ethyleneglycol)-Poly(propylenesulfide)-Poly(ethyleneimine) (PEG-b-PPS-b-PEI) block copolymer to deliver nucleic acid. We hypothesize that delivery of plasmids carrying Runx2 and HIF-1 into bone lesions by using these micelles will significantly help bone regeneration through two different ways: i) enhancing osteoblast differentiation and ii) increasing bone vascularization.

HIF-1 α and HIF-1 α Δ ODD (HIF-1 α lacking the oxygen-sensitive degradation domain) cDNAs were subcloned in pIRES2-EGFP vector and transfected in HEK293T cells by using PEG-b-PPS-b-PEI micelles, thus confirming the potential of the new vector to mediate in vitro cell transfection (Figure 1).

Although the promising in vitro results, the same micelles were not able to mediate in vivo transfection. Indeed, the delivery of micelles complexed with plasmids encoding for reporter genes such as GFP and Luciferase did not mediate cell transfection in a calvarial bone lesion model in rats.

The inability of the micelles to mediate an efficient transfection in vivo encouraged us to develop new micelles, easily internalizable by cells. Indeed, an ideal carrier should be nanometer sized and should show, as viruses, a high efficiency to cross cell membranes. Viruses first bind to cell surface proteins, carbohydrates and lipids, leading to activation of cellular signaling pathways. Cells respond by internalizing viruses using one of several endocytic mechanisms. In this context, integrins are involved in the binding of different virus types, among them reo- and adeno-viruses. Fibronectin is an extracellular matrix glycoprotein that binds to different integrins, promoting integrin endocytosis and recycling. Taking advantage from this biological process we sought to develop novel micelles, easily internalizable by cells and with a high capacity to cross cell membranes.

Fluorophore-labeled PEG-PPS (AB) micelles were functionalized with recombinant FNIII9-10/12-14 fibronectin fragment (Figure 2), after which the binding and uptake by different cell types were investigated. When NIH3T3 cells were treated with either functionalized or unfunctionalized micelles a higher internalization of FNIII9-10/12-14-functionalized micelles was observed, thus confirming the potential of integrin targeting to increase micelle uptake. The involvement of endocytotic pathways was demonstrated by the inhibition of uptake at 4°C. Finally, confocal microscopy analysis further confirmed micelle uptake (Figure 3), no toxicity was observed for all the tested micelles.



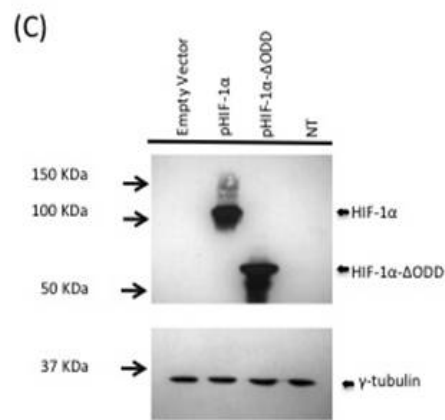
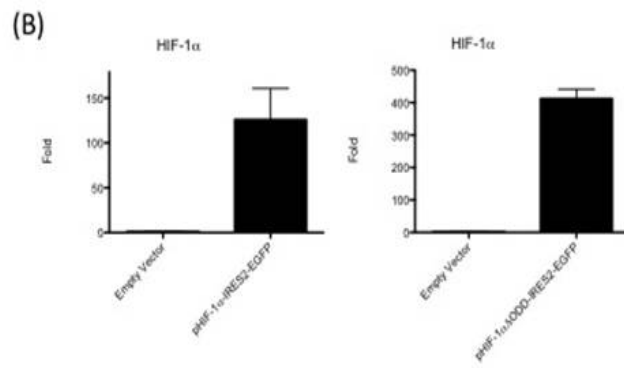


Figure 1: (A) HEK293T cells transfected with pIRES2-EGFP, pHIF-1α-IRES2-EGFP and p HIF-1αΔODD-IRES2-EGFP, fluorescence microscopy analysis. (B) HIF-1α mRNA expression, real time PCR analysis (n=2). (C) HIF-1α expression, western blot analysis.

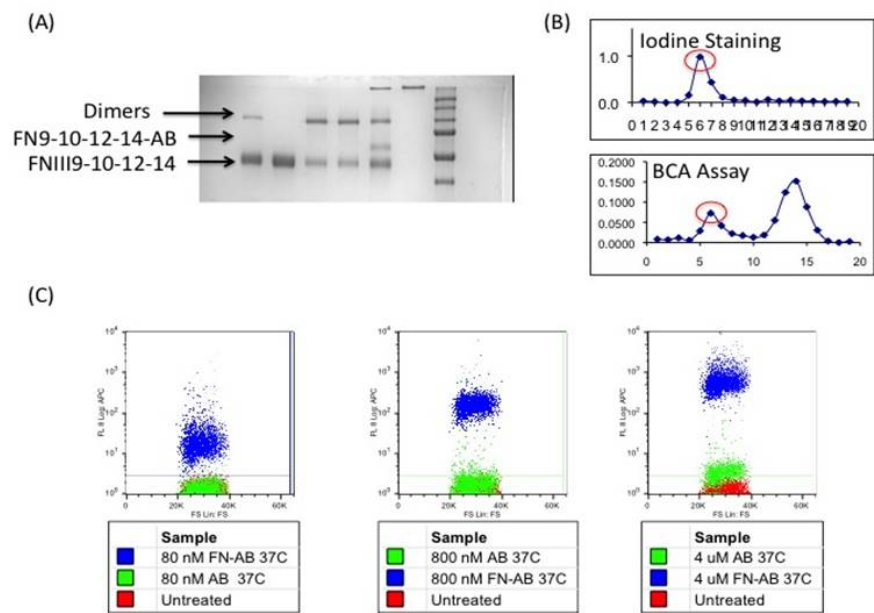
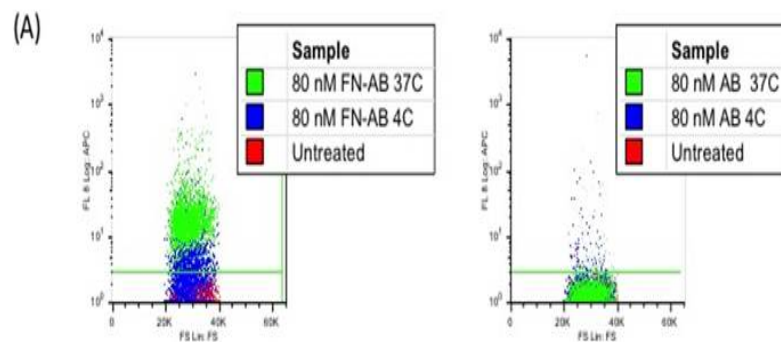
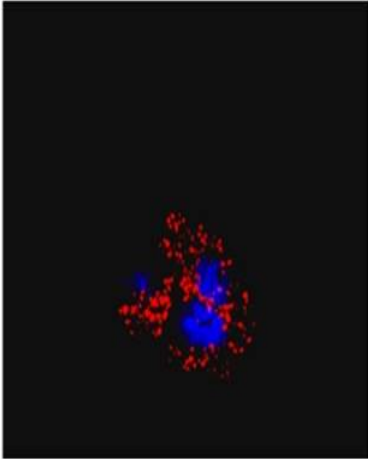
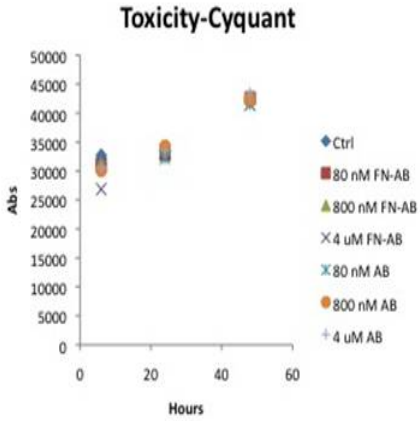


Figure 2: Micelle functionalization with FNIII9-10/12-14 fragment. (A) SDS Page gel. Lane 1: Cys-FN fragment; lane 2: Reduced Cys-FN Fragment; lane 3,4: FN fragment-functionalized PEG-PPS micelles; lane 5,6: PEG-PPS micelles. (B) Size exclusion chromatography, elution profile (BCA assay and Iodine staining). Elution 6 showed a positive staining for both iodine and BCA assays, thus confirming the presence of functionalized micelles. (C) Micelle uptake FACS analysis. NIH3T3 were treated with either Alexa 647-FNIII9-10/12-14-functionalized or Alexa 647-unfunctionalized micelles.



	<div style="display: flex; justify-content: space-around;"> <div style="text-align: center;"> <p>(B)</p>  </div> <div style="text-align: center;"> <p>(C)</p>  </div> </div> <p><i>Figure 3: (A) NIH3T3 were treated at either 37°C or 4°C with Alexa 647-FNIII9-10/12-14-functionalized- or Alexa 647-unfunctionalized-micelles. Uptake was measured by FACS analysis. (B) Confocal microscopy analysis showed uptake in NIH3T3 cells treated with Alexa647-FNIII9-10/12-14-functionalized micelles. (C) No toxicity was observed when NIH3T3 (n>4) were grown in presence of different concentration of either Alexa 647-FNIII9-10/12-14-functionalized- or Alexa 647-unfunctionalized-micelles (Cyquant cell proliferation assay).</i></p>
Publications	None
Patents	None
Other	None
Work to be performed in year 3	Bound genes for morphoregulators and transcription factors for morphoregulators will be de-emphasized in Years 3 and 4, given that work on the bound morphogens themselves has progressed so well. Continuing technology development will only be carried out in the context of the hyaluronic acid gel-based matrices, and in Year 3 this will be at the development level but with validations in bone and cardiac repair.

No.	Title	Lead Scientists	Start Month	End Month
-----	-------	-----------------	-------------	-----------

WP2 has not produced peer-reviewed publications in this period.

We have completed the two tasks according to schedule as outlined in the original proposal and have also completed task 2.3-3, which was not finalised during year 1.

There were no changes to the original proposal with respect to collaborations and staff. However as reported last year in the original DoW we erroneously indicated that Andreas Zisch (now Martin Ehrbar) would be involved in work package 3 for 40 months of effort.

Collaborations within the work package are as follows.

Exchanges of staff
<ul style="list-style-type: none"> Ossipov Group: Prof. Livne group (Technion, Israel) examined the new HA-HP hydrogels in subcutaneous and calvarial mice model
Exchanges of reagents

- Ehrbar lab sent TG-VEGF121 and EMP peptides to Dimmeler lab for pilot experiments
- Hubbel lab sent fibrin gels containing PEG-b-PPS-b-PEI micelles carrying a Luciferase expression plasmid to Livne's lab for implantation and in vivo imaging in rats.
- Hubbells-lab has also made the following material exchanges to:
 - Eschanhagen's lab: Fn 9-10, Fn 9-10/12-14, TGVEGF-165, TG-IGF
 - Cossu's lab: Fn 9-10, Fn 9*-10, Fn 9-10/12-14, Fn 9-10*/12-14, TG-IGF
 - Redl's lab: TG-VEGF165
 - Banfi's lab: TG-VEGF164, TG-aprotinin
 - Dimmeler's lab: FN IIIV, Fn 9-10, Fn 12-14
 - Fawcett's lab: Fn 9-10, Fn 12-14, Fn EDA, Fn 9-10/12-14, TG-aprotinin
 - Miltenyi's lab: Fn 9-10, Fn 9-10/12-14, Fn 9-10/12-14V15
 - Seliktar's lab: Fn 12-14, Fn 9-10/12-14
 - Hilborn's lab: Vs-FN 9*-10
 - Ehrbar's lab: Fn 9-10, Fn 9*-10, Fn 12-14, Fn IIIV, Fn EDA, Fn 9-10/12-14, Fn 9*-10/12-14, Fn 9-10/12-14V15
 - Werner;s lab: Fn 9-10, Fn 9-10/12-14
 - Blanco's lab: TG-aprotinin

Work package number	3	Start date or starting event:					Month 1		
Work package title	Fundamental Characterization: Angiogenesis								
Activity Type	RTD		Workpackage Leader				Melody Swartz		
Participant number	1	6	7	8	9	10	15	16	
Principal Investigator	JAH/MS	CW	AB	ED	SD	ME	HR	PB	
Planned Person-months for whole WP duration	70	0	36	36	36	40	0	0	
Actual Person-months so far	28.65	2.5	33	11	23	12.12	24	2.5	

REPORT OVERVIEW: WP3 – Angiogenesis

3.1 To evaluate the potential of fibronectin fragments and engineered VEGF-laminin fusion protein for therapeutic angiogenesis, we (**JAH**) generated FN fragments containing the FN's cell binding (FN III9-10) with or without the GF binding domain (FN III12-14). Enhanced and prolonged GF receptor phosphorylation was obtained with fibronectin fragments FN III9-10/12-14. The FN fragments also delayed the GF (VEGF-A165 and PDGF-BB) release. When GFs are delivered with FN III9-10/12-14 we detected better wound healing and more granulation tissue in the diabetic mouse model and angiogenesis was drastically improved. Thus FN III9-10/12-14 act in synergy with VEGF-A and PDGF-BB and the synergy is mostly dependant on the integrin $\alpha_5\beta_1$, suggesting that **GFs should be delivered in the presence of integrin ligands, in order to potentiate their signalling**. We are currently testing the effect of fibrin gels containing ephrin-mimetics, TG-VEGF121 (**SD**) or FN fragments (**SD, JAH**) on endothelial differentiation from human bone marrow mesenchymal progenitors in culture systems.

3.2. We (**MS, AZ**) have developed a fibrin-binding TG-VEGF-C with a matrixmetalloproteinase (MMP)-degradable sequence, TG-MMP-VEGF-C, that provides a slow and cell-demanded release. TG-VEGF-C and TG-MMP-VEGF-C improves lymphatic endothelial cell (LEC) proliferation and capillary formation compared with wildtype VEGF-C. In vivo, TG-MMP-VEGF-C drove the most efficient functional lymphatic regeneration in a tail dermal wound healing model. Preliminary studies of coculture of LEC with subtypes of macrophages producing different cytokine profiles suggest that LEC motility is higher in an anti-inflammatory environment.

3.3 We (**ED and JAH**) have designed, cloned and expressed a vascular endothelial (VE)-cadherin chimeric protein that increased ring formation of endothelial cells. The chimeric protein consists of the first 4 extracellular domains of VE-cadherin, fused to the N-terminus of a FC domain, which is itself fused to a TG sequence.

3.4 and 3.5. The threshold between normal and aberrant angiogenesis depends on the balance between VEGF and PDGF-BB signalling. To co-deliver recombinant VEGF and PDGF-BB in a controlled fashion, we (**AB, HR**) are in the process of achieving precise co-localization of VEGF and PDGF-BB gradients by TG binding to fibrin and PEG-TG hydrogel or by encapsulation technology. Modified recombinant VEGF was bound into either fibrin or PEG-TG hydrogels. The degradation rate of fibrin gels in mouse muscle was found to be controlled mainly by fibrinogen concentration, rather than that of cross-linking enzymes. The correlation between hydrogel degree of cross-linking and rate of degradation was biphasic. Moreover, preliminary results show that the *in vivo* degradation of PEG hydrogels, on the other hand, was affected both by PEG-monomer concentration and by chemical modifications that impart different MMP susceptibility. Inflammatory infiltrates responsible for degradation were detected in both fibrin and PEG hydrogels. The kinetics of *in vivo* degradation as a function of the degree of cross-linking are currently being determined by real-time imaging, in collaboration with H. Redl in Vienna.

To validate the Zebrafish as a model to test biomaterials which was developed in year 1, we (**ED**) implanted fibrin gels fragments subcutaneously in *fli:GFP* adult fishes, in which endothelial cells express GFP. Newly formed vessels could be observed within the gel few days post implant and VEGF clearly induced higher levels of angiogenesis. The fluorescent implant was more clearly visible in transgenic Casper fishes that have transparent skin. We have now obtained Casper/*fli:GFP* fishes that combine skin transparency with fluorescent vessels. This powerful model will allow rapid and minimally invasive tests to screen for different biomaterial/morphogen combinations before moving to larger animals.

HR has shown that TG-VEGF121 activated fibrin matrix at low concentrations of VEGF121 (1µg) were most effective in reducing tissue necrosis on day 7 post surgery in the rodent epigastric flap model. In a tube model in the Sprague Dawley rat the fibrin sealant tended to induce greater neovessel formation. Furthermore, preliminary analysis showed also distinct induction of angiogenesis via rhVEGF165 released from a fibrin biomatrix.

3.6 no work was performed on VEGF-Syndecan fusions this year

3.7. We (**CW and SD**) continued the work from the first year with regard to SDF and have developed a new starPEG-heparin hydrogels to deliver SDF-1 in a matrix-bound vehicle to enhance recruitment of endothelial progenitor cells (EPCs) and to aid in the neovascularization of the injured myocardium. After characterization of the new biomimetic material, we found that SDF-1 enhanced EPC migration by the hydrogels in a dose-dependent manner. Increased cell infiltration, vessel formation and matrix remodelling were detected in vivo too. Degradation of the starPEG-heparin hydrogels matrix established a SDF-1 gradient and further enhanced angiogenesis and cellularity.

Beneath we tabulate the progress towards our original objectives with details for each project that has been initiated & highlighting significant results:

3.1	BVP's related to fibronectin fragments			
Checkpoint	3.1	JAH	6	24
Deliverable	D3.1-1. Role of $\alpha v\beta 3$ vs. $\alpha 5\beta 1$ in angiogenesis \pm VEGF D3.1-2. Role of $\alpha v\beta 3$ vs. $\alpha 5\beta 1$ in endothelial progenitor cell differentiation D3.4-3 Influence of matrix bound vs. free VEGF in endothelial progenitor cell differentiation			
Task update	<p>Growth factors (GFs) are widely used in regenerative medicine and tissue engineering with various successes. Indeed, GFs are rapidly cleared and degraded in vivo. Consequently, in order to improve the overall regenerative efficiency of GFs, systems that control their release from hydrogels, have been developed. Many of these systems are inspired from the natural interactions that exist between GFs and the extracellular matrix (ECM), since in fact, ECM binds and release GFs. However, the ECM/GF interactions do not serve only for the sequestration and release of GFs. For example, ECM can directly modulate GFs signaling through integrins. For instance, joint integrin/GF-receptor signaling can be generated by the formation of GF-receptors/integrins clusters that are mediated by specific complexes between ECM proteins and GFs. Recently, we found that the second heparin binding domain of FN, FN III12-14, acts as a promiscuous GF binding site and could serve as a generic approach to deliver GFs from hydrogels. For example, GFs from the VEGF/PDGF, and FGF families showed strong affinity to FN III12-14. The reasons for such promiscuous binding capacity are still unclear, but evidences suggest that the close proximity of the major cell-binding domain of FN, FN III9-10, allows strong crosstalk between GFs and integrins. Therefore, we hypothesized that GF-induced tissue repair and regeneration would be enhanced, when GFs are delivered within a well defined integrin microenvironment. Accordingly, we generated FN fragments containing the FN's cell binding (FN III9-10) with or without the GF binding domain (FN III12-14). The fragments were engineered to be covalently crosslinked into fibrin, a clinically relevant and widely used matrix in regenerative medicine for GFs delivery. Using VEGF-A165 and PDGF-BB as GFs models, in vitro analysis showed that only, FN III9-10/12-14, the fragment containing both the cell binding and GF binding domains allows synergistic signals between GF-receptors and the integrins $\alpha 5\beta 1$ and $\alpha v\beta 3$. In vivo, while using really low dose of VEGF-A165 and PDGF-BB, we found that cutaneous wound healing and angiogenesis, in diabetic mice were greatly improved, when the GFs were delivered using fibrin matrices functionalized with FN III9-10/12-14. As a second in vivo model, we used epigastric flap in rat. In this model, a clear trend to less</p>			

necrosis is observed in the group treated with fibrin containing VEGF-A165, PDGF-BB and III9-10/12-14. However, more animals should be added in this study, in order to achieve a powerful statistical analysis.

We designed fusion protein containing VEGF121 and an angiogenic laminin peptide. Expression of VEGF-laminin, control proteins and preliminary experiments were performed within WP2 morphogen development project. In vitro biological activity of the engineered protein in 3D fibrin environment was confirmed by using a flow chamber model developed in Swartz lab. In vivo evaluation is ongoing.

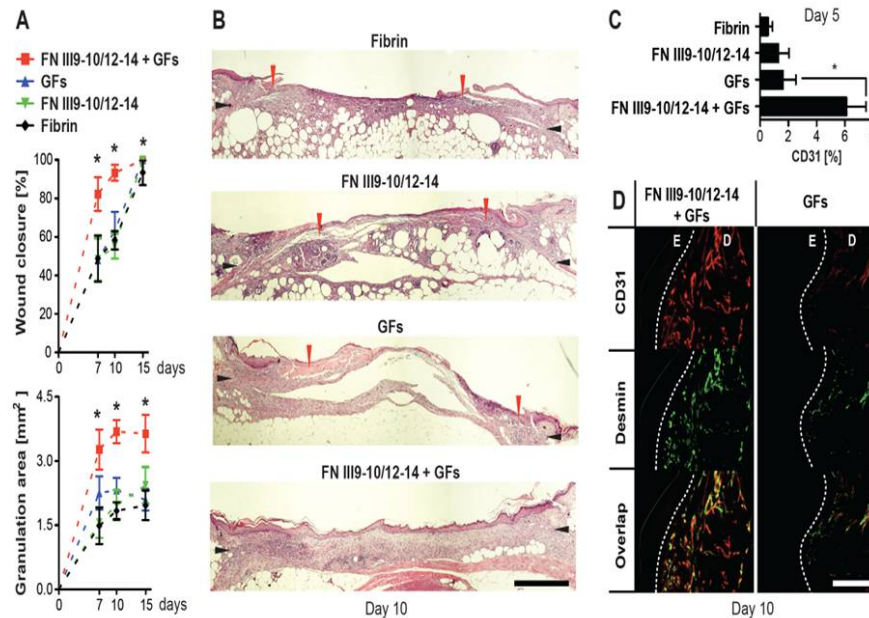


Figure 1. Delivering low dose of GFs, using FN III9-10/12-14 enhances wound healing and angiogenesis. After wounding, wounds were filled with fibrin matrices functionalized with or without FN III9-10/12-14 and GFs (VEGF-165 and PDGF-BB). **A)** Wound closure and granulation tissue area measurements. After 7, 10 and 15 days, wound closure and granulation tissue area were measured based on histology. Determined by the formation of a new epithelium, only the wounds where GFs have been delivered using FN III9-10/12-14 are significantly closed more rapidly (student t-test, * $p < 0.05$, $n = 7$). Similarly, only the wounds where GFs have been delivered, using FN III9-10/12-14 contained significantly more granulation tissue, compared to fibrin only (* $p < 0.05$, Student's t test, $n = 7$). **B)** Representative histology of wounds at day 10. Black arrows indicate the wound edges, while red arrows indicate the end of the new epithelium (haematoxylin and eosin staining, scale bar = 1mm). **C)** Recruitment of endothelial cells within the wounds. After 5 days, wound tissues were extracted and digested, in order to recover cells. The percentage of endothelial cells (CD31+) was determined by flow cytometry. Much more endothelial cells could be recruited, when GFs were delivered with FN III9-10/12-14 (* $p < 0.05$, Student's t test, $n = 6$). **D)** Angiogenesis within granulation tissue. Wound tissues were stained at day 10 for endothelial cells (CD31) and smooth muscle cells (desmin). More blood vessels can be formed within granulation tissue, when GFs were delivered with FN III9-10/12-14. Representative pictures are shown (E = epidermis, D = dermis, scale bar = 0.2mm).

We also investigated the effects of distinct integrin-specific 3-dimensional biomaterials on the endothelial differentiation / functionality of progenitor cells. Specifically, the improvisational extracellular matrix protein fibronectin contains in the FN III9-10 fragment binding sites for the $\alpha 5 \beta 1$ -integrin (PHSRN and RGD sequence) and in the fragments FN III12-14 and FN III V (CS1-peptide) binding sites specific for the $\alpha 4 \beta 1$ -integrin. Therefore, we investigated the effects of fibrin gels containing the fibronectin fragments FN III9-10, FN III12-14 and FN III V on the endothelial gene expression of human mesenchymal stem cells (MSC) growing in the presence of VEGF165 (100

ng/ml) in comparison to MSC growing in 2-dimensional culture (n=7 for each condition). Specifically, we assessed with real time PCR the expression of KDR, VE-Cadherin and endothelial NO-synthase (eNOS) after 5 days of culture. MSC growing in fibrin gels containing the fibronectin fragments FN III9-10, FN III12-14 or FN III V did not display significant differences in the expression of KDR and VE-Cadherin in comparison to MSC growing in gels containing only fibrin or in comparison to MSC growing in 2-dimensional culture. Interestingly, gels containing the $\alpha 5\beta 1$ -integrin-binding fragment FN III9-10 led to an increased expression of eNOS, while gels containing the fragment FN III 12-14 led to a significantly reduced expression of eNOS in MSC in comparison to gels containing only fibrin. However, in all conditions MSC displayed an overall very low expression of eNOS, VE-Cadherin and KDR in comparison to mature endothelial cells (HUVEC). In ongoing studies we are investigating the effects of long term (14 d) culture of MSC in fibrin gels containing the above mentioned fibronectin fragments on the expression of endothelial genes. Moreover, we are also assessing the effects of fibronectin fragments on the expression of endothelial genes in early outgrowth endothelial progenitor cells (myeloid EPC) in a short term and long term 3-dimensional culture. Since progenitor cells are also contributing to angiogenesis in a paracrine manner, we additionally plan to assess the effects of fibrin gels containing the above mentioned fibronectin fragments on the expression of angiogenic growth factors in MSC and early outgrowth EPC.

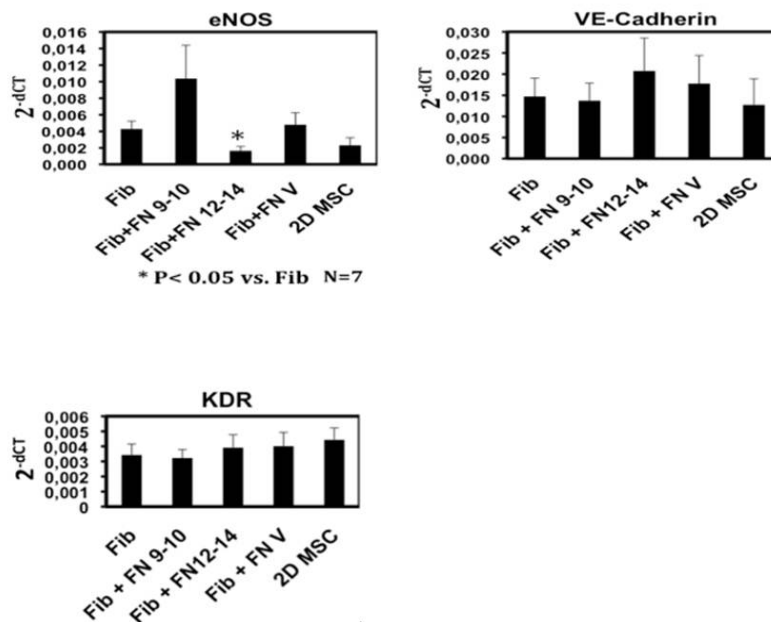


Figure 2. Effect of distinct integrin-specific 3-dimensional biomaterials on the endothelial differentiation / functionality of progenitor cells.

Publications	Martino M.M, Hubbell J.A. The 12th-14th type III repeats of fibronectin function as a highly promiscuous growth factor-binding domain. <i>FASEB J.</i> 2010 Aug 4. Chavakis E, Koyanagi M, Dimmeler S. Enhancing the outcome of cell therapy for cardiac repair: progress from bench to bedside and back. <i>Circulation.</i> 2010 Jan 19;121(2):325-35. Chavakis E, Dimmeler S. Homing of Progenitor Cells to Ischemic Tissues. <i>Antioxid Redox Signal.</i> 2010 Sep 2.
Patents	None
Other	None
Work to be performed in year 3	With regard to modulation of angiogenesis induced by VEGF-A in the presence of the fibronectin fragments, this work will continue to the status of publication of results. With regard to presentation of growth factors in the context of EPC proliferation and differentiation, in Year 3 the consortium will investigate the potential activity of the

	fibronectin fragments in modulating the release or activity of SDF-1a, which is the main morphogen for recruitment of EPCs to sites of tissue injury, in addition to other stem cells; and will continue in validating the effects of matrix-bound integrins with VEGF-A or other morphogens in EPC proliferation and/or differentiation. For these factors, both angiogenesis (<i>per se</i>) validation and angiogenesis (in clinical indications, such as skin repair) will be pursued in Year 3.
--	--

No.	Title	Lead Scientists	Start Month	End Month
3.2	BVP's related to ephrins			
Checkpoint	3.1	SD	12	24
Deliverables	D3.2-1. Role of EphB4, EphA2, EphB2 in angiogenesis ± VEGF D3.2-2. Role of EphB4, EphA2, EphB2 in endothelial progenitor cell differentiation ± VEGF			
Task update	<p>Progenitor and stem cells mobilized from the bone marrow or systemically administered to patients with ischemic disorders are recruited to ischemic tissues and contribute to tissue neovascularization and regeneration. Cell therapy has emerged as a promising option to treat myocardial infarction or heart failure. However, clinical studies demonstrated only a modest effect of progenitor cells on left ventricular function after myocardial infarction. In line with this fact, only a small fraction of administered progenitor cells homed and are remaining in the ischemic tissues. In addition, adult progenitor and stem cells display only a restricted potential to differentiate to endothelial cells and to other cell types. Therefore, there is a need for the development of new approaches, in order to improve differentiation potential and functional capacity of progenitor/stem cells. VEGF/VEGF-receptor- and Ephrin/Ephrin-receptor- signaling were shown to affect endothelial differentiation and fate of progenitor/stem cells. The aim of the task is to investigate the effects of distinct 3-dimensional biomaterials containing ephrin-mimetics or TG-VEGF121 on the endothelial differentiation/functionality of progenitor cells. Synthetic peptides acting as ephrin-mimetics and TG-VEGF121 were developed from the group of Andreas Zisch. The YSA-peptide acts as ephrin A1-mimetic activating EphA2 receptor, the SNEW-peptide acts as an ephrin B1-mimetic activating the EphB2 receptor and the TNYL-RAW- peptide acts as an ephrin B2-mimetic activating EphB4.</p> <p>In order to assess the effects of ephrin-mimetics and TG-VEGF121 on endothelial differentiation, human mesenchymal stem cells (MSC) derived from the bone marrow were grown in fibrin gels containing 5 µM YSA-peptide (ephrin A1-mimetic), 5 µM SNEW-peptide (ephrin B1-mimetic), 5 µM TNYL-RAW- peptide (ephrin B2-mimetic), 1000 ng/ml TG-VEGF121 and where indicated soluble VEGF 165 for 5 days in comparison to MSC growing in 2-dimensional culture (n=3 for each condition). RNA was isolated from the gels and real time PCR was performed, in order to assess the expression of endothelial genes such as KDR (VEGFR2), VE-Cadherin and endothelial NO-synthase (eNOS). 3-dimensional culture of MSC led to an increased (albeit not significant) expression of the KDR, VE-Cadherin in comparison to MSC growing in 2-dimensional culture. However, gels containing the YSA-peptide, the SNEW-peptide, the TNYL-RAW- peptide or the TG-VEGF121 or external stimulation with soluble VEGF165 did not further enhance the expression of KDR, VE-Cadherin and eNOS in MSC in comparison to MSC growing in control fibrin gels (without any stimulation). In all conditions MSC displayed an overall very low expression of eNOS, VE-Cadherin and KDR in comparison to mature endothelial cells (HUVEC). Taken together, the YSA-peptide, SNEW-peptide, TNYL-RAW-peptide and the TG-VEGF121 under these conditions did not regulate endothelial marker gene expression in MSC. In ongoing studies we are investigating the effects of long term (14 d) culture of MSC in fibrin gels containing higher concentrations (25 µM) of the above mentioned ephrin-</p>			

mimetics or TG-VEGF121 on the expression of endothelial genes. Moreover, we are also assessing the effects of ephrin-mimetics and of VEGF121 on the expression of endothelial genes in early outgrowth endothelial progenitor cells (myeloid EPC) or mixed cultures (EPC and MSCs) in short term and long term culture. Since progenitor cells are also contributing to angiogenesis in a paracrine manner, we additionally plan to assess the effects of fibrin gels containing the above mentioned ephrin-mimetics or TG-VEGF121 on the expression of angiogenic growth factors in MSC and early outgrowth EPC.

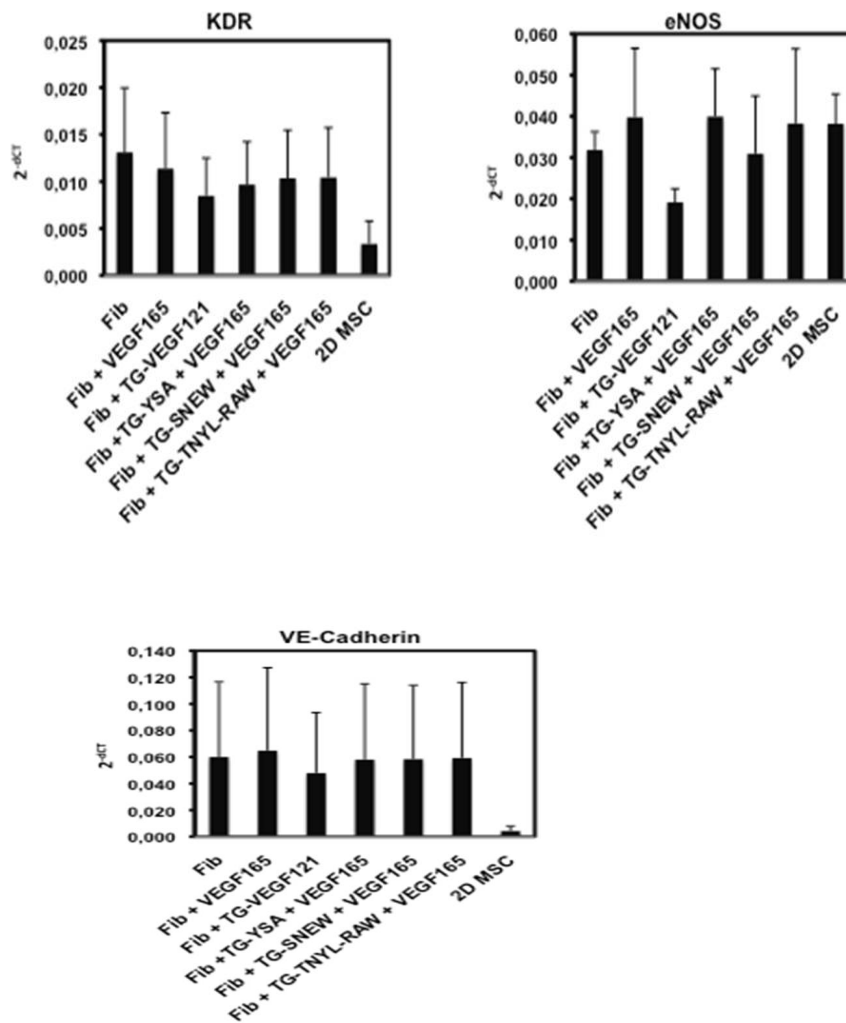
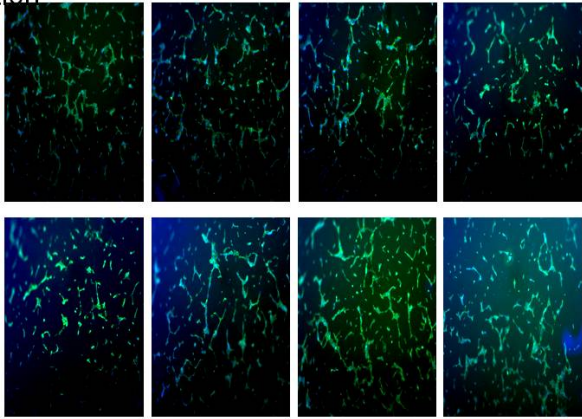


Figure 1: Effect of ephrin-mimetics and TG-VEGF121 on endothelial differentiation (n=3 for each culture condition)

Publications	<ul style="list-style-type: none"> • Chavakis E, Koyanagi M, Dimmeler S. Enhancing the outcome of cell therapy for cardiac repair: progress from bench to bedside and back. <i>Circulation</i>. 2010 Jan 19;121(2):325-35. • Chavakis E, Dimmeler S. Homing of Progenitor Cells to Ischemic Tissues. <i>Antioxid Redox Signal</i>. 2010 Sep 2.
Patents	None
Other	None
Work to be performed in year 3	Based on the work in development of the novel ephrin class of morphogens in regenerative medicine, the consortium will continue in validation of the morphogen in angiogenesis assays both alone within fibrin and in combination with fibrin-bound VEGF-A. The results of these angiogenesis validations will be used to guide further validation studies with this new morphogen and morphogen combinations in angiogenesis validation models in Year 3, with subsequent translation to other tissue

	repair validation models.
--	---------------------------

No.	Title	Lead Scientists	Start Month	End Month
3.3	BVP's related to cadherins			
Checkpoint	3.1	ED, JAH	24	48
Deliverable	None in this reporting period			
Task update	<p>After expression and purification of the VE-cadherin fusion protein, the tube formation of endothelial cells were studied within fibrin matrixes containing the VE-cadherin construct. A slight increase in ring formation of endothelial cells were observed with a moderate concentration of VE-cadherin FC-tg fusion.</p> <p>VE cadherin concentration 0 nM 0.2 nM 2 nM 20 nM</p>  <p>Figure 1: HUVEC cells seeded within a fibrin matrix with varying amounts of VE-cadherin FC-tg and media supplemented with VEGF. After 72 hours of incubation the endothelial cells began to form ring like structures within in the 3D matrix with moderate levels of VE cadherin.</p>			
Publications	None			
Patents	None			
Other	The work was presented at the TOPEA meeting in Barcelona during the summer of 2010.			
Work to be performed in year 3	The protein engineering challenge in developing the VE cadherin morphogen was substantial, but this is now complete. Results will be published, however, only with validation results in angiogenesis. It is not known a priori whether the VE cadherin will promote angiogenesis, or whether it will alter the quality of angiogenesis by inducing a more morphologically mature angiogenic response. These differences will be the main sought-after characteristics in the validation experiments in angiogenesis.			

No.	Title	Lead Scientists	Start Month	End Month
-----	-------	-----------------	-------------	-----------

3.4	BVP's related to VEGF-A																															
Checkpoint	N/A	AB, HR	6	36																												
Deliverable	D3.4-1. Dose response behavior of matrix bound VEGF																															
Task update	<p>Local delivery of vascular endothelial growth factor (VEGF) is an attractive approach for therapeutic angiogenesis in ischemic diseases. Using a highly controlled cell-based platform for in vivo gene delivery we have previously established that, in order to induce normal and stable angiogenesis, it is necessary to deliver VEGF at controlled and homogeneous levels in the microenvironment, and for at least 4 weeks. Local delivery of growth factors via biodegradable matrices is a convenient and fully customizable approach to translate this biological concept into a clinical application. Therefore, here we aim to induce normal and stable angiogenesis by controlled delivery of VEGF from a state-of-the art matrix-bound system, based on transglutaminase (TG) reaction to bind the modified recombinant factor into either fibrin or PEG-TG hydrogels. These could afford different and complementary profiles of degradation time, persistence <i>in vivo</i> and release rate of the morphogen. Since fibrin gels polymerize very rapidly, we determined the range of matrix components concentrations (fibrinogen, thrombin and Factor XIII) to allow hydrogel injection while still liquid. The upper limits, to ensure a polymerization time > 15s, were 25 mg/ml for fibrinogen, 4 U/ml for thrombin and 5 U/ml for Factor XIII. Furthermore, fibrinogen concentration had the greatest influence on decreasing the polymerization time. Next, in order to define how hydrogel composition controls the duration of release, we evaluated the degradation rate of different matrix compositions, within the above-defined limits, in mouse muscle tissue. We found that the <i>in vivo</i> degradation rate of fibrin gels is controlled mainly by fibrinogen concentration, rather than that of cross-linking enzymes. In fact, gels were still detectable after 9 days when fibrinogen was high and enzymes low, whereas the opposite combinations were already degraded after 4 days. In order to determine the correlation between hydrogel degree of cross-linking and rate of degradation, gels were prepared with the highest fibrinogen concentration (25 mg/ml) while varying the amount of cross-linking enzymes (Table 1). Surprisingly, the <i>in vivo</i> correlation was not linear, but biphasic. In fact, increasing the amount of cross-linking enzymes led to an initial decrease in degradation rate, followed by an unexpected increase, rather than further decrease or stabilization, so that gels with the highest concentration of enzymes were degraded as fast as gels with the lowest (Fig. 1).</p> <table border="1" data-bbox="363 1406 1046 1662"> <thead> <tr> <th>Conditions</th> <th>Fibrinogen (mg/ml)</th> <th>Factor XIII (U/ml)</th> <th>Thrombin (U/ml)</th> </tr> </thead> <tbody> <tr> <td>1</td> <td>25</td> <td>1</td> <td>2</td> </tr> <tr> <td>2</td> <td>25</td> <td>1</td> <td>4</td> </tr> <tr> <td>3</td> <td>25</td> <td>2</td> <td>2</td> </tr> <tr> <td>4</td> <td>25</td> <td>2</td> <td>4</td> </tr> <tr> <td>5</td> <td>25</td> <td>5</td> <td>2</td> </tr> <tr> <td>6</td> <td>25</td> <td>5</td> <td>4</td> </tr> </tbody> </table> <p>Table 1. Fibrin gel compositions used to study the relationship between degree of crosslinking and gel persistence <i>in vivo</i>.</p>				Conditions	Fibrinogen (mg/ml)	Factor XIII (U/ml)	Thrombin (U/ml)	1	25	1	2	2	25	1	4	3	25	2	2	4	25	2	4	5	25	5	2	6	25	5	4
Conditions	Fibrinogen (mg/ml)	Factor XIII (U/ml)	Thrombin (U/ml)																													
1	25	1	2																													
2	25	1	4																													
3	25	2	2																													
4	25	2	4																													
5	25	5	2																													
6	25	5	4																													

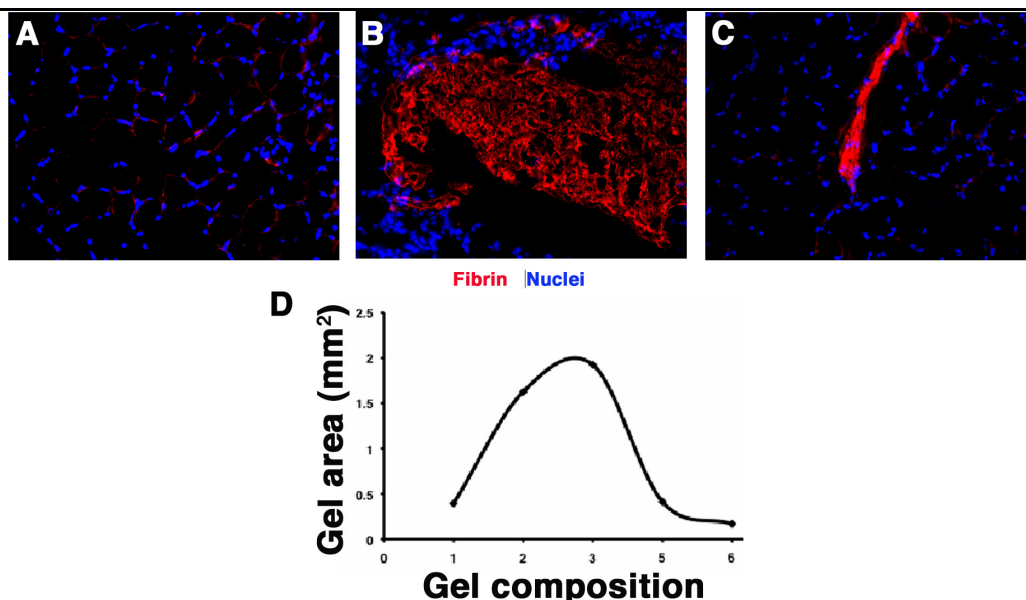


Figure 1. Quantification of *in vivo* fibrin hydrogel persistence. Gels were prepared with the compositions shown in Table 1 and were injected in the Gastrocnemius muscles of immunodeficient SCID mice to avoid reactions to the human fibrin and enzymes ($n=3/\text{condition}$). Tissues were harvested 4 and 9 days after injection, fresh-frozen and cryosections were immunostained with a monoclonal antibody specifically recognizing human fibrin, but not non-polymerized fibrinogen. (A-C) Representative immunofluorescence staining of uninjected muscle (A), or tissue injected with hydrogel composition 2 (25 mg/ml fibrinogen, 1 U/ml Factor XIII and 4 U/ml Thrombin) 4 days (B) and 9 days (C) after injection. Fibrin is shown in red and nuclei in blue. (D) Quantification of the total gel area remaining 4 days after injection of hydrogels made with the different compositions indicated in Table 1. Quantification was performed on similar images as those shown in panels A-C.

The kinetics of *in vivo* degradation as a function of the degree of cross-linking is currently being determined by non-invasive real-time imaging, in collaboration with H. Redl in Vienna. To investigate the mechanism of this biphasic degradation behaviour, experiments are also currently ongoing with an *in vitro* macrophage degradation assay, to test the hypothesis that increasing gel stiffness above a threshold can biologically activate macrophages.

Preliminary results show that the *in vivo* degradation of PEG hydrogels, on the other hand, was affected both by PEG-monomer concentration and by chemical modifications that impart different MMP susceptibility (Table 2 and Fig. 2). MMP-resistant hydrogels were practically undegraded both 4 and 9 days after injection and will not be useful to achieve a significant release of angiogenic factors. Therefore, the next experiments will focus on the MMP-sensitive chemistry and will investigate the persistence of PEG compositions designed to achieve 3 different stiffness values: 250, 500 and 1000 KPa. Persistence will be quantified on cryosections of injected muscles similarly to the fibrin hydrogels shown in Figure 1. H&E staining showed in both fibrin and PEG hydrogels a massive inflammatory infiltrate that is responsible for their gradual degradation. The quantity and cellular make-up of this infiltrate in the different gel compositions are currently being determined by immunofluorescent staining.

Condition	1	2	3	4
Degradability	MMP-resistant	MMP-sensitive	MMP-resistant	MMP-sensitive
Stiffness	1000Pa (Stiff)	1000Pa (Stiff)	500Pa (Soft)	500Pa (Soft)
PEG concentration	2.41%	2.41%	1.95%	1.95%

Table 2. PEG gel compositions used to study the relationship between stiffness and MMP-susceptibility and gel persistence *in vivo*.

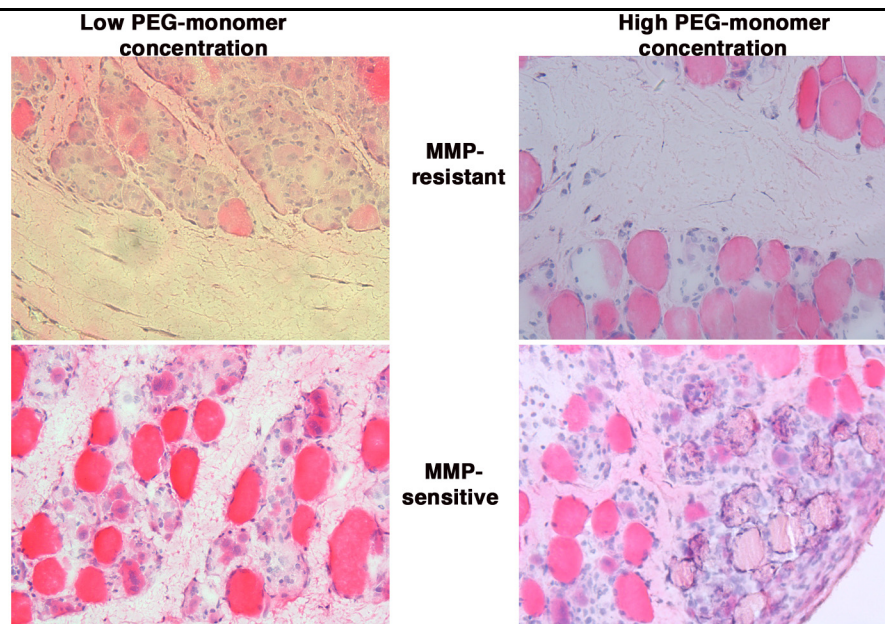


Fig.3 In vivo persistence of PEG-TG hydrogels of different composition. Gels were prepared with the compositions shown in Table 2 and were injected in the Gastrocnemius muscle of immunodeficient SCID mice ($n=2/\text{condition}$). Tissues were harvested 4 days after injection, fresh-frozen and cryosections were stained with Hematoxylin and Eosin.

In the second part of the project, the gel compositions ensuring the slowest degradation rate will be loaded with recombinant TG-VEGF, to determine the therapeutic window of TG-VEGF. Vascular perfusion and morphology will be studied by intravascular lectin injection and by immunofluorescent staining of frozen sections as well as by SLS micro-CT of tissue corrosion casts. Based on these results, selected conditions will be tested in a functional ischemia model (epigastric flap) with 2D Doppler imaging of blood flow.

Additionally using the specific binding technology with the TG-hook, we (**HR**) bound VEGF121 to the fibrin biomatrix and tested in an ischemic flap model. A standard rodent epigastric flap model was used. Recipient sites were treated either with sprayed fibrin sealant (FS) alone or in combination with VEGF121. For the later, VEGF121 in two different concentrations (1 and 10 μg) was simply added to the FS (FS/rhVEGF121) or the specific binding technology was used (FS/TG-rhVEGF121). Development of necrotic flap tissue was documented by digital photography over a 1 week period and quantified using planimetric analysis. Flap perfusion was measured using 2D laser Doppler imaging. To show treatment induced angiogenic response von Willebrand factor (vWF) and smooth muscle actin (sma) protein expression was determined by means of immunohistochemistry.

The preliminary results showed that the low concentrations of VEGF121 (1 μg) were most effective in reducing tissue necrosis on day 7 post surgery regardless of whether the TG-hook technology was used or not, although no statistical significant differences were detected with current numbers of experiments/group compared to the control group. Immunohistochemical as well as perfusion analysis are currently performed.

VEGF121 seems to have a positive effect on reducing necrotic tissue in this model. Low concentrations are performing better than higher concentrations. The TG-hook binding technology in this model with the current number of experiments was not able to further decrease necrosis. Further experiments have to be performed to get statistical relevant data sets.

As part of this work it became evident that relevant screening tools were absent for the assessment of the angiogenic effect of the materials+bioactives. We

therefore implemented experiments to develop tools which would permit us both quickly and cost effectively to measure the effect of the materials.

Zebra fish has been previously assessed as an excellent tool to study angiogenesis during larvae development as well as in the adulthood (1,2). Upon external fertilization Zebra fish eggs develop rapidly (24-48 hours) into transparent larvae. Transgenic fish models (fli:GFP) are available where endothelial cells express GFP protein under an endothelial specific promoter allowing the analysis of vascular development in the larvae or, with some limitations, in the adult fish.

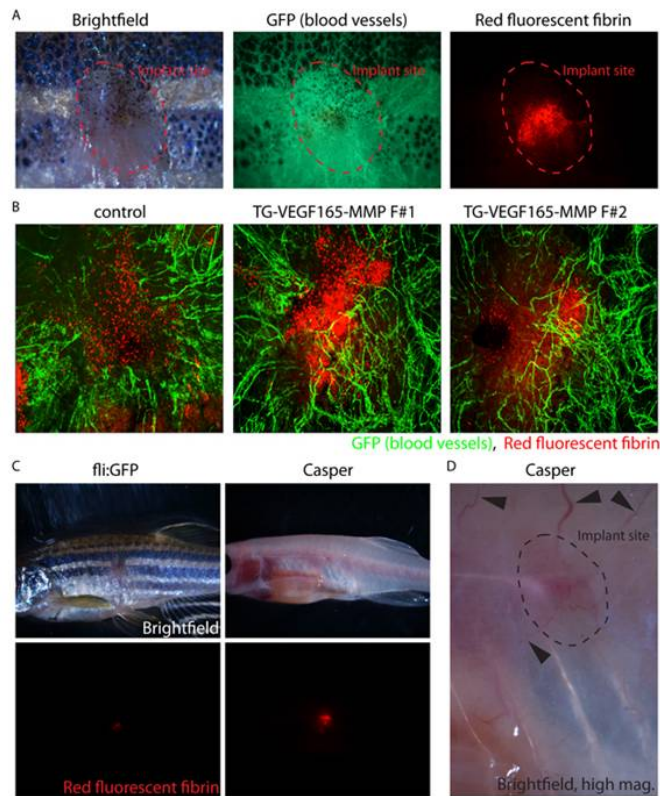


Figure 2. A) Typical subcutaneous implant 7 days after implantation in fli:GFP fishes. Skin has been completely regenerated, but pigmentation is still incomplete in the implant site and scales have not yet been regenerated. In central and left panels, fluorescent vessels and fluorescent implant are partially visible through the skin. B) Confocal stacks of control fibrin gel (left panel) and two tg-VEGF165-MMP/fibrin gel implanted fli:GFP fishes (central and right panel). Angiogenesis toward and within the gel (red) can be

observed (in green, GFP positive vessels); the presence of VEGF into the gel induces higher levels of angiogenesis compared to control. C) Example of implant in fli:GFP (left panels) and Casper (right panels) fishes. Bottom panels are intended to show the intensity of fluorescence passing through the skin of Casper transparent fishes (bottom-right) in comparison to fli:GFP (bottom-left); image has been acquired with equal magnification and exposure time. D) Higher magnification of the implant shown in panel C for Casper fish. The red fragment of fibrin gel, as well as blood vessels (arrowhead), is clearly visible through the skin in brightfield microscopy.

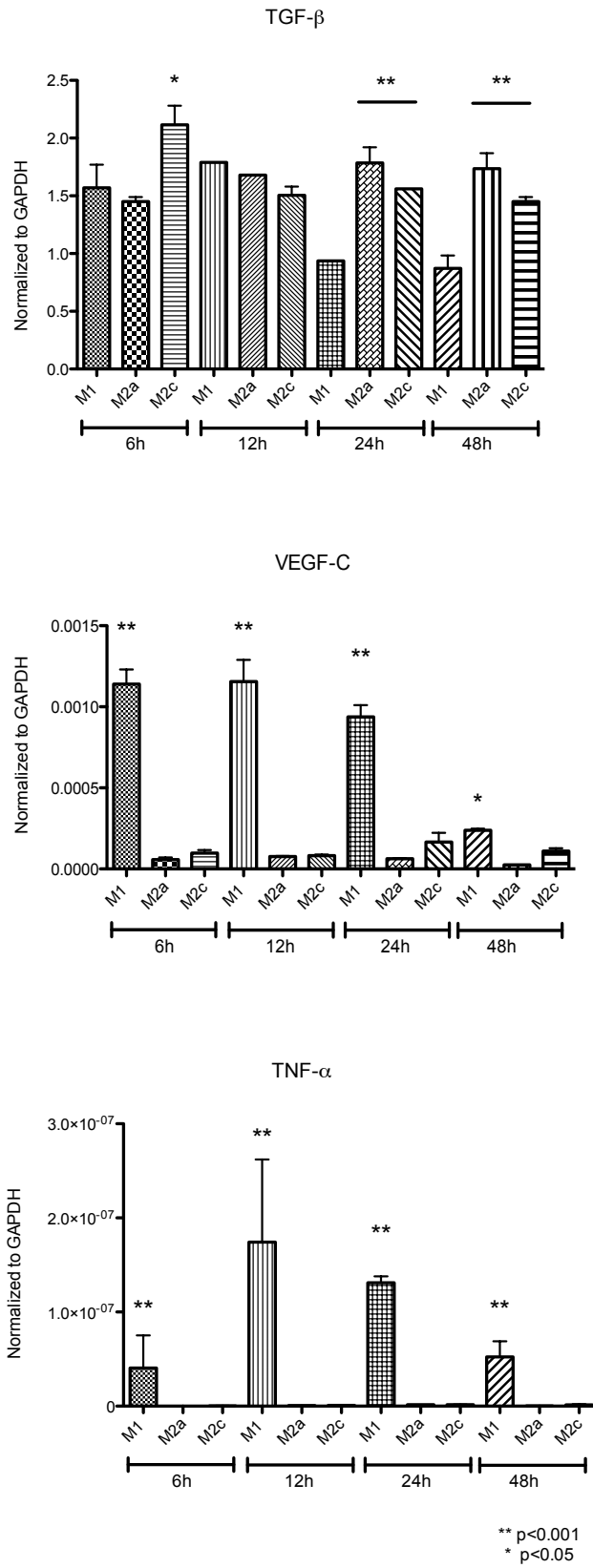
Tg-VEGF165-MMP: engineered form of VEGF165 capable to bind fibrin gels to TG fragment, but also to be cleaved out from the gel through the action of matrix-metalloproteases.

We (ED) developed a protocol to surgically implant fibrin gel fragments in fli:GFP adult fishes: after scales removal the gel fragment can be implanted subcutaneously (fig 2A). Observation of newly formed vessels within the gel can be observed few days post implant (fig 2B). In the experiment shown in figure 2B, fibrin gels with (right) or without (left) VEGF were implanted. VEGF clearly induces higher levels of angiogenesis around and within the fluorescent (red) gel compared to wild type, however opacity and pigmentation of the skin dramatically reduced the quality of the analysis. To overcome this intrinsic limit of the system, we took advantage of *nacre* and *roy* double transgenic fishes (Casper) that present transparent skin (2). The characteristic adult pigmentation pattern of the zebrafish consists of three distinct classes of pigment cells arranged in stripes: black melanophores, reflective iridophores, and yellow xanthophores (3). The *nacre* mutant (*nacre* $-/-$) has a complete lack of melanocytes while the spontaneous *roy*

	<p><i>orbison</i> (<i>roy</i> <i>-/-</i>) mutant has a complete lack of iridophores, uniformly pigmented eyes, sparse melanocytes, and a translucency of the skin. Casper fishes demonstrate a complete lack of all melanocytes and iridophores in both embryogenesis and adulthood (2). Therefore, we performed an implantation test on this fishes (fig 2C) and the results are promising; the fluorescent implant is much clearly visible through the transparent skin of Casper fish in comparison to <i>fli</i>:GFP even at low magnification. Interestingly, at higher magnification, the gel fragment implanted is already visible through the skin in brightfield (fig 2D). Casper fishes were breed with <i>fli</i>:GFP to obtain transparent adult fishes with fluorescent vessels. This breeding will generate different genetic combinations. Among the other, triple mutant <i>nacre</i> <i>-/-</i>, <i>roy</i> <i>-/-</i>, <i>fli</i>:GFP (Casper/<i>fli</i>) fishes are the most interesting. We already obtained this fish line and we are now expanding colony to have enough fishes for the experiments. In conclusion we are developing an <i>in vivo</i> assay, which will allow a rapid and minimally invasive test to screen for different biomaterial/morphogen combinations before moving to larger animals.</p> <p>As an extension of this development (HR) aimed to develop a validated rodent model to study angiogenesis induced by various growth factors which are delivered locally from different biomatrices. In the inguinal region of Sprague Dawley rats longitudinal incisions were made after depilation.</p> <p>Preliminary immunohistological analysis (vWF, sma) showed distinct induction of angiogenesis via rhVEGF165 at 200ng released from a fibrin biomatrix. Currently, analyses are conducted of 50 implanted tubes.</p>
<p>Publications</p>	<p>Misteli H., Wolff T., Füglistaler P., Gianni-Barrera R., Gürke L., Heberer M. and Banfi A. High-throughput FACS purification of transduced progenitors expressing defined VEGF levels induces controlled angiogenesis in vivo. <i>Stem Cells</i> 28: 611-619 (2010).</p> <p>Dejana E, Simons M, Ratcliffe P, Maxwell P, Carmeliet P. The role of wnt signaling in physiological and pathological angiogenesis. <i>Circ Res.</i> 2010 Oct 15;107(8):943-52. IF: 9,99</p> <p>Hermans K, Claes F, Vandeveldel W, Zheng W, Geudens I, Orsenigo F, De Smet F, Gjini E, Anthonis K, Ren B, Kerjaschki D, Autiero M, Ny A, Simons M, Dewerchin M, Schulte-Merker S, Dejana E, Alitalo K, Carmeliet P. Role of synectin in lymphatic development in zebrafish and frogs. <i>Blood</i> 2010 Oct 28;116(17):3356-66. IF: 10,43</p> <p>Corada M, Nyqvist D, Orsenigo F, Caprini A, Giampietro C, Taketo MM, Iruela-Arispe ML, Adams RH, Dejana E. The Wnt/beta-catenin pathway modulates vascular remodeling and specification by upregulating Dll4/Notch signaling. <i>Dev Cell.</i> 2010 Jun 15;18(6):938-49. IF: 12,88</p> <p>Lampugnani MG, Orsenigo F, Rudini N, Maddaluno L, Boulday G, Chapon F, Dejana E.CCM1 regulates vascular-lumen organization by inducing endothelial polarity. <i>J Cell Sci</i> 2010 Apr 1;123(Pt 7):1073-80. IF:6,25</p> <p>Murakami M, Francavilla C, Torselli I, Corada M, Maddaluno L, Sica A, Matteoli G, Iliev ID, Mantovani A, Rescigno M, Cavallaro U, Dejana E. Inactivation of junctional adhesion molecule-A enhances antitumoral immune response by promoting dendritic cell and T lymphocyte infiltration. <i>Cancer Res.</i> 2010 Mar 1;70(5):1759-65. IF:7,51</p>
<p>Patents</p>	<p>None</p>
<p>Other</p>	<p>None</p>
<p>Work to be performed in year 3</p>	<p>Although work with VEGF-A is now mature, work will continue in validation projects in angiogenesis and in skin healing on effects and dose-responsiveness with VEGF-A in fibrin and in the PEG hydrogels n angiogenesis validations. Work on valudation of new angiogenesis models will continue.</p>

No.	Title	Lead Scientists	Start Month	End Month
3.4 and 3.5	BVP's related to VEGF-A BVP's related to VEGF-C			
Checkpoint	3.1	MS, ME	9	48
Deliverable	D3.4-2 Influence of matrix bound vs. free VEGF in angiogenesis D3.5-1 Role of matrix bound vs. free VEGF C in lymphangiogenesis			
Task update	<p>The lymphatic system plays important roles in immunity and tissue regeneration by providing a route for immune cell trafficking and by transporting soluble antigens, cytokines and various danger signals to the lymph nodes. After development, lymphangiogenesis occurs in wound healing, inflammation and cancer, and blocking lymphangiogenesis has shown positive effects on diseases like chronic inflammation and tumor metastasis. Still, there is huge gaps in our knowledge of how lymphangiogenesis functionally affects the inflammatory microenvironment, and conversely how different inflammatory cues can differentially affect lymphangiogenesis and functional drainage to the lymph node. Such an understanding is necessary to develop effective strategies for therapeutic lymphangiogenesis.</p> <p>Macrophages are known mediators of lymphangiogenesis during inflammation. However these cells have heterogenous phenotypes and can release different cytokines as well as levels of the main lymphatic growth factor VEGF-C; for example, the classically activated macrophages (M1) release pro-inflammatory cytokines, whereas alternatively activated macrophages (M2a and M2c) can secrete type II or immunosuppressive cytokines. Our hypothesis is that lymphatic endothelial cell (LEC) proliferation and lymphangiogenesis influenced by macrophage subtypes and their associated cytokine environments.</p> <p>The dose and the time of the delivery of the VEGF-C is important for the development of functional lymphangiogenesis not only for the success of the <i>in vivo</i> studies but also for the future therapeutical applications. We recently developed a fibrin-binding TG-VEGF-C with a matrixmetalloproteinase (MMP)-degradable sequence, TG-MMP-VEGF-C, that provides a slow and cell demanded release. We showed that in our 9-well radial flow culture chamber (Bonvin et al 2010), TG-VEGF-C and TG-MMP-VEGF-C improves LEC proliferation and capillary formation compared with wildtype VEGF-C. <i>In vivo</i>, TG-MMP-VEGF-C drove the most efficient functional lymphatic regeneration in a tail dermal wound healing model (manuscript in preparation). We are working on the development of gel plug assays in order to develop a faster and high throughput <i>in vivo</i> models for matrix-bound growth factors.</p> <p>In the second year we have generated and characterized these three human macrophage subtypes from THP-1 monocytes (Figure 1). Secondly we have co-cultured macrophage subtypes and LECs in 2D chamber devices. LECs that were cultured together with anti-inflammatory (M2c) type of macrophages showed higher motility than the other macrophage co-cultures. Furthermore, we have examined the macrophage-mediated cytokine effect on the LEC motility and proliferation. Our first studies showed that LECs have higher motility in anti-inflammatory cytokine environments, correlating with the result of macrophage coculture experiments. However we could not see significant differences in the expression of LEC proliferation genes.</p> <p>Together with our ongoing studies, our aim will be to describe the importance of the inflammatory conditions for the initiation and the functional lymphangiogenesis and to understand the <i>in vivo</i> applications of engineered growth factors in future therapeutic applications.</p> <p>Figure 1. The expression of the TGF-β, VEGF-C and TNF-α in macrophages. M1, M2a</p>			

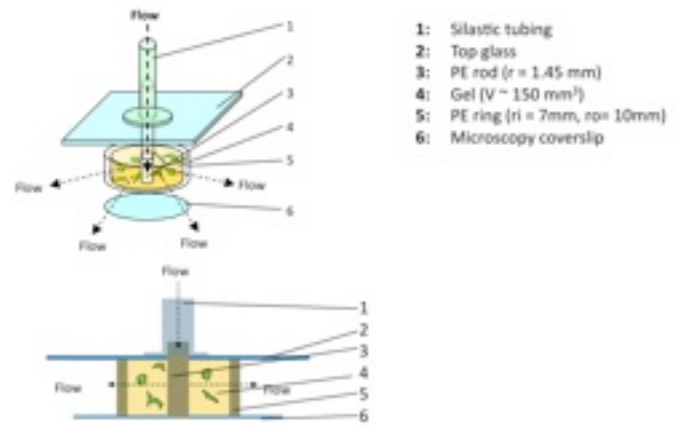
and M2c macrophages are differentiated with 6, 12, 24 and 48h of cytokine stimulation. Macrophage subtypes are statistically compared in each incubation time points (n=3, two tailed t-test * p<0.05, ** p<0.001)



Publications

C Bonvin, J Overney, AC Shieh, JB Dixon, and MA Swartz (2010). A multichamber fluidi

	device for long-term 3D cultures under interstitial flow with live imaging. <i>Biotechnol Bioeng</i> 105(5):982-91. JA Pedersen, S. Lichter, and MA Swartz (2010). Cells in 3D matrices under interstitial flow: Effects of pericellular matrix alignment on cell shear stress and drag forces. <i>J Biomech</i> 43:900-905.
Patents	None
Other	None
Work to be performed in year 3	One of the most exciting observations with fibrin-bound VEGF-C is its role in modulating inflammation and immunological interactions, a previously unknown function that appears to be due to induction of lymphangiogenesis and induction of secondary chemokine secretion (such as CCL21) from cells in the lymphangiogenic microenvironment. In Year 3, these applications will be explored with validation in lymphangiogenesis and the consequences of immune modulation within the lymphangiogenic microenvironment. This is to say, work will continue in angiogenesis validation models, further with a focus on understanding the immunological implications of angiogenesis.

No.	Title	Lead Scientists	Start Month	End Month
3.6	BVP's related to VEGF-Syndecan fusions			
Checkpoint	No milestone associated with this task in this period	JAH, MS, ED	21	48
Deliverable	3.6-1 Dose response of matrix bound VEGF Syndecan 3.6-2 Influence of matrix bound VEGF syndecan in endothelial progenitor cell differentiation			
Task update	<p>VEGF-syndecan (here we call VEGF-AG) was designed, cloned and produced previously. The aim of this task to determine whether VEGF-AG has angiogenic activity and whether this molecule could be a potent substitute of wild type VEGFs.</p> <p>Chamber model was used compare VEGF-AG and wild type VEGFs for human umbilical vein endothelial cell behavior in microfluid environment (Figure 1). This in vitro chamber model that can demonstrate 3D physiological microfluid environment was used to compare role of VEGF-AG, VEGF121, and VEGF165.</p>  <p>Figure 1. Single radial flow chamber for visualizing capillary morphogenesis under slow flow</p>			

Human umbilical vein endothelial cells (HUVECs) were cultured in fibrin gel in the presence of 500 ng/ml of either VEGF-AG, VEGF-121, VEGF165, or 200ug/ml of ECGS and cultured for 3 days with flow. After 3 days of flow, HUVEC cells in fibrin gels in the radial flow chamber were fixed and stained by actin-FITC and nucleus (Hochest). Cells were visualized via confocal microscopy and 3D stacs were generated. In addition, different concentrations (50, 200, 500 ng/ml) of VEGF-AG were examined.

When cells were grown in the static condition in 3D fibrin gel, they remained rounded within the gel (data not shown). In contrast, we found that interstitial flow drove organization of HUVECs. HUVECs responded to flow and organized capillary morphogenesis.

With flow alone, cells in 3D fibrin gel spread and formed single-cell structures (Figure 2), in the presence of VEGF-AG and ECGS, cells formed multi-structures containing lumen and more organized and denser (Figure 2). Those capillaries formed more extensively and faster compared to those in the presence of VEGF121 and VEGF165 (Figure 2).

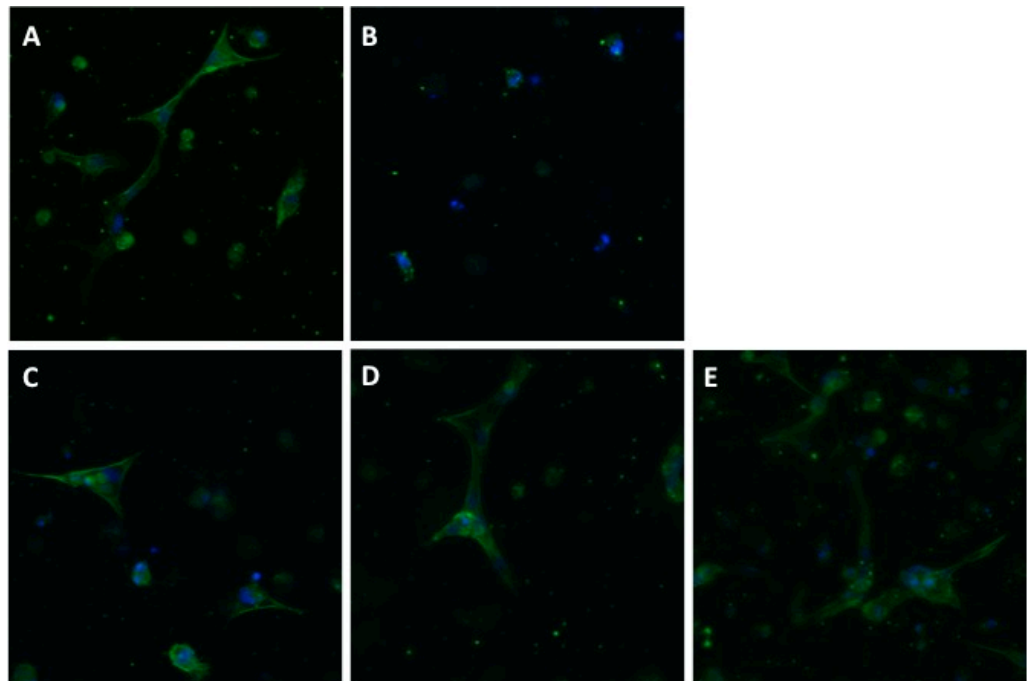


Figure 2 Effect of VEGFs on HUVECs in 3mg/ml fibrin gel in radial flow chamber after 3 days of flow. HUVECs formed structures in fibrin in the presence of microfluid. Green: actin, blue: nucleus. A: positive control ECGS, B negative control fibrin only, C 500 ng/ml of wild type VEGF121, D 500ng/ml of wild type VEGF165, and E 500ng/ml of VEGF-AG

Quantitatively, the presence of VEGF-AG led to increases of number of structures per area, total fiber length and cell numbers/structure in dose dependent manner (Figure 3 and 4).

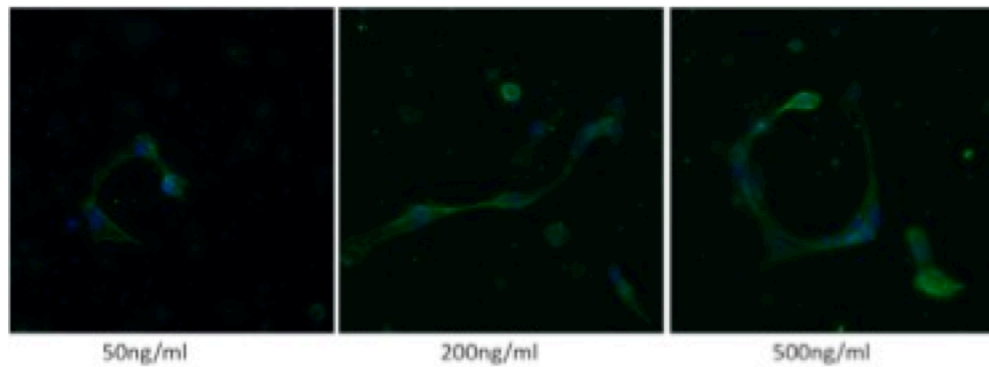


Figure 3 Effect of VEGF-AG on HUVECs in 3mg/ml fibrin gel in radial flow chamber after 3 days of flow. HUVECs formed multi-structures in VEGF-AG dose-dependent manner. Green: actin, blue: nucleus. 50, 200, and 500 ng/ml of VEGF-AG were applied in fibrin gel.

This result suggests that VEGF-AG promote human umbilical endothelial cell differentiation in 3D environment.

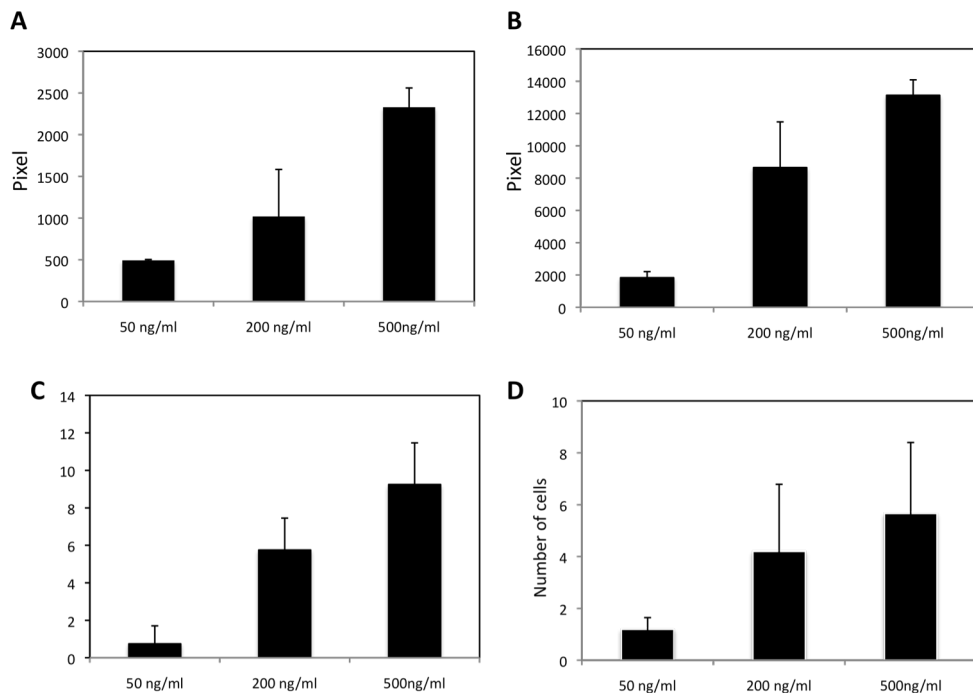


Figure 4 Effect of VEGF-AG on HUVECs in 3mg/ml fibrin gel in radial flow chamber. From images of confocal microscopy, A; total structure area, B; fiber length, C; total number of structures, and D: cells per structures were quantified (n=3).

Receptor phosphorylation assay was performed to see whether VEGF-AG activity was linked to growth factor-receptor phosphorylation. The effect of laminin sequence (AG) in VEGF-AG to VEGF receptor phosphorylation is unknown even though it was found as angiogenic molecule.

With the result of chamber model as described above, we assumed that VEGF-AG promote angiogenesis by synergistic signal from VEGF121 and AG sequence. To answer this question, we performed receptor phosphorylation ELISA assay.

Human umbilical vein endothelial cells (HUVECs) were starved prior to the experiment and stimulated by adding 5 ng/ml of VEGF-AG, VEGF121, VEGF165 for 20 and 40 min. Each cell lysate was used for phosph-ELISA kits to quantify phosphorylated VEGFR receptor 2 (pVEGF-R2) and extracellular signal-regulated kinase1/2 phosphorylation (pERK1/2) which is in the downstream of the growth factor-signaling pathways.

Phosphorylation of VEGF-R2 (pVEGF-R2) and ERK 1/2 (pERK 1/2) was greater when cells were stimulated with VEGF-AG or VEGF165 while phosphorylations were weak when cells were stimulated by VEGF121 (Figure 5).

pVEGF-R2 and pERK1/2 were dose independent with VEGF-165, VEGF-121 and VEGF-AG. The curve of phosphorylation was same with VEGF-121, VEGF-165, and VEGF-AG. This suggests that VEGF-AG does not keep longer phosphorylation compared to VEGF-161 but simply has strong initial phosphorylation to be angiogenic. This result suggests that VEGF-AG induces receptor phosphorylation by synergistic effect of VEGF121 and AG sequence.

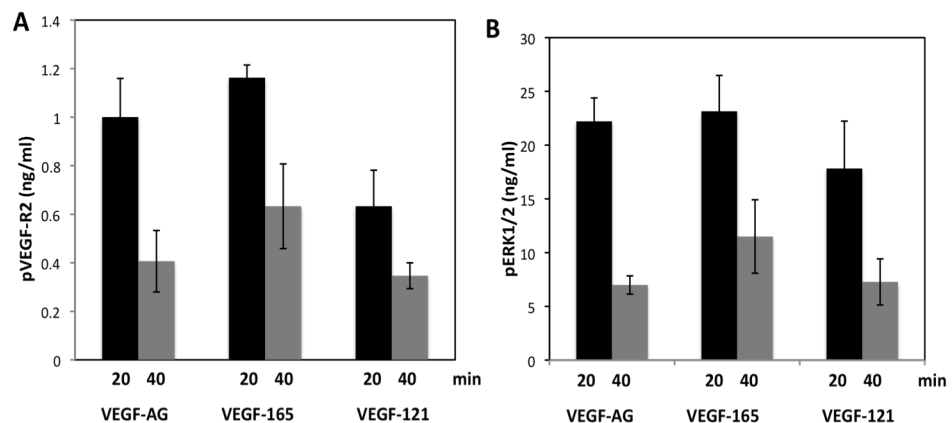


Figure 5 VEGF receptor 2 and ERK 1/2 phosphorylation

Growth factor signaling is enhanced by VEGFs. 20 and 40 min after the stimulation by adding 5ng/ml of VEGF-AG, wild type VEGF-165, and wild type-VEGF-121, phosphorylated VEGF-R2 (A) and ERK 1/2 (B) were quantified (n>3).

in vivo wound model developed by Sabine Eming's lab was performed. we used the *db/db* mouse, which is a genetic mouse model of type-1 diabetes mellitus that provides a well-established experimental system of impaired wound healin. This mouse strain heals wounds principally by the formation of granulation tissue rather than by contraction, and its impairment is notably due to lower levels of several morphogens and receptors. C57BLKS/J-m/Lepr db (db/db) male mice were 10 to 12 weeks old at the start of the experiments. Their backs were shaved and 4 full-thickness punch-biopsy wounds (6 mm in diameter) were created in each mouse. Directly after, fibrin matrices (10 mg/mL fibrinogen) were polymerized on the wounds. Fibrin matrices contained 500ng or 100ng of VEGF-AG, 500ng of recombinant wild type VEGF121 or no morphogens respectively. After 10 days, animals were sacrificed and the wounds were harvested. For histological analysis, an area of 8 mm in diameter, which includes the complete epithelial margins, was excised. Wounds were cut on one edge and embedded. Histological analysis was performed on serial sections until the central portion of the wound. The extent of re-epithelialization and granulation tissue formation was measured by histomorphometric analysis of tissue sections (hematoxylin and eosin stain). For analysis of re-epithelialization, the distance that the epithelium had traveled across the wound was measured. The

muscle edges of the panniculus carnosus were used as indicator for the wound edges. Re-epithelialization was calculated as the percentage of the distance of edges of the panniculus carnosus muscle. For granulation tissue quantification, the area covered by a highly cellular tissue was determined and normalized with the distance of muscle edges of the panniculus carnosus, in order to obtain the area at the center of the wound.

We evaluated whether this microenvironment engineering approach could be used to enhance angiogenesis and skin healing in an animal model. All proteins were covalently attached to fibrin via transglutaminase sequence and controlled-released from the matrix. The wounds were histologically analyzed after 10 days. High concentration of VEGF-AG shows most angiogenesis and wound closure. Compared to the wounds treated with fibrin only, the wounds that received fibrin matrices containing high dose of VEGF-AG led to significantly faster wound closure and greater development of granulation tissue. While high concentration of VEGF-121 has slight difference from wounds treated with fibrin only, lower concentration of VEGF-AG did not differ from wounds treated with VEGF-121, in either amount of granulation tissue or extent of wound closure (Figure 6).

VEGA-AG showed most wound healing and angiogenesis effect on db/db mice. Moreover, the activity was dose-dependent. The components of VEGF-AG, wild type VEGF121 is known to be angiogenic and laminin derived sequence is also found to be angiogenic and promote wound healing. Therefore, it is suggested that two components of VEGF-AG showed synergistic effect for angiogenesis and wound healing in vivo.

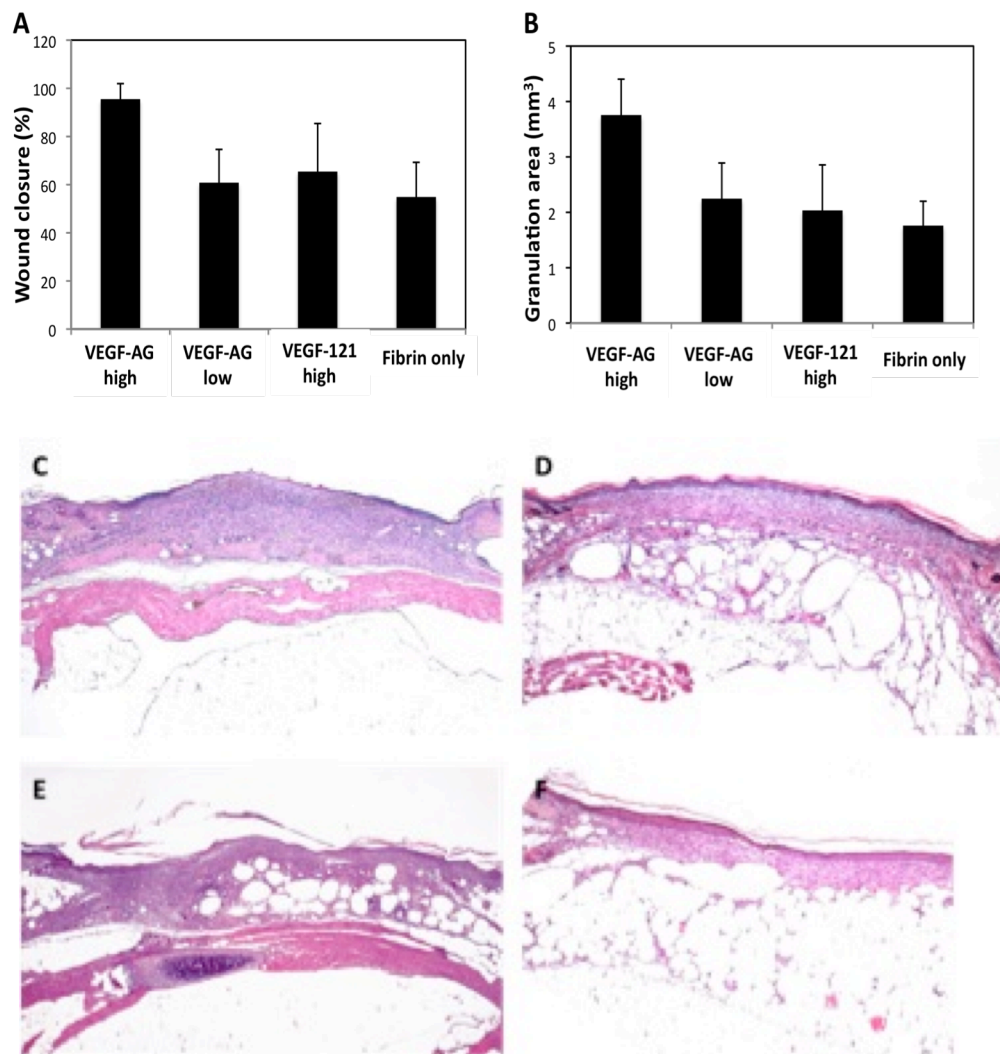


Figure 6. wound healing assay

Delivering VEGF-AG greatly enhanced skin wound healing in diabetic mice.

After 10 days, wound closure (A n=3) and granulation tissue area (B n=3) were measured by histology. Representative histology at day 10. C; VEGF-AG high concentration, D; VEGF-AG low concentration, E; VEGF-121 high concentration, F; fibrin only.

3. in vivo permeability assay was performed as pilot study.

Recent paper revealed that heparan sulfate of heparan sulfate proteoglycan (HSPG) is directly involved in VEGF165- and VEGF121-mediated vascular hyperpermeability in vivo (Xu et al, J.B.C. 2011). VEGF-AG was designed to contain VEGF121 and laminin derived HSPG binding domain while VEGF165 contains heparin binding domain and VEGF121 not. Therefore, here, we asked whether VEGF-AG has same or less (or more) permeability activity as wild type VEGF.

As a pilot experiment, we performed modified the Miles assay. The Miles assay is a classic method to assess alterations in vessel permeability mediated by a number of molecules including VEGF and this technique has been published to be appropriate method for evaluation in pre-clinical trials of anti- VEGF drugs.

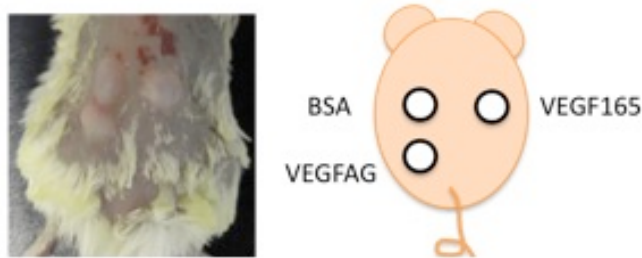
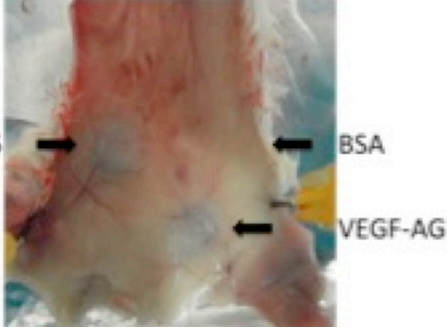


Figure 7. Vascular permeability assay

The effect of VEGFs on vascular permeability was examined by injecting morphogens on the back of mice. The picture shows mice back just after injecting components topically. The mice received iv injection of evans blue dye 15 min before injecting morphogens.

In brief, male mice back was shaved. Tested components (50 ng of VEGF-AG, recombinant wild type VEGF165, or bovine serum albumin (BSA)) were dissolved in PBS. The mice received intravenous injection of 50ul of 1% evans blue dye via the tail vein. 15 min after injecting dye, mice received intradermal injection of 50ul of VEGF-AG, recombinant wild type VEGF165, and BSA (Figure 7). BSA was used as negative control and the recombinant wild type VEGF165 was used as basis activity as it was known to promote more vascular leakage than VEGF121. Mice back skin was monitored and photographed at 30 min after the injection. The skin was opened and exposed to document any blood leakage into the dermal tissue by assessing the intensity of evans blue dye extravasation. The areas of blue (vascular leaks) were photographed (Figure 8). Leakage of evans blue was detected on the place of injecting VEGF165 and VEGF-AG but not on the place of injecting BSA. Similar effect was noted with VEGF165 and VEGF-AG-induced vascular leaks. As result, the VEGF-AG induced more permeability than control BSA but more or less same as VEGF165 does. The results are not quantified and not statistically significant.

	 <p>Figure 8. Vascular permeability from inner skin side The mouse was sacrificed and back skin was opened to see the effect of VEGFs after 30 min. While negative control BSA does not show any vascular leakage, leakage was observed by detecting blue ink at the places of injecting VEGF165 and VEGF-AG. The experiments were repeated several times and showed similar results (n>3).</p> <p>Following these promising results in vivo and in vitro, permeability in vivo assay will be completed and further signalling investigation and new animal model will be performed in future.</p>
Publications	None
Patents	None
Other	None
Work to be performed in year 3	The VEGF-Syndecan protein has been produced, and Year 3 will focus on validation in angiogenesis assays. The protein has been demonstrated to be active, yet the distinct advantages, if any, of conjugation to the syndecan-binding domain as engineered remain to be investigated. Year 3 will also include an IP analysis regarding this novel fusion protein.

No.	Title	Lead Scientists	Start Month	End Month
3.7	BVP's related to SDF			
Checkpoint	No milestone associated with this task in this period	CW, SD	1	48
Deliverable	None in this reporting period			
Task update	Promoting effective tissue repair after myocardial infarction is an important research area due to the limited dividing capacity of cardiomyocytes, which restricts the regeneration of ischemic tissue. Following a myocardial infarction, stromal cell-derived factor-1 (SDF-1), a heparin-binding chemokine and a potent chemoattractant for hematopoietic stem cells, is released by the injured myocardium to initiate the homing of circulating endothelial progenitor cells (EPCs), which are thought to improve the neovascularization of ischemic tissue. To enhance recruitment of EPCs and further aid in the neovascularization of the injured myocardium, a novel biomimetic hydrogel system was developed as a means to provide a matrix-bound delivery vehicle for providing SDF-1 to the site of the injury. This hydrogel system combines the flexibility and nonadhesiveness of synthetic poly(ethylene glycol) (starPEG) with the glycosaminoglycan heparin which naturally has a high affinity for the reversible binding of different chemokines, cytokines and other extracellular molecules. Moreover, the starPEG-heparin hydrogels allow for independent tuning of physical properties while maintaining a constant level of biofunctionalization.			

	<p>ELISA and radiolabeling studies were performed to determine the uptake and release profiles of the hydrogels with varying crosslinking degrees (e.g. mechanical properties). A constant level of SDF-1 functionalization (e.g. initial immobilized amounts) was found across hydrogels with varying degrees of crosslinking. Furthermore, the amount of SDF-1 released by the scaffolds correlates well with the concentration of initially applied SDF-1, thus enabling the specific adaptation of the released cytokine amount for the desired application. Additionally, hydrogels incorporating matrix metalloprotease- (MMP-) sensitive cleavage sites could be applied to increase the amount of SDF-1 released.</p> <p>To investigate the attraction of EPCs to SDF-1-loaded starPEG-heparin gels, the chemotactic properties of starPEG-heparin gels were investigated in a transwell migration assay. Studies revealed that EPC migration is enhanced by establishing a gradient of SDF-1 by the hydrogels in a dose dependent manner with a maximum of migration at SDF-1 loading concentrations of 10 µg/ml. Equivalent experiments with soluble SDF-1 in the bottom well instead of SDF-1 released by the biohybrid gel system showed a similar but slightly decreased migration of the EPCs, suggesting that the long-term gradient provided by the hydrogels is beneficial to promoting chemotactic migration. Moreover, vertical migration of EPCs from collagen gels into MMP-cleavable starPEG-heparin gels loaded with different concentrations of SDF-1 confirmed the chemotactic properties of the hydrogel system. In this context, the MMP-sensitive cleavage sites incorporated as crosslinking moieties allowed for cell-mediated remodeling and invasion into the hydrogels. Increasing amounts of SDF-1 immobilized in the matrix likewise augmented the migration depth of the EPCs into the gels.</p> <p>Since the results of the in vitro analysis suggested an improvement in the hydrogel-mediated EPC migration, first in vivo experiments in nude mice were performed. Subcutaneous implantation of SDF1-loaded MMP-cleavable hydrogels revealed an increase in cell infiltration, vessel formation, and matrix remodelling compared to control-hydrogels without SDF-1. Moreover, combining an intravenous injection of YFP-bone marrow mononuclear cells (BMCs) immediately following implantation of SDF-1-functionalized hydrogels revealed that by establishing a SDF-1 gradient through starPEG-heparin hydrogels matrix remodelling (i.e. gel degradation), angiogenesis, and cellularity was further enhanced.</p> <p>Following these promising in vitro and in vivo studies, experiments to determine the degree of EPC attraction to unloaded and SDF1-loaded hydrogels will be performed in a hind limb ischemia model in mice. Following the procedure, vascularization and perfusion of the limb will be assessed.</p>
Publications	None
Patents	None
Other	<p>Poster presentation: Silvana Prokoph, Kandice Levental, Andrea Zieris, Karolina Chwalek, Uwe Freudenberg, Carsten Werner. “Biomimetic starPEG-heparin hydrogels as well-defined delivery matrices for SDF-1 to promote cardiac progenitor cell chemotaxis.” 3rd International Congress on Stem Cells and Tissue Formation. Dresden, Germany (July 2010).</p>
Work to be performed in year 3	<p>Now that approaches have been developed to present SDF-1 in healing environments from matrices, work in Year 3 will continue in validation models in angiogenesis, and more generally in stem cell recruitment to tissue defect sites.</p>

WP3 has produced 12 peer-reviewed publications in this period.

We have completed our tasks according to schedule as outlined in the original proposal.

There have been changes to the original proposal with respect to collaborations and staff as indicated previously. Martin Ehrbar's team is extensively involved in WP2, therefore the effort engagement in this work package will be decreased accordingly. The work on SDF, which was reported and approved in the first years report has also been continued this year. Heinz Redl's, have also initiated collaborations as part of this work package. The effort of Ralph Muller which was specifically linked to the imaging aspect, for strategic reasons has been reallocated to the horizontal work package on imaging which is indicated at the end of this section.

Collaborations within the work package are as follows.

Exchanges of staff

M Swartz's work involves collaborations with Algirdas Ziogas from the Zisch group (University of Zurich), Kuros, and the Hubbell lab.

Mikaël Martino visited Eming's lab to perform and learn the wound healing model. Mikaël Martino brought materials to Redl's lab to perform the epigastric flap model.

Carmen Schön from Stefanie Dimmeler's laboratory visited J Hubbell's laboratory to learn and get trained in fibrin gel formation and working with the biomaterials.

Exchanges of reagents

A Banfi received the following from the EPFL

Fibrin, TG-mouse VEGF₁₆₄ and TG-Aprotinin and PEG-TG hydrogel.

E Dejana's lab has supplied the Hubbell lab with the human VE cadherin gene and antibodies towards VE cadherin.

J Hubbell lab has supplied the Dejana lab with reagents to form fibrin matrixes with fluorescent fibrinogen. Also an expression plasmid for mammalian cell expression of proteins fused to an FC domain with a transglutaminase peptide sequence

starPEG-heparin hydrogels were prepared in C Werner's laboratory by Silvana Prokoph and sent to S Dimmeler for subsequent subcutaneous implantation into the backs of nude mice.

Work package number	4			Start date or starting event:					Month 1				
Work package title	Translation: Bone Repair												
Activity Type	RTD			Workpackage Leader					Thomas Engstrand				
Participant number	1	2	3	4	5	11	1 2	16	17	22	2 6	27	32
Principal Investigator	JAH /ML	JH	JP	EL	K S	JB	R M	PB	RC	NZ	M A	DF	PB
Planned Person-months for whole WP duration	56	28	24	48	1 2	24	4 2	48	48	48	2 4	2	45
Actual Person-months so far	14. 5	6	5.7 3	47. 87	8	0	0	3	27. 3	27. 75	1 8. 5	0.2 5	2.6 8

REPORT OVERVIEW: WP4 – Bone Repair

4.1 Many systems that control growth factor (GF) release from hydrogels are inspired from the natural interactions that exist between GFs and the extracellular matrix (ECM), such as sequestration and release, but also modulation of GFs signaling through integrins. To evaluate the potential of fibronectin fragments for osteogenesis, we (**JAH**) hypothesized that GF-induced tissue repair and regeneration would be enhanced, when GFs are delivered within a well defined integrin microenvironment. Accordingly, we generated FN fragments containing the FN's cell binding (FN III9-10) with or without the GF binding domain (FN III12-14). The fragments were engineered to be covalently crosslinked into fibrin and tested in two distinct rodent models of osteogenesis. Ectopic bone formation was improved when GFs were delivered within a fibrin matrix functionalized with FN III9-10/12-14 in nude mice and significantly more progenitor cells could be recruited when GFs were delivered with FN III9-10/12-14 in the rat calvarial model.

4.2 A spinal fusion model in rabbits was applied (**PB**) where a limited vascular network in different implants may correlate to lack of bone formation and non-fusion. Osteoprogenitors in combination with fibrin, HA, PLA +/- osteoconductive materials +/- VEGF were evaluated in a heterotopic model aiming to find a novel concept for bone regeneration. The design of constructs optimized with respect to vascularization must be fine-tuned taking into account the needs to a) immobilize cells; b) prevent premature reabsorption of the scaffold; c) ensure the presence of an osteoconductive material.

Preliminary results (**EL, PB**) indicated in vitro osteogenic capabilities of purified human bone marrow CD146+ MSC as attested by positive alkaline phosphatase activity. Samples of cells transfected with VEGF165 were ectopically transplanted in athymic nude mice for testing their ability to enhance bone and vascularisation.

We (**JP**) have developed a calcium phosphate bioactive glass biomaterial for tissue engineering with pro-angiogenic properties and found that the composite promotes angiogenesis through biochemical and mechanical cues in bone marrow-derived endothelial progenitors which is being validated prior to conjugation with factors for bone repair testing.

4.3 No work was performed on VEGF-Syndecan fusions in this period

4.4 We (**EL**) have continued the comparative analysis of the ability of multiple AngioScaff scaffolds complexed with BMP-2 to induce bone formation in standardized in vivo animal models. To validate hydrogel scaffolds and deliver morphogens in a model of local treatment of osteoporosis, we (**JH**) initiated a new pilot study using delivery of BMP-2 in an animal model of osteoporosis in ovariectomized rabbits. This pilot study unexpectedly showed that the hydrogel alone had promising effects on bone density and highlighted potential draw-backs of utilizing BMP-2 to locally improve existing bone quality.

BMP-heterodimeric growth factors possess higher osteoinductive potential than their homodimeric variants. Accurate quantification of BMP2/7 release, either by cells or biomaterials is crucial for determination of release kinetics and produced factor. Therefore we (**HR**) are developing an ELISA assay specific for BMP2/7 heterodimer. We eliminated cross-reactivity for BMP2 and BMP7 homodimers. The setup will be further optimized for the detection of low amounts (pg/ml range) of BMP2/7 as required for transfection experiments in cell culture.

Cells for transplantation Based on the idea of combining a fully degradable polymer (Poly(ϵ -caprolactone); PCL) with a thermoresponsive polymer (polyethylene glycol methacrylate (PEGMA)) a scaffold was developed by **KS**. This scaffold liquefies when exposed to 4°C degrees and solidifies at body temperature. Adipose-derived mesenchymal stem cells (ASCs) have the potential to differentiate into various lineages, including osteocytes. In this new project, we (**HR**) will combine the novel material with human ASC to generate an osteogenic construct. So far, we have optimized biomaterial seeding for the primary ASCs and characterized their survival and persistence within the 3D material. Furthermore, methods for characterization of both the material and the cellular differentiation capacity were adjusted to the use of the thermoresponsive scaffold. This included the preparation for scanning electron microscopy, RNA isolation and the preparation for cross sections for further histological analysis.

To isolate, characterize and experimentally manipulate rare cell populations relevant, we are optimizing two new protocols to isolate: *i*) mesenchymal stem cells and endothelial progenitor cells from liposuction material (**HR**); *ii*) circulating endothelial cells from blood (**MA**). Preliminary results obtained from a single donor suggest a selective medium supports CD133⁺CD34⁺ mesenchymal stem cells from liposuction material. Mature endothelial cells in whole human blood have been detected, magnetically isolated and characterized by flow cytometry.

Beneath we tabulate the progress towards our original objectives with details for each task that has been initiated & highlighting significant results:

No.	Title	Lead Scientists	Start Month	End Month
4.1	BVP related to fibronectin fragments			
Checkpoint	No milestone associated with this task in this period	JAH, RC, Biorigen	12	36
Deliverable	None in this reporting period			
Task update	<p>Growth factors (GFs) are widely used in regenerative medicine and tissue engineering with various successes. Indeed, GFs are rapidly cleared and degraded <i>in vivo</i>. Consequently, in order to improve the overall regenerative efficiency of GFs, systems that control their release from hydrogels, have been developed. Many of these systems are inspired from the natural interactions that exist between GFs and the extracellular matrix (ECM), since in facts, ECM binds and release GFs. However, the ECM/GF interactions do not serve only for the sequestration and release of GFs. For example, ECM can directly modulates GFs signaling through integrins. For instance, joint integrin/GF-receptor signaling can be generated by the formation of GF-receptors/integrins clusters that are mediated by specific complexes between ECM proteins and GFs. Recently, we found that the second heparin binding domain of FN, FN III12-14, acts as a promiscuous GF binding site and could serve as a generic approach to deliver GFs from hydrogels. For example, GFs from the VEGF/PDGF, FGF and TGF-β families showed strong affinity to FN III12-14. The reasons for such promiscuous binding capacity are still unclear, but evidences suggest that the close proximity of the major cell-binding domain of FN, FN III9-10, allows strong crosstalk between GFs and integrins. Therefore, we hypothesized that GF-induced tissue repair and regeneration would be enhanced, when GFs are delivered within a well defined integrin microenvironment. Accordingly, we generated FN fragments containing the FN's cell binding (FN III9-10) with or without the GF binding domain (FN III12-14). The fragments were engineered to be covalently crosslinked into fibrin, a clinically relevant and widely used matrix in regenerative medicine for GFs delivery. Using BMP-2 and PDGF-BB as GFs models, <i>in vitro</i> analysis showed that only, FN III9-10/12-14, the fragment containing both the cell binding and GF binding domains allows synergistic signals between GF-receptors and the integrins $\alpha 5\beta 1$ and $\alpha v\beta 3$. <i>In vivo</i>, while using really low dose of BMP-2 and PDGF-BB, we found that formation of bone ectopically in nude mice was improved, when GFs were delivered within a fibrin matrix functionalized with FN III9-10/12-14. As a second <i>in vivo</i> models, we used calvarial defect in nude mice and rats. In nude mice, a clear trend to better bone regeneration</p>			

was observed in the group treated with fibrin containing BMP-2, PDGF-BB and FN III9-10/12-14. However, in this model, fibrin alone showed a unexpected good capacity to induce bone repair. In rat, we found that the delivery of BMP-2 and PDGF-BB with FN III9-10/12-14 induced recruitment of much more progenitor cells (CD90+/CD45-/CD54+/CD29+) (Figure 1). Currently, the matrices are tested in the rat calvarial defect model for long term bone regeneration.

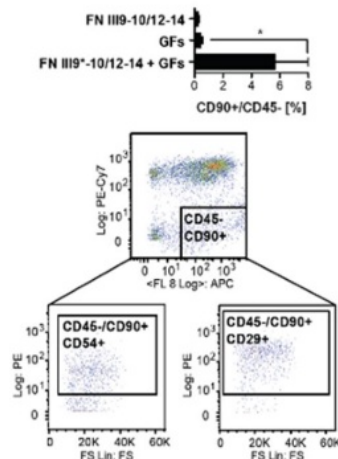


Figure 1. Delivering of BMP-2 and PDGF-BB with FN III9-10/12-14 induce recruitment of progenitor cells. Rat calvarial defect (8mm diameter) were field with fibrin matrices functionalized with or without FN III9-10/12-14 and GFs (BMP-2 and PDGF-BB). After 5 days, matrices were extracted and digested with collagenase and trypsin, in order to recover cells. The percentage of progenitor cells

(CD90+/CD45-/CD54+/CD29+) was determined by flow cytometry. Much more progenitor cells could be recruited, when GFs were delivered with FN III9-10/12-14 (* $p < 0.05$, Student's t test, $n = 5$).

In the bone tissue engineering field, the creation of bioactive materials derived by the combination of a synthetic scaffold with the suitable growth factor preparation could enhance the angiogenic process thereby improving osteogenesis. Bioactive factors contained in platelets modulate different biological functions in the frame of the wound healing process. For many years, the use of platelet rich plasma (PRP) as a therapeutic agent has found several applications in different medical and surgical procedures due to its fibrin and fibronectin components. The availability of a stable and biologically active product could greatly improve the possibility to use these bioactive products in a clinical setting. With this aim, we have performed a series of experiments to verify the maintenance of biological activity and product stability of a standardized platelet rich plasma preparation as well as testing possible delivery vehicles. At the same time, parallel experiments have been performed to evaluate the effect of various growth factors on progenitor cell recruitment profiles within the bone regeneration niche. On a larger scale, experiments are currently underway to evaluate such products in an orthotopic animal model. Techniques for analysis include the optimization of corrosion casting to evaluate enhanced angiogenesis and osteogenesis.

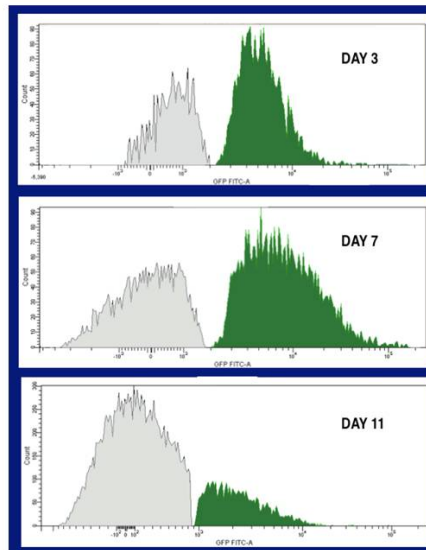
Following ectopic implantation of porous ceramic cubes seeded with mouse GFP labeled mesenchymal stem cells (MSC) into syngenic mice, we investigated the event cascade leading to bone formation. Implants harvested at different times were enzymatically digested to generate single-cell suspensions. Recovered cells were sorted to separate GFP+ implanted MSC and host recruited GFP- cells.

We (RC) isolated and characterized two different "waves" of cells, migrating from the host to the MSC-seeded ceramic. The first migrated cell population, recovered 7 days after implantation, was enriched in CD31+ endothelial progenitors, while the second one, recruited at day 11, was enriched in CD146+ pericyte-like cells. Both populations were not recruited into the scaffold following implantation of a non MSC seeded ceramic.

Pericyte-like cell mobilization was dependent on the first migrated endothelial cell

population. Pericyte-like cells retained properties distinctive of stem cells, such as capacity of performing a high number of in vitro cell divisions and showed an osteogenic potential.

A representative figure and its legend from a recent publication is presented below. Time-dependent recruitment of host-derived cells within MSC/bioscaffold constructs. Representative sorting of cells derived from constructs of GFP+ MSC/bioceramic implanted in C57Bl/6 recipient mice and recovered after 3, 7, and 11 days. The grey curve represents GFP- endogenous cells recruited within the pores of the implants, the green curve indicates seeded GFP+ MSC.



Although all goals related to this specific task and considered in the initial application have been reached, we will continue to investigate this aspect. In particular we will focus on nature, properties and different origin (bone marrow, local, other?) of the recruited cells and on the inducing agents (growth factors and other active molecules) associated with the stem cell conditioned media.

To identify the factors and the cytokines secreted by the different cell populations several methods, including “Luminex” technology are being adopted by RC and Biorigen. Nevertheless, this part of the study is just initiated and results to be included in the present report are not available yet. The bioactive factors contained in the platelets modulate different biological functions in the frame of the wound healing process: cell chemo-attraction and angiogenesis, inflammation regulation and control, cell proliferation, extracellular matrix synthesis.

Since many years, the use of platelet rich plasma (PRP) as a “therapeutic agent” has found several applications in different medical and surgical procedures. In the tissue engineering field the creation of a bioactive material derived by the combination of a synthetic scaffold with a platelet derived growth factor preparation could enhance the angiogenic process which underlies the repair and regeneration processes. The availability of a stable and biologically active product could greatly improve the possibility to use the PRP.

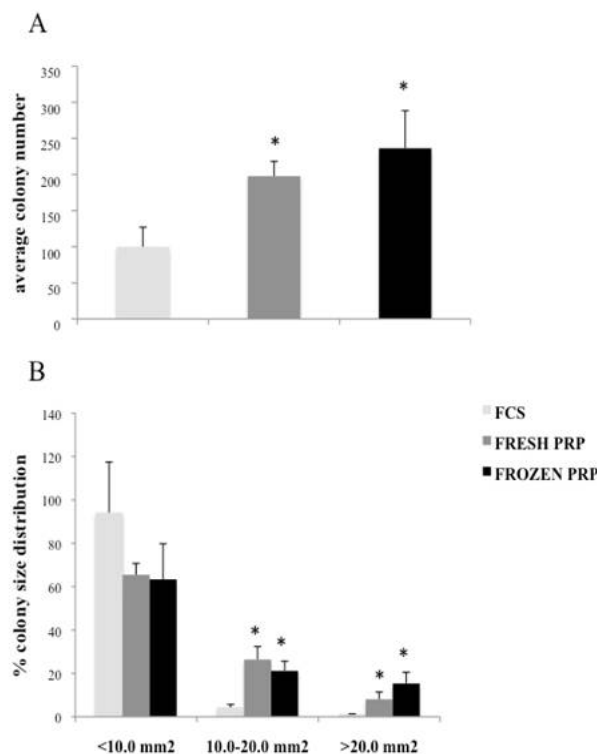
With this aim, Biorigen developed and optimized protocols for freeze drying and gamma-irradiation of platelet lysates and platelet rich plasma preparations. The maintenance of the biological activity and the stability of the product(s) over time was tested by means of an in vitro bone marrow mesenchymal stromal cells (BMSC). clonogenic test (CFU-f) specifically developed for this purpose. Additionally the optimal platelet lysate concentration to be used to sustain BMSC proliferation was defined. The long term stability of the freeze-dried platelet products could dramatically change the practice of the use of platelet derived products for wound healing applications.

A figure from a manuscript in preparation and its legend are presented below.

Effect of the Platelet Rich Plasma as culture medium supplement on number and size colony forming unit - fibroblasts (CFU-f) from human bone marrow aspirates.

Panel A: Average colony number obtained in the presence of FCS, PRP stored at 4°C (fresh PRP), PRP stored at -80°C (frozen PRP). A significant increase ($p < 0.05$) in the colony number occurred in response to PRP addition to the culture.

Panel B: Percentage of colony size distribution obtained in the presence of FCS, fresh PRP, frozen PRP. Colonies were selected for their size according to three different area ranges: $<10 \text{ mm}^2$, $10\text{-}20 \text{ mm}^2$, $>20 \text{ mm}^2$. Clonogenic growth was induced by PRP with a significant increase ($p < 0.05$) in the number of colonies with a larger size. **Data represent the mean \pm standard error (se) of values from 3 independent experiments each one with three different PRP preparations.**



Two different types of scaffold have been produced for the development of a platelet growth factors/glass/polymeric scaffold composite: i) a composite, combining the glass G5 with the polymer (PLA) fabricated by solvent-casting and particulate leaching; ii) a control scaffold without glass (G5). The capacity of the composite(s) to sustain bone formation in vivo when seeded with

bone marrow derived MSC was tested in the ectopic bone formation mouse model. Both scaffolds presented some problems with regard to the cell adhesion. We tested different seeding protocols in the attempt to improve the cell adhesion to the scaffolds.

We (**RC**) did not succeed to show bone formation in the glass/polymer scaffold seeded with MSC and we discontinued this work.

RC is also developing novel scaffolds for delivery of Platelet Derived Growth Factors. So far they have defined the optimal combination of platelet derived GFs for delivery by scaffolds.

The lyophilized, sterilized platelet derived product maintained biological activity and remained stable when stored at -20°C for at least 6 months as compared to other storage and sterilization conditions. When the product was lyophilized overnight and then sterilized using gamma irradiation, it maintained stable concentrations of PDGF-BB and VEGF comparable to the frozen product (control). When used as a cell culture supplement for human bone-marrow derived stromal cells, the product also showed higher performance in terms of colony formation number, colony size and cell

	<p>proliferation.</p> <p>In-vivo testing of developed scaffolds for bone regeneration potential in conjunction with bone marrow derived stromal cells: polylactic acid scaffold/bioactive glass composites, calcium phosphate cement scaffolds with different physical properties.</p> <p>Polylactic acid-glass composite scaffolds (PLA-G5) were prepared by Planell's group incorporating calcium phosphate glass particles of less than 40 mm in size in the PLA polymer solution, to achieve final porous composite scaffolds using a solvent casting/particulate leaching technique. Scaffolds with or without bioactive glass were loaded with sheep bone marrow derived stromal cells and implanted ectopically in nude mice. After 2 months, histological evaluation of implants did not show any bone formation in the implants and hence further experiments were no longer programmed.</p> <p>Calcium phosphate cements were also prepared by the Technical University of Catalonia, UPC (third party from Planell's group). Two different particle sizes of alpha-tricalcium phosphate (α-TCP), i.e. coarse and superfine, were used for the production of the calcium phosphate scaffolds. Very briefly, scaffolds were obtained by mixing the solid phase with a liquid foam which resulted in a paste that was allow to harden (via dissolution precipitation mechanism) yielding the solid scaffold. Using coarse and superfine α-TCP powders rendered scaffolds with similar macroarchitecture but very different microarchitecture. This difference in microarchitecture is believed to affect differently the retention of proteins from the blood and the attachment of cells.</p> <p>Superfine and Coarse scaffolds were loaded with sheep bone marrow derived stromal cells and implanted ectopically in nude mice. After 2 months, histological evaluation of implants showed that these cements could support bone formation. In addition, cartilage-like islands could be seen particularly with the superfine samples. Both cements were invaded with blood vessels emphasizing enhanced angiogenesis.</p> <p>A pilot study to evaluate bone regeneration of a critical long bone defect has been performed in a rabbit model by Biorigen where an osteo-angiogenic platelet derived membrane in association with a poliurethane scaffold, containing hydroxyapatite particles, was used to treat a critical size ulnar gap. In this model, a 1.5 cm defect is created in the distal part of the ulna, the periosteum is removed from each side of the proximal and distal remaining fragment and the scaffold is press fitted into the gap. The fixation of the ulna is not necessary because the radius acts as an internal fixator for the ulna thanks to the union between radius and ulna.</p> <p>The rabbits were monitored by X-rays postoperatively and then every 4 weeks thereafter and the specimens are analyzed by histological analysis. Preliminary results on ulnar defect treated with the poliurethane scaffold wrapped with a platelet derived membrane indicate new bone formation at the peripheries of the defect which appears more pronounced at the lateral border opposite to the radial side. This new bone is of endochondral origin since there were well defined areas where hypertrophic chondrocytes undergoing mineralization were present. Blood vessels were clearly detectable inside the scaffolds.</p>
<p>Publications</p>	<p>Tortelli F., Tasso R., Loiacono F., Cancedda R.: The development of tissue-engineered bone of different origin through endochondral and intramembranous ossification following the implantation of mesenchymal stem cells and osteoblasts in a murine model. <i>Biomaterials</i> 31:242-249, 2010</p> <p>Tasso R., Fais F., Reverberi D., Tortelli F., Cancedda R.: The recruitment of two consecutive and different waves of host stem/progenitor cells during the development of tissue-engineered bone in a murine model. <i>Biomaterials</i> 31(8): 2121-2129, 2010</p> <p>Komlev V., Mastrogiacomo M., Pereira R., Peyrin F., Rustichelli F., Cancedda R.: Biodegradation of porous calcium phosphate scaffolds in an ectopic bone formation model studied by x-ray computer microtomography. <i>Eur Cell Mater.</i> 19:136-46, 2010</p>

	Martino M.M, Hubbell J.A. The 12th-14th type III repeats of fibronectin function as a highly promiscuous growth factor-binding domain. FASEB J. 2010 Aug 4.
Patents	None
Other	None
Work to be performed in year 3	Work on the fibronectin fragments will continue in Year 3 to the status of publication in skin and bone validation models, including probing the role of angiogenesis in skin and mesenchymal stem cell infiltration in bone repair induced by growth factors bound to the fibronectin fragment. Work will continue on finding economical alternatives to purified fibrinogen, including exploration of autologous-derived blood plasma product. Work will continue in Year 3 on combination of the fibrin/fibronectin technologies with structural materials, including the calcium phosphate materials, in bone repair validation models.

No.	Title	Lead Scientists	Start Month	End Month
4.2	BVP related to VEGF-A			
Checkpoint	No milestone associated with this task in this period	PB, EL, JP	12	36
Deliverable	None in this reporting period			
Task update	<p>We (PB) have designed a heterotopic transplantation assay in which neovessel form from transplanted endothelial cells, under the direction of a co-transplanted mesenchymal progenitor population. Inasmuch as neither growth from preexisting vessels (angiogenesis) nor de novo differentiation of endothelial cells (vasculogenesis) is involved, we refer to the formation of neovessels in this system as angiopoiesis. We used three different kinds of clonogenic progenitors (CFUF), all sharing an identical surface phenotype (CD146+CD34-CD45-CD105+CD90+ALP+/-) but from different tissue sources (human postnatal BM, human postnatal muscle, human cord blood). When transplanted alone in Matrigel in the epifascial space of the back of SCID mice, BM-CFUF did not generate any differentiated tissue; M-CFUF generated myotubes, myofibers and a unique kind of muscle spheres replicating the differentiation features, but not the shape, of myotubes; CB-CFUF generated histology-proven hyaline cartilage although no chondroinductive cues (BMP-6, TGFb3) was ever applied ex vivo or in vivo. When the same kind of progenitors were co-transplanted with HUVECs, functional blood vessels formed in 3 weeks, and in the case o BM-CFUF matured to near-perfect arterial and venous structures over the next 5 weeks. As shown by LV-GFP labeling, progenitor cells were in all cases recruited to a mural cell fate. Silencing CD146 gene in progenitor cells perturbed the formation of neovessels, leading to the appearance of tubes without a lumen or of irregular uncoated, non functional vascular structures. Silencing of Ang-1 led in contrast to the development of vessel-associated adipocytes. Myogenic differentiation of M-CFUF was halted in the presence of angiopoiesis. Co-transplantation of CB-CFUF and HUVECs resulted in the formation of a unique kind of cartilage-armoured functional blood vessels, which have no equivalent in nature. Interestingly, this system revealed that endothelial cells can introduce a specific spatial pattern in an otherwise isotropic distribution of differentiating mesenchymal progenitors.</p> <p>The use of either smart scaffolds alone, or of constructs comprising scaffolds and osteoprogenitor cells, is a dominant paradigm in bone tissue engineering. We (PB) have developed an extreme model of bone tissue engineering aiming at posterolateral spinal fusion in the rabbit. The model is extreme inasmuch as it represent a unique type of more than critical size defect in a non-osseous enviroment. The space between consecutive transverse processes is greater than</p>			

critical size, and the new bone is expected to form outside of bone. We have shown that in this model, cell populations and mineral-based material that are perfectly able to form bone and to conduce bone formation, respectively, in a heterotopic transplantation system, fail to generate a continuous osseous phase. We have further shown that a limited development of a vascular network in the central portion of the graft associates with failure to generate a continuous osseous phase. With the aim of screening novel material better apt to conduce neovascularization under similar or related conditions, we generated cell-material constructs using either human or rabbit osteoprogenitors and a) fibrin gels, b) hyaluronic acid based hydrogels, with or without an osteoconductive phase (Pro-Osteon™); c) PLA and PLA glasses. All constructs were implanted with or without the addition of VEGF. All the constructs were tested in a heterotopic transplantation model. At 3 weeks post-implantation all the different combinations of Fibrin gel with or without VEGF and hBMMCs had been reabsorbed. Transplants with PLAglass or HA were harvested after 8 weeks and embedded in glycol-methacrylate or paraffin for histology. Strong inflammatory reaction with numerous giant multinucleated cells was present in both PLA and PLAglass heterotopic transplants and no bone formation was observed. Hyaluronic acid, with or without VEGF, did not improve bone formation compared to control.

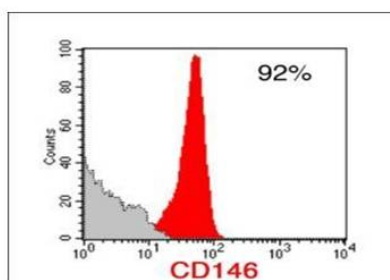
Design of constructs optimized with respect to vascularization must be fine-tuned taking into account the needs to a) immobilize cells; b) prevent premature re-absorption of the scaffold; c) ensure the presence of an osteoconductive material.

In collaboration with the **PB** lab human bone marrow MSCs were sorted by FACS for CD 146+ and sent to Livne's lab. Cells sorted for CD146+/- were evaluated for their osteogenic capabilities in vitro as well as in vivo.

Cells were sorted for CD146 +/- (Fig. A) and were cultured in inductive and osteogenic media for up to 4 weeks. Cultures were tested for the presence of osteogenic markers including alkaline phosphatase activity, Alizarin Red S staining and CD146+ immunostaining. Results indicated a high percentage of CD146 cells obtained from fresh bone marrow sorting and marked positive CD146 immunostaining following cell expansion after sorting (Fig. B). Positive alkaline phosphatase activity in CD146+ cultured cells (Fig. C) and strong alizarine-Red-S (Fig. D) staining were obtained. Samples of cells transfected with VEGF165 were ectopically transplanted in athymic nude mice for testing their ability to enhance bone and vascularisation.

Lentivirus expression system of VEGF165 was constructed by our lab and CD146 sorted cells were infected with VEGF165 containing lentiviruses. The infected cells are being tested for VEGF secretion in vitro and will be followed by in vivo subcutaneous transplantation in mice. In vivo results will be analyzed for both bone formation as well as for transplant vasculature by x-ray and laser Doppler, respectively. Ex-vivo evaluations will be performed on tissue samples of transplant processed for histology and evaluated in both labs.

Figure A: FACS analysis of fresh human bone marrow



Alkaline Phosphatase

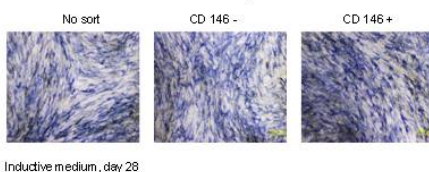
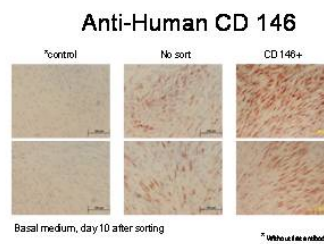


Figure C: Alkaline phosphatase activity of CD146 sorted cells

Figure B: Positive CD146 immunostaining sorted MSCs.



Alizarin-Red-S

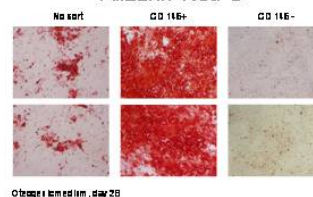


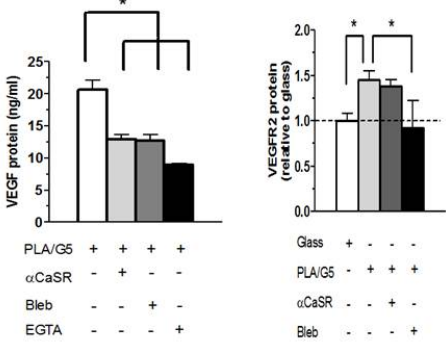

Figure D: Alizarin-Red-S staining of CD146 sorted cells

JP has developed a **calcium phosphate bioactive glass biomaterial** for tissue engineering for bone with pro-angiogenic properties. In this work we intended to elucidate the biochemical and matrix-related mechanical signals responsible for this effect prior to conjugating with pro angiogenic factors.

The bioactive glass (G5) consists in soluble particles of calcium phosphate in the system $P_2O_5-CaO-Na_2O-TiO_2$ and was designated G5. The biodegradable composites of PLA and G5 were produced by the solvent casting method. Porosity was ~95%, with pore size diameter in the 80-210 μm range and high pore interconnectivity. BM-Endothelial progenitors were cultured on the scaffolds.

Staining for fluorescence visualization of cells showed spontaneous formation of tube-like structures suggesting a pro-angiogenic effect on the biomaterial. This point was later confirmed by real time RT-PCR for an array of angiogenic and endothelial differentiation genes, SEM and confocal microscopy. Calcium released in the vicinity of the cells induced bioactivity through the activation of the CaSR (calcium-sensing receptor) promoting chemotaxis and translocation of the transcription factor NF-KB to the nuclei, where it up-regulated VEGF transcription and protein synthesis. Blocking CaSR receptor with specific antibodies abolished this effect. Matrix stiffness -which was determined by both G5 glass and PLA-promoted the nuclear translocation of GATA2 with little to no change of TFII-I, resulting in up-regulated VEGFR-2 transcription and protein at the membrane. The Non-Muscle Myosin II inhibitor blebbistatin (which prevents the matrix stiffness response) eliminated GATA2 nuclear translocation and VEGFR-2 synthesis.

Results indicated below ($n = 2$, with 4 replicates per experiment) demonstrate the proangiogenic potential of the PLA/G5 composite, as well as highlighting the importance of controlling the cell microenvironment -both biochemical and physical- for directing the differentiation process.

	<p><i>Figure 1. PLA/G5 increases VEGF protein production. Treatment with αCaSR, EGTA or blebbistatin eliminates it.</i></p>  <p><i>Figure 2. The proangiogenic gene expression program activated by PLA/G5 is partly abolished by αCaSR or blebbistatin, although by different pathways.</i></p> 
Publications	<p>Aguirre A, González A, Planell JA, Engel E. Extracellular calcium modulates in vitro bone marrow-derived Flk-1+ CD34+ progenitor cell chemotaxis and differentiation through a calcium-sensing receptor. <i>Biochem Biophys Res Commun.</i> 2010 Feb 26;393(1):156-61. Epub 2010 Feb 1.</p> <p>Aguirre A, Planell JA, Engel E. Dynamics of bone marrow-derived endothelial progenitor cell/mesenchymal stem cell interaction in co-culture and its implications in angiogenesis. <i>Biochem Biophys Res Commun.</i> 2010 Sep 17;400(2):284-91. Epub 2010 Aug 21.</p>
Patents	None
Other	<p>Oral presentation at ESB 2010, Tampere, Finland A Calcium Phosphate Bioactive Glass Composite Promotes Angiogenesis through Biochemical and Mechanical Cues in BM-derived Endothelial Progenitors. A. Aguirre, A. González, M. Navarro, O. Castaño, J.A. Planell, E. Engel</p> <p>Poster presentation at TERMIS 2010, Galway, Ireland Extracellular Calcium as a Differentiation Factor on Bone Marrow's MSC and EPC. Arlyng G. González V, Aitor Aguirre, Josep A. Planell, Elisabeth Engel.</p> <p>Poster presentation at 3rd IBEC Symposium 2010, Barcelona, Spain Extracellular Calcium in Bone Tissue Regeneration through CaSR. A. González_Vázquez, A. Aguirre, J. Planell, E. Engel.</p> <p>Oral presentation at TOPEA meeting 2010, Barcelona, Spain.</p> <p>Transeuro, Optistem, Plasticise, Endostem and Angioscaff consortia. Extracellular Calcium's Role on the Progenitor Bone Marrow Cells Behavior. Relation in Bone Tissue Engineering. A.González, A.Aguirre, J. Planell, E. Engel.</p>
Work to be performed in year 3	In Year 3, work will continue on the validation of VEGF within fibrin in bone repair validation models as well as on the calcium phosphate material with and without VEGF in bone repair validation models.

No.	Title	Lead Scientists	Start Month	End Month
4.3	BVP related to VEGF-Syndecan fusions			
Checkpoint	No milestone associated with this task in this period	NA	24	48
Deliverable	None in this reporting period			
Task update	No work was performed on this task in this period			
Publications	None			
Patents	None			
Other	None			
Work to be performed in year 3	Based on the very positive results from other projects on growth factor-induced bone repair, we have prioritized bone repair validation on other factors. The management has stopped bone repair validation of the VEGF-Syndecan.			

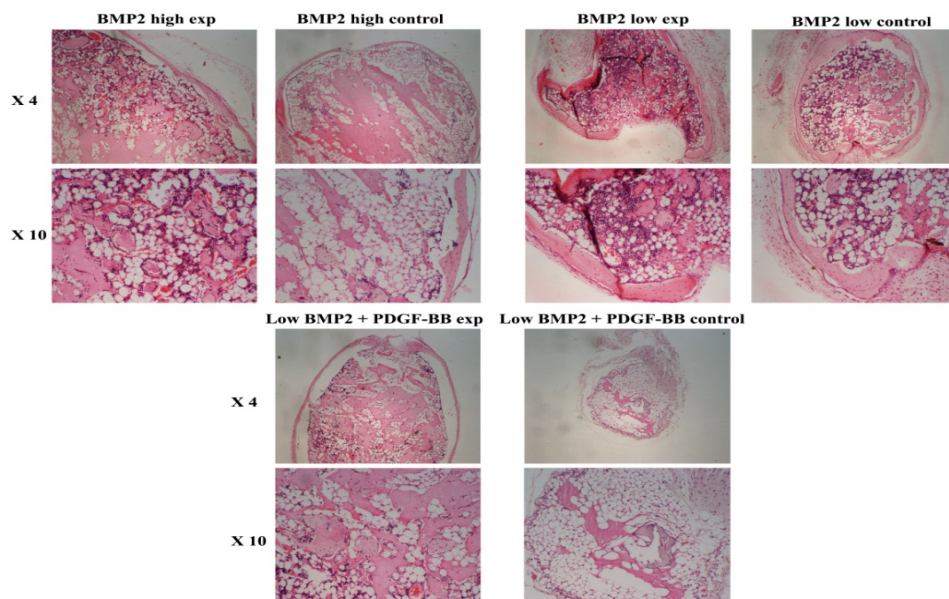
No.	Title	Lead Scientists	Start Month	End Month
4.4	BVP's related to BMP2			
Checkpoint	No milestone associated with this task in this period	EL, JH, JP	6	48
Deliverable	D4.4-1 Activity of wild type BMP 2 released from click chemistry gelled hyaluronic acid			
Task update	<p>The aim of this task was to test the ability of Angioscaff various scaffolds complexed with the osteogenic morphogen BMP-2, for in vivo bone formation in subcutaneous and cranial defect animal models. The screening test of all scaffolds has been performed under the same conditions where all scaffolds were treated according to the same protocol regarding their preparation, handling and sterilization and in addition, each material was tested +/- the morphogen (BMP-2). All groups have used the same morphogen, purchased from the same supplier. The insertion of BMP-2 into the scaffold was performed according to protocol submitted to all the groups by Livne's lab. Also, prior to transplanting the complexed scaffolds, BMP-2 release pattern and alkaline phosphatase in vitro bioassay has been tested in vitro on MSCs for the assessment of the osteogenic potential of released BMP-2 prior to their transplantation in subcutaneous and cranial defects in athymic nude immunodeficient animals.</p> <p>The various scaffolds designed by Angioscaff members (Hilborn, Shakesheff, Hubbell, Seliktar, Planell) were sent to our lab (scaffold+BMP-2) and from each lab the representative colleagues came to our lab for transplanting their material:</p> <p>The table below summarizes the different materials and the collaborative work performed (n= 5 mice per condition):</p>			

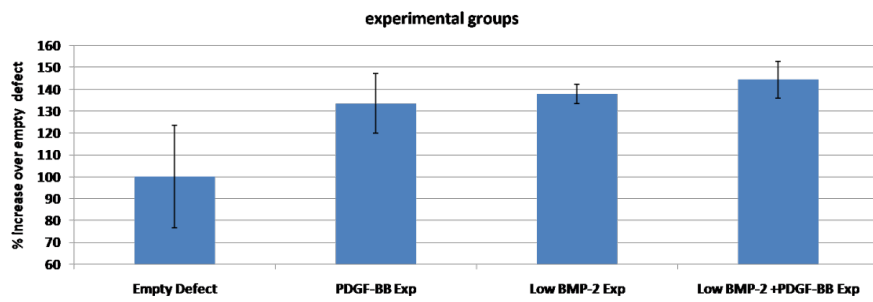
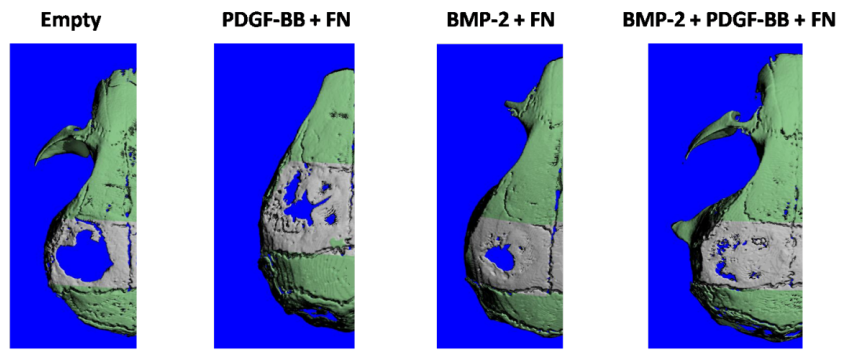
Name/ /PI/WP	Scaffold	Control	Subcut. implantation	Cranial implantation	Histology	MicroCT
Mikael Martino Hubbell WP1	Fibrin+FN III9*-10-GBD +BMP-2 (low)	Fibrin+ BMP-2 (low)	*	*	*	*
	Fibrin+FN III9*-10-GBD +BMP-2 (low)+PDGF- BB	Fibrin+BMP-2 (low)+PDGF-BB	*	*	*	*
	Fibrin+FN III9*-10-GBD +BMP-2 (high)	Fibrin+ BMP-2 (high)	*	*	*	*
Oomenn/ Dmitri Hilborn WP4	HA- heparin+BMP-2	HA-heparin	*	*	*	*
Cheryl Shakeseff WP1	<i>Porous scaffold PLGA/PEG+ BMP-2</i>	Porous scaffold PLGA/PEG	*	*	*	*
Keren Seliktar WP1	PEGylated fibrin+BMP-2	PEGylated fibrin	*	*	*	*
Montse/E dgar Planell WP4	CaCO ₃ (αTCP) +BMP-2	CaCO ₃ (αTCP)	*	*	*	*
Dror Livne WP4	ES PCL/collagen +BMP-2	PCL/collagen	*	*	*	*

At the end of the experiment X-ray radiology was performed and the transplants were carefully dissected and fixed in NBF. Scaffolds containing hydroxyapatite or calcium carbonate were demineralized in EDTA and further processed for paraffin embedding for histology analysis. Cranial defects were sent for μ CT imaging to Ralph Muller's lab for imaging and analysis.

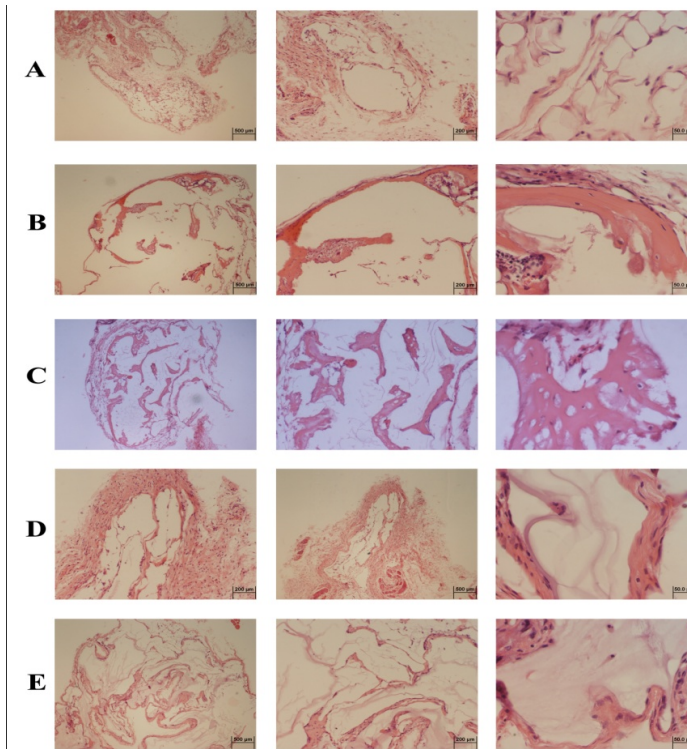
Below are figures that show the results obtained for each material.

Hubbell april –october 2010 (Fibrin±FN III9*-10-GBD+BMP-2 (low)+PDGF-BB)





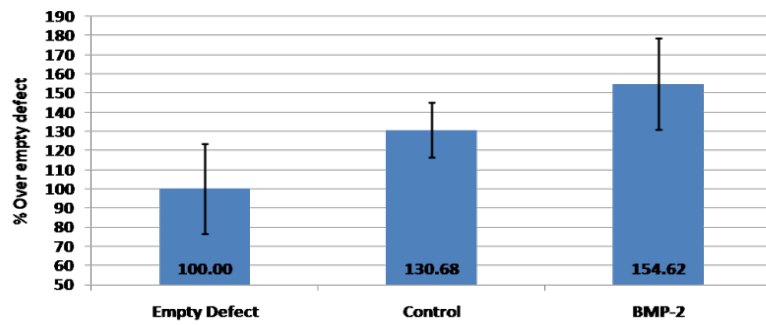
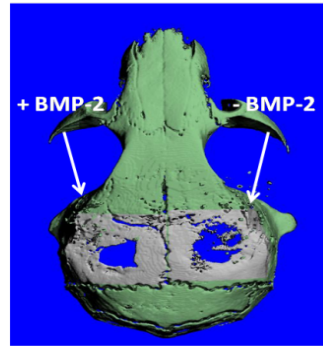
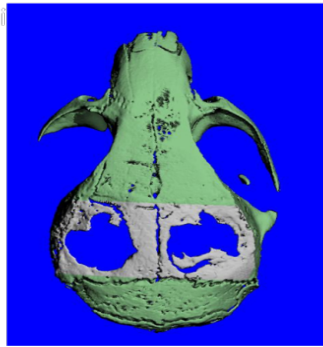
Hilborn april 2010 (HA-heparin±BMP-2)



- (A) - (HA-aldehyde + Heparine-aldehyde) + PVA-hydrazide - negative control
- (B) - (HA-aldehyde + Heparine-aldehyde) + (PVA-hydrazide + 0.5 ug BMP-2)
- (C) - (HA-aldehyde + Heparine-aldehyde) + (PVA-hydrazide + 1 ug BMP-2)
- (D) - (HA-aldehyde) + (PVA-hydrazide + 1 ug BMP-2) - control without heparine
- (E) - (HA-aldehyde) + (PVA-hydrazide + 0.5 ug BMP-2) - control without heparine

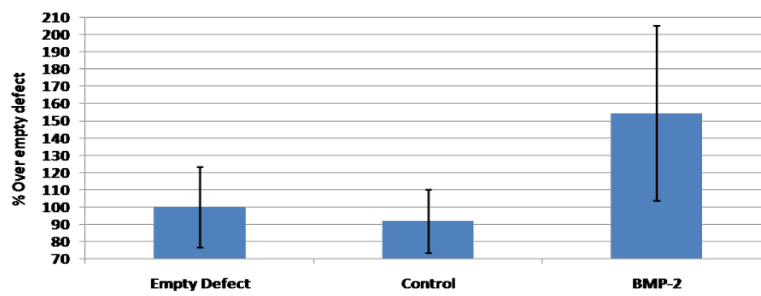
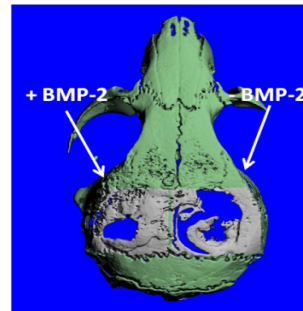
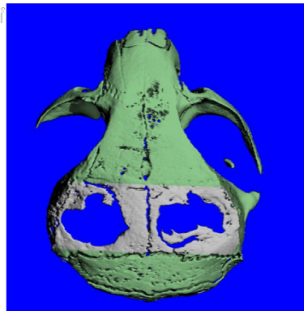
Shakesheff - June 2010 (*Porous scaffold PLGA/PEG±BMP-2*)

Empty defects

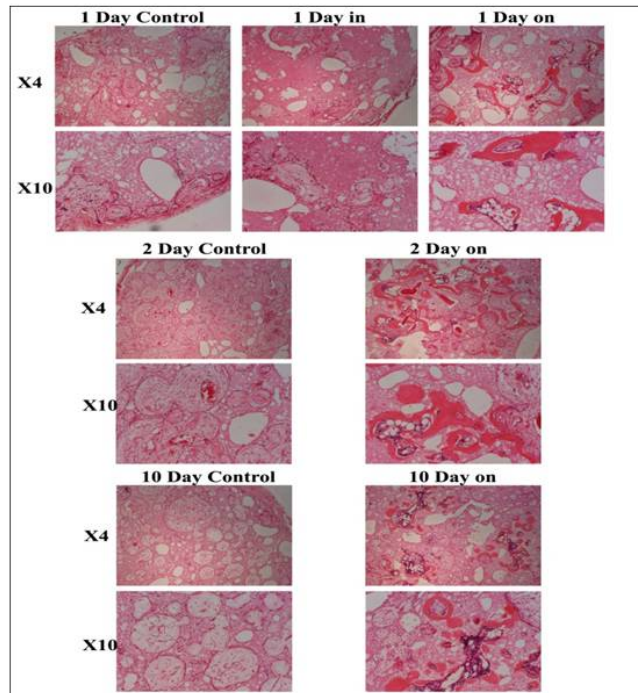


Seliktar - June 2010 (*PEGylated fibrin±BMP-2*)

Empty defects



Plannel – may 2010 ($CaCO_3$ (α TCP) \pm BMP-2)



JH has also synthesized new aldehyde derivative of heparin (HP-al) by grafting 1,2-diol side groups to the heparin backbone followed by their selective periodate oxidation. The same procedure has been used to synthesize aldehyde derivative of hyaluronic acid (HA-al). These functionalized glucosaminoglycans (GAGs) formed strong hydrogels within half a minute upon mixing the GAGs' aqueous solution with an aqueous solution of poly(vinyl alcohol)-based cross-linker bearing carbazate groups (PVA-carb) (see Scheme 1). To evaluate the role of heparin in sequestering of bone inducing growth factor (BMP-2) in a hydrogel matrix, four hydrogel samples have been prepared [(HA-al + PVA-carb), (HA-al + PVA-carb + BMP-2), (HP-al + HA-al + PVA-carb), and (HP-al + HA-al + PVA-carb + BMP-2)] and implanted subcutaneously into mice (n=3 per group). The volume of each implant was 130 μ L and the concentration of BMP-2 was varied between 0.5 μ g/implant and 1.0 μ g/implant. After 4 weeks histological examination revealed formation of new bone where (HP-al + HA-al + PVA-carb+ BMP-2)-hydrogel was implanted and not in other three groups (see Figure 1). The same hydrogels were also examined in calvarial mice model (implant volume - 20 μ L, BMP-2 concentration - 1.0 μ g/implant). The studies on BMP-2 release from the hydrogels as well as the studies on toxicity of the hydrogels and their biodegradation products are now in progress.

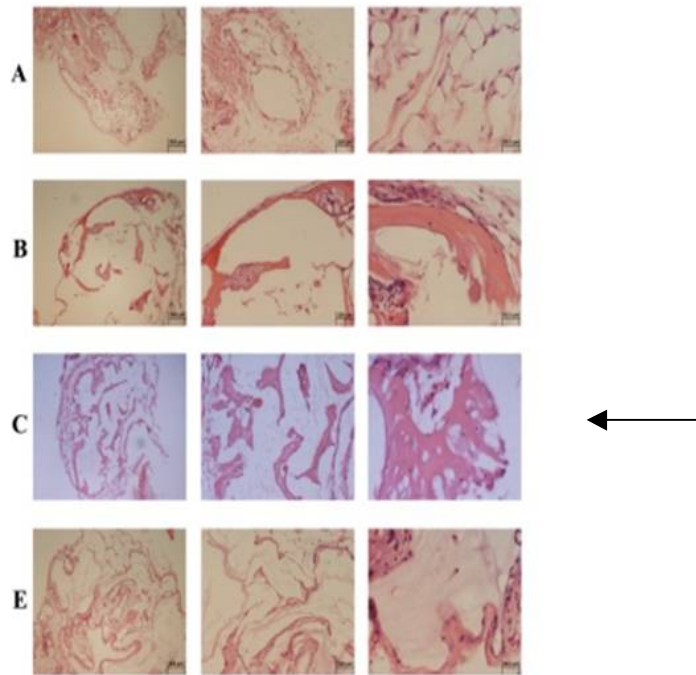
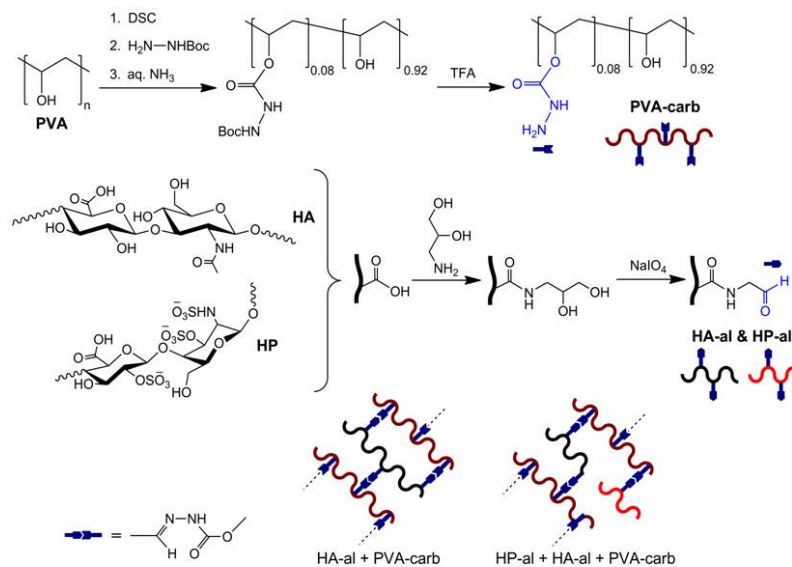


Figure 1. Arrow shows the group of (HP-al + HA-al + PVA-carb + BMP-2) hydrogel



Scheme 1. Synthesis of PVA-carb, HP-al, and HA-al.

Considering the fact that osteoconductive BMPs implanted together with a suitable carrier induce bone formation at ectopic and orthotopic sites JH intended to investigate the capacity of BMP-2 to locally enhance bone density within existing bone. BMP-2 (InducOs, Wyeth) at concentration of 250 $\mu\text{g}/\text{ml}$ of hydrogel delivered by a hyaluronan-based hydrogel containing hydroxyapatite particles (Termira, Sweden) was injected into the bone marrow space of distal femurs in ovariectomized (OVX) New Zealand white rabbits (Fig.2 A and B). Five weeks later the animals were sacrificed and femurs were examined by histology (Fig. 3), scanning electron microscopy (SEM), and by histometrical analysis. SEM was used to distinguish newly formed bone from the host tissue. Histometrical results

showed that there was lower bone density (Fig. 4 A) with thinner trabeculae (Fig. 4 B) in femurs treated with BMP-2 as compared to sham operated controls at this time-point whereas femurs treated with the hydrogel alone demonstrated higher bone density with thicker trabeculae. In one animal the hydrogel alone induced a more unified bone mass at the injection site. Although the results are preliminary this pilot study indicates the potential draw-backs of utilizing BMP-2 to locally improve existing bone quality. Unexpectedly, the hydrogel alone here shows promising effects on bone density and may be favorable for the local treatment of weak bone.

Figure 2A shows the the surgical approach and injection of the gel through the medial epicondyl of the distal femur. A cortical hole was created by drilling before the injection. **B:** Radiography demonstrates the site of injection



Figure 3: Histological examinations 5 weeks after injections indicate increased trabecular bone content in distal femurs in OVX rabbits treated with hydrogel alone as compared to bmp-2 treatment and sham operated controls (bone gets red or pink by van Gieson's staining).

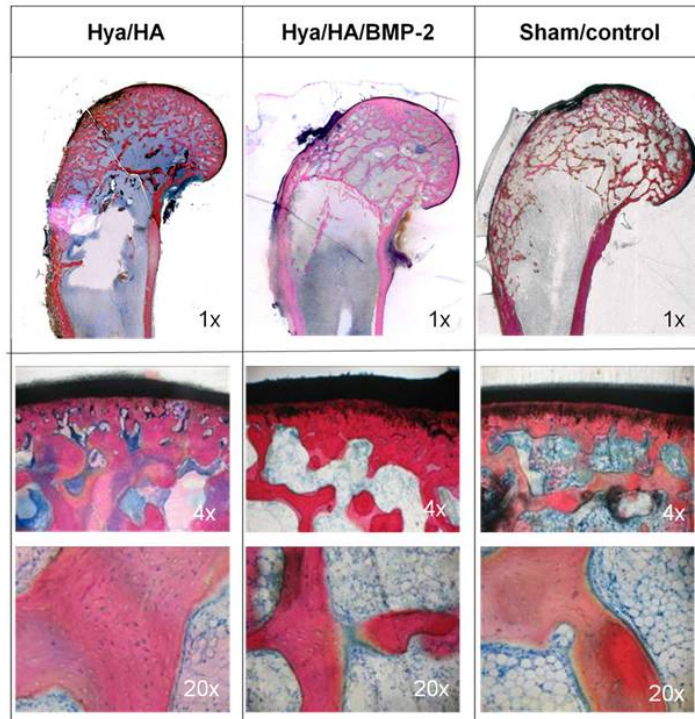
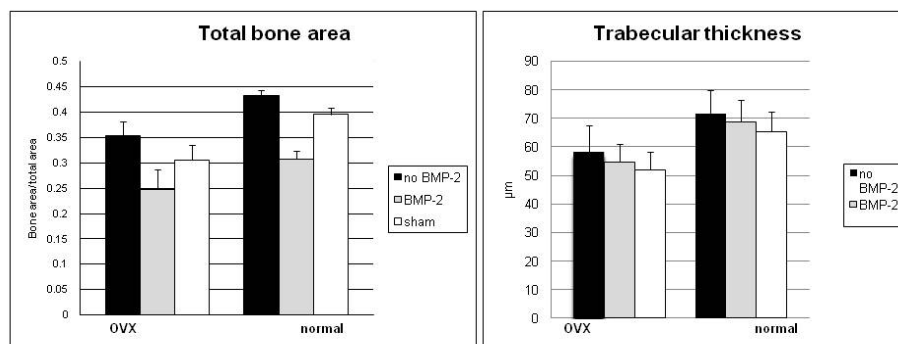


Figure 4: Histomorphometric analysis from histological sections on distal femurs injected with hydrogel alone, hydrogel + BMP-2 or sham operated controls. The analyses were performed 5 week after surgery.



BMP-heterodimeric growth factors have been shown to possess higher osteoinductive potential than their homodimeric variants (Israel *et al.*, 1996). Therefore heterodimeric BMP2/7 has been selected for osteoinduction, either through transfection based BMP2/7 co-expression strategies or by direct application of recombinant growth factor. Accurate quantification of BMP2/7 release, either by cells or biomaterials is crucial for determination of release kinetics and produced factor. Therefore HR aimed to develop a BMP2/7 heterodimer specific sandwich ELISA assay. Special focus was set on cross-reactivity of this assay with homodimeric BMP7 and the respective optimization of blocking and loading buffers on its compatibility with standard cell culture medium containing FCS.

ELISA protocol

Capture antibody and coating protocol:

Anti-human BMP2/7 heterodimer antibody (R&D Systems, 1µg/ml) in carbonate coating buffer, 100µl/well in a Nunc Maxisorp 96-well plate. Coating was carried out over night at 4°C.

Wash 4-5x, 1xPBS 0,05% Tween20, 1min each

Blocking:

Blocking buffer (1xPBS 5% dry milk + 2% bovine serum albumin), 100µl/well, 1h RT.

Wash 4-5x, 1xPBS 0,05% Tween20, 1min each

Sample (standard) loading:

Recombinant proteins in sample loading buffer (1xPBS+1%BSA), 100µl/well, 1h RT.

Standard curve for BMP2/7 heterodimer: 0-100ng/ml recombinant BMP2/7 (R&D Systems).

Controls for BMP2 and BMP7 homodimers: 25 and 50ng/ml recombinant BMP2 (Pfizer) or BMP7 (R&D Systems).

Spiked standard in DMEM+10% FCS: 25 and 50ng/ml.

Wash 4-5x, 1xPBS 0,05% Tween20, 1min each

Detection antibody:

Biotinylated anti-human BMP2 antibody (R&D Systems, 1µg/ml), 1h RT in 1xPBS 1%BSA 100µl/well

Wash 4-5x, 1xPBS 0,05% Tween20, 1min each

Detection:

Streptavidin-HRP conjugate (Roche Diagnostics)1:5000 in 1xPBS 1%BSA 100µl/well 30min RT

Wash 4-5x, 1xPBS 0,05% Tween20, 1min each

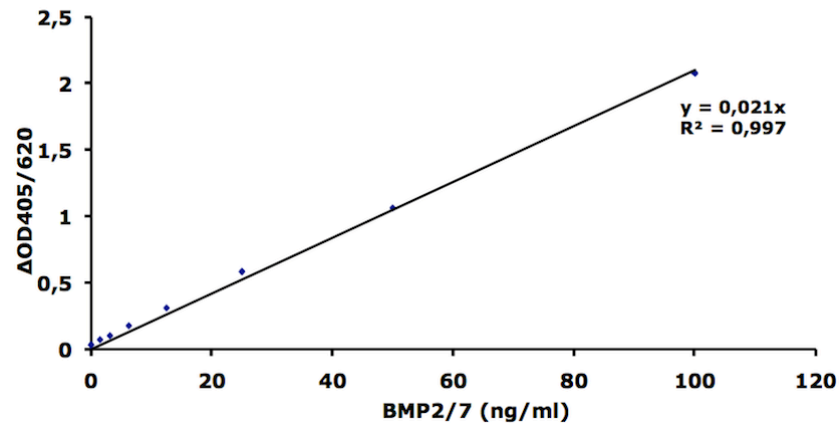
BM Blue POD substrate solution (Roche Diagnostics), 7min RT 100µl/well

STOP with 4M H2SO4 100µl/well

Readout: 405/620nm in a plate photometer

average, n=2

BMP2/7 ELISA standard curve



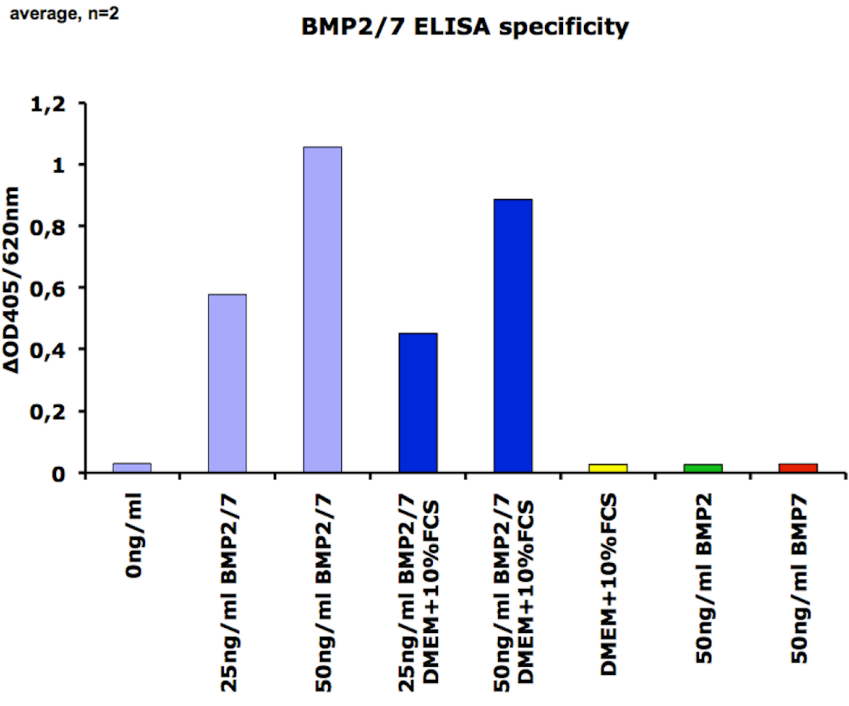


Figure 5: Standard curve for BMP2/7 (A). Standards and control samples (B).

The developed sandwich ELISA showed a consistent standard curve for 1,5-100ng/ml recombinant BMP2/7 heterodimeric growth factor (Figure 5A). Through the application of the custom ELISA protocol it was possible to eliminate cross-reactivity for BMP2 and BMP7 homodimers (Figure 5B). Furthermore, it has been shown for the spiked samples that this ELISA setup is compatible with DMEM+10%FCS cell culture medium and that there is no BMP2/7 heterodimeric growth factor present in FCS (Figure 5B). The setup will be further optimized for the detection of low amounts (pg/ml range) of BMP2/7 as required for transfection experiments in cell culture.

At present work is progressing on entrapping BMP2/7 in the FN-GBD gel for application in bone tissue regeneration.

Publications	<p>Srouji S, Ben-David D, Lotan R, Livne E, Avrahami R, Zussman E. Slow-release hrBMP-2 embedded within electrospun scaffolds for regeneration of bone defect: in vitro and in vivo evaluation. Tissue Eng Part A. 2010 Aug 28. [Epub ahead of print]</p> <p>Ben-David D, Kizhner TA, Kohler T, Müller R, Livne E, Srouji S. Cell-scaffold transplant of hydrogel seeded with rat bone marrow progenitors for bone regeneration. J Craniomaxillofac Surg. 2010 Oct 12. [Epub ahead of print]</p>
Patents	None
Other	None
Work to be performed in year 3	Results in Years 1 and 2 have been very encouraging in the use of BMP-2 in the scaffold materials deriving from Angioscaff. Given the high priority of this area from the perspective of industrial translation and the enthusiasm of the industrial partners, validation of these applications in bone repair will continue in Year 3 in the use of BMP-2 with the fibronectin fragment, the fibrinogen-polymer matrix, the hyaluronic acid-based matrices, the porous biomaterials, and the calcium phosphate biomaterials. Each has different characteristics in terms of healing, mechanics, and application, and each may be useful in different bone repair indications/products.

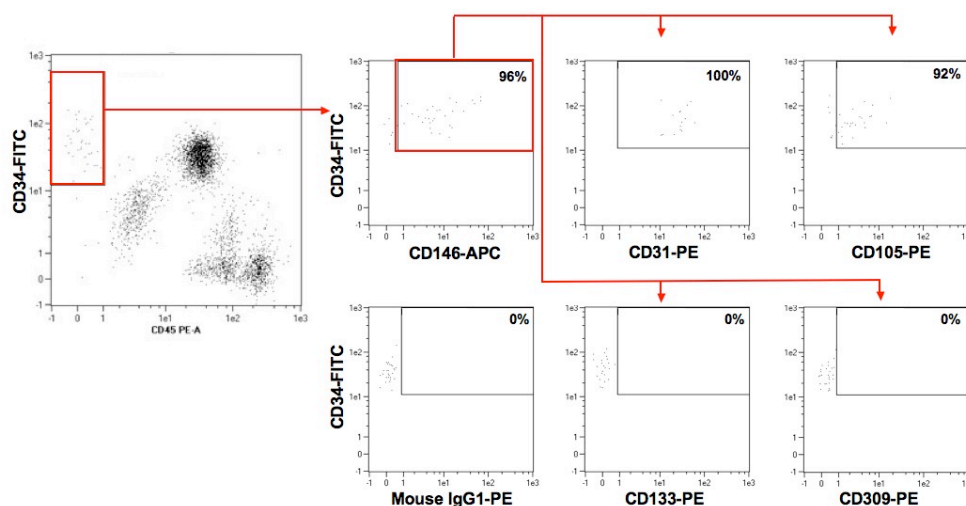
No.	Title	Lead Scientists	Start Month	End Month
4.5	BVP related to TGFβ1			
Checkpoint	No milestone associated with this task in this period	NA	18	42
Deliverable	None in this reporting period			
Task update	No work was performed on this task in this period			
Publications	None			
Patents	None			
Other	None			
Work to be performed in year 3	Given the very positive results on other members of the TGF- β superfamily (with BMP-2, see above), work was prioritized already in Year 2 on these other members, rather on TGF- β itself. In Year 3, no work will be carried out on TGF- β . This factor is a very pleiotropic growth factor, and the management believes based on the positive results with BMP-2 that resources are better used on these factors with more specific activities.			

No.	Title	Lead Scientists	Start Month	End Month
4.6	BVP related to IGF-1			
Checkpoint	No milestone associated with this task in this period	NA	12	42
Deliverable	None in this reporting period			
Task update	No work was performed on this task in this period			
Publications	None			
Patents	None			
Other	None			
Work to be performed in year 3	Given the very positive results with BMP-2 (see above), work was prioritized already in Year 2 on this factor, rather than IGF-1 in bone repair. In Year 3, no work will be carried out on IGF-1 in bone repair. This factor is a very pleiotropic growth factor, and the management believes based on the positive results with BMP-2 that resources are better used on these factors with more specific activities. Work on IGF-1 will focus on muscle repair.			

No.	Title	Lead Scientists	Start Month	End Month
4.7	BVP related to gene delivered Runx2			
Checkpoint	No milestone associated with this task in this period	NA	18	48

Deliverable	None in this reporting period
Task update	No work was performed on this task in this period
Publications	None
Patents	None
Other	None
Work to be performed in year 3	Although work with BMP-2 in bone is very encouraging, use of RUNX2 transfection presents an attractive opportunity. The use in scaffolds has been focused in Year 3 on the use in the calcium phosphate materials, to determine if adequate transfection can be obtained to induce local bone morphogenesis.

No.	Title	Lead Scientists	Start Month	End Month
Cells	Cells for transplantation			
Checkpoint	No milestone associated with this task in this period	HR, MA	1	48
Deliverable	None in this reporting period			
Task update	<p>Generally, cEC are described as cells expressing endothelial markers like CD146, CD34, CD31 and Ulex europaeus agglutinin-1 in the absence of typically hematopoietic markers, such as CD45 and CD14. To differentiate cECs from endothelial progenitor cells (EPC), which seems to play a role in angiogenesis, it is usual to look at CD133 or CD309.</p> <p>Because of the very low frequent of CECs (between 0.01% and 0.0001% of mononuclear cells in normal peripheral blood), it is very difficult to accurately quantify their numbers. To do this, it is often necessary to employ cell enrichment techniques combined with specific cell marker labeling.</p> <p>The goal is to develop a standardized procedure for the enumeration of circulating endothelial cells (CECs) in human blood sources. This goal is planed to be reached in three Phases: <u>Phase 1</u>: Detection of mature endothelial cells in human whole blood samples. <u>Phase 2</u>: Characterization of mature endothelial cells in human whole blood samples. <u>Phase 3</u> :Optimization of the enrichment and enumeration strategy for a flow cytometry based assay.</p> <p>cECs have been detected by using different cEC markers in combination with the MACS system (magnetic activated cell sorting). We have compared enrichment of cECs with CD31, CD34 and CD146 MicroBeads and CD34 showed the best performances related to purity and recovery of the cECs. The cells have been characterized as CD146, CD34, CD31, UEA-1, CD105 positive and CD45, CD133 and CD309 negative.</p> <p><i>Only viable mononuclear cells after enrichment with CD34 MicroBeads are shown</i></p>			



In phase 3, that is ongoing, we are optimizing a protocol that includes the reliable enrichment and enumeration of cECs by flow cytometry. At the time, we are able to enrich cECs and analyze the sample automatically by using the MACSQuant® Analyzer, which is a cell analyzer for multicolor flow analysis, containing a MACS® Cell Enrichment Unit. For enumeration we use a 5 mL whole blood sample, lyse the red blood cells and label the remaining cells with CD34 MicroBeads and different antibody-fluorochrome conjugates (e.g. CD34, CD146 and CD45) for detection. Remaining steps can be done by the MACSQuant® Analyzer. At the time, merely the gating has to be done by the operator again. The optimization of the protocol is ongoing.

Furthermore, Umbilical cord blood (UCB) is also a rich source of primitive cells with clinical potential matching that of the far more controversial embryonic stem cells (ESCs). A decade ago, an endothelia progenitor cell (EPC) population was described to be the source of de novo formed vascular structures in the adult. Subsequent studies however indicated that endothelial progenitor cells (EPCs) do not differentiate into endothelial cells but rather might contribute to vessel formation by paracrine signalling. Now it is widely accepted that only a subset of these EPCs named "colony forming endothelial cells" (ECFCs) should be considered as progenitors of endothelial cells. These cells are thought to play an important role in the vascularization of damaged tissues or cancers and are considered as potential cell source for tissue engineering applications. They are typically purified from the mononuclear cell fraction of UCB through adhesion and colony formation by tissue plastic adherence and are characterized by expression of several markers including panendothelial-specific marker vWF, CD31, CD146 CD105, CD34 and CD133. In a series of experiments we compared the conventional isolation procedure with the isolation and enrichment of ECFC using magnetic beads coupled to anti-CD146 and CD133 antibodies. In all cases, unselected mononuclear cells formed colonies after 12 days of culture whereas CD146 or CD133 selected cells failed to give colonies. To exclude impaired viability of ECFC after MAC sorting we initiated a new series of isolations where defined numbers of CD146 and CD34 positive ECFC cells, in presence or absence of fresh cord blood, are selected based on CD146 or CD34 expression. Furthermore, we attempt to analyze the expression profile of ECFC in more detail to determine new markers that can potentially be used for enrichment.

Due to their low frequency in blood we also aimed to identify other sources of MSC and ESC for potential clinical application; primarily from discarded liposuction material due to the lower ethical restrictions. As the cell yield in the fluid portion of the lipoaspirate is too low for experiments (data not shown) cell isolation is performed by collagenase digestion. The obtained stromal vascular fraction (SVF) is then treated in different ways to enrich the EPC portion in this mixture of cells. First of all, culture flasks were coated with 1% gelatin to test the hypothesis that CD34 expression is preserved by this coating procedure. Even though high donor

variability was observed we clearly showed that CD34 expression is not maintained by gelatine coating (figure 1).

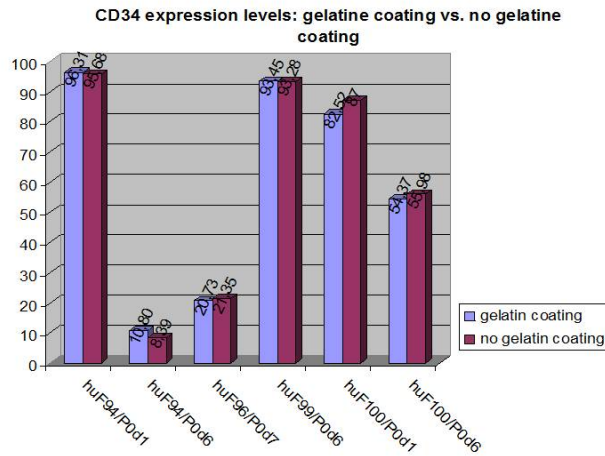


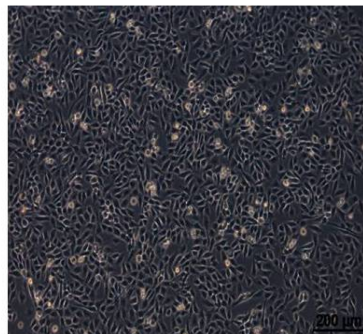
Figure 1. Flow cytometric data of CD34 expression of cells cultured on gelatine vs. cells cultured without coating.

Another approach to enrich EPCs in the stromal vascular fraction was the usage of a selective medium (Xue, et al. 2010, Neuroscience Letters) in contrast to the routinely used EGM-2 medium (Lonza). First, cells were cultured in DMEM/Ham's F12/FCS during passage 0 and from passage 1 the selective medium was used. Second, selective medium was used right away for freshly isolated cells (from passage 0).

Preliminary results suggested that the switch to selective medium in passage 1 supports the existence of CD133⁺CD34⁺ cells. Unfortunately, these results could not be verified by further donor testing. Therefore, another strategy was tested next. EPC enrichment was tried to be done by culturing a late adhesion fraction. After cell isolation from the stromal vascular fraction, cells were seeded in culture flasks and incubated over night for adhesion of MSCs (mesenchymal stem cells). The supernatant was replated 24 hours after the initial seeding (on fibronectin coated flasks) to obtain a so called late adhesion fraction of cells.

About 9 to 12 days after replating colonies of cells with cobblestone-like morphology appeared (figure 2a). The cells were part of a cell mixture as colonies of spindle shaped MSCs were also still present (figure 2b).

A



B

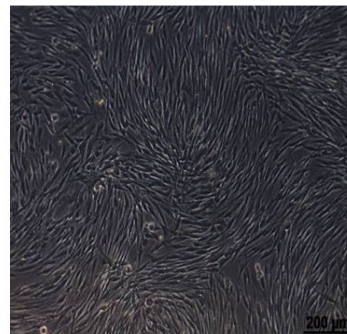


Figure 2. Mixture of cells 12 days after replating onto fibronectin coated flasks. A, cells showing cobblestone like morphology typical for endothelial cells. B, cells showing spindle-like morphology typical for MSCs.

The cell mixture, as shown in figure 2 A and B, was separated by MACS technology (CD34 or CD133 microbead kit), expanded and stained for FACS analysis or used in Matrigel assays.

So far, FACS analysis of EPC markers (CD31, CD34, CD133, CD146, CD309) has not delivered clear results yet. Nevertheless, it seems like CD31, CD133 and CD146 are expressed more highly than CD34 and CD309. CD34 enriched cells of a single donor did not succeed in building tube-like structures in Matrigel assays. Therefore, more donor testing is necessary.

To date, several approaches have been taken to repair bone defects using tissue engineering methods. In tissue engineering, the natural process of bone repair is imitated by applying cells capable of differentiation into osteoblasts, by exposure to inductive growth and differentiation factors, or by using bioresorbable scaffolding matrices to support cellular attachment, migration and proliferation. One class of bioresorbable matrices are hydrogels, crosslinked polymers via chemical bond or physical interactions, which are widely used in tissue engineering applications because of their three-dimensional network, their tissue-like water content, structure stability, and biocompatibility to homogeneously encapsulate cells.

Based on the idea of combining a fully degradable polymer (Poly(ϵ -caprolactone); PCL) with a thermoresponsive polymer (polyethylene glycol methacrylate (PEGMA)) a scaffold was developed at the Center of Biomolecular Science at the University of Nottingham. This scaffold liquefies when exposed to 4°C degrees and solidifies at body temperature.

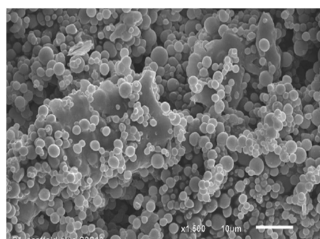
Mesenchymal stem cells are amongst the most promising cell sources for tissue engineering. They are present in several tissues, including adipose tissue. Adipose-derived mesenchymal stem cells (ASCs) can be used in an autologous way and show the potential to differentiate into various lineages, such as adipocytes, chondrocytes and osteocytes.

In this project, the novel material will be combined with human ASC to generate an osteogenic TE construct. Therefore, we have optimized biomaterial seeding for the primary ASCs and characterized their survival and persistence within the 3D material. Furthermore, methods for characterization of both the material and the cellular differentiation capacity were adjusted to the use of the thermoresponsive scaffold. This included the preparation for scanning electron microscopy, RNA isolation and the preparation for cross sections for further histological analysis.

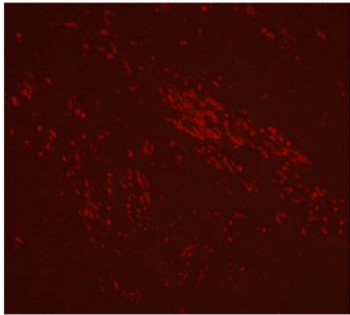
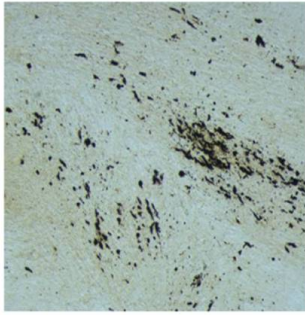
1×10^5 cells were seeded 3D in 150 μ l of the scaffold. Cells were found even distributed in all scaffolds. Prior to cell seeding the scaffolds were coated with standard medium, fetal bovine serum, 0.01% Poly-L-Lysine or 0.1% Gelatine solution. Cells were not viable on Poly-L-Lysine treated scaffolds, but showed a higher viability on Gelatine-treated scaffolds.

Mineralisation of osteoblastic cultures can be examined non-invasively by using fluorescent dyes, such as Xylenol Orange or Calcein Blue. The osteogenic differentiation capacity of ASCs were studied using both fluorescent dyes compared with two standard staining methods.

Xylenol Orange (20 μ M working solution) as well as Calcein Blue (30 μ M working solution) are suitable for staining mineralization. In this trial the fluorescent signal of Xylenol Orange was stronger and more sensitive compared to that of Calcein Blue.



1x

	 
	<p style="text-align: center;">Xylenol Orange Staining Von Kossa Staining</p>
Publications	None
Patents	None
Other	Work presented at the Biomaterial Symposium, Vienna, Austria, 15-17 November 2010.
Work to be performed in year 3	Work will continue in Year 3 on optimization of cell purification approaches and technologies to enable efficient and economical supplementation of scaffolds with osteogenesis-inducing cells. This will continue in validation models of bone repair.

WP4 has produced 6 peer-reviewed publications in this period.

We have completed our tasks according to schedule as outlined in the original proposal.

There were no changes to the original proposal with respect to collaborations and staff except that the effort of Ralph Muller and Jeronimo Blanco's teams which were specifically linked to the imaging aspect, for strategic reasons has been reallocated to the horizontal work package on imaging which is indicated at the end of this section.

Collaborations within the work package are as follows.

Exchanges of staff
Veronika Hruschka from the LBIT visited Kevin Shakesheff to learn the handling with the material for the period 28.2.2010-6.3.2010
Exchanges of reagents
The PCL particles as well as the polymer PEGMA were fabricated in Nottingham by Kevin Shakesheff and then sent by mail to the Ludwig Boltzmann Institute for experimental and clinical Traumatology.
Hubbell's lab sent materials to Livne's lab to perform the invivo experiments in nude mice. Skulls have been scanned and analyzed in Müller's lab.
Fibrin gels containing PEG-b-PPS-b-PEI micelles carrying a Luciferase expression plasmid were sent to Livne's lab for implantation and in vivo imaging in rats.

Work package number	5		Start date or starting event:				Month 1			
Work package title	Translation: Skin Repair									
Activity Type	RTD			Workpackage Leader				Sabine Eming		
Participant number	1	8	11	12	13	15	24	28	10	
Principal Investigator	JAH/MS	ED	JB	RM	SE	HR	PK	DF	ME	
Planned Person-months for whole WP duration	50	6	24	12	49	48	4	2	0	
Actual Person-months so far	11.5	0	0	0	23.91	33	1.6	0	6	

REPORT OVERVIEW: WP5 – Skin Repair

5.1 To assess whether the PEGylated Fibrinogen (PEG-Fib) hydrogel can be used as a morphogen slow release matrix for skin regeneration we (**AZ, MS, JAH, SE**) tested it either alone or with the addition of Fibronectin fragments (PEG-Fib-FN) with a growth factor binding domain developed in the Hubbell lab to increase the VEGF₁₆₅ immobilization and residence time in the matrix. PEG-Fib alone showed enhanced VEGF₁₆₅ affinity while the FN fragments appeared to immobilize more VEGF₁₆₅ in the matrix, which is important for many applications requiring on-demand, cell-mediated release of VEGF₁₆₅ by proteolysis of the encapsulating hydrogel.

To improve skin regeneration, we (**SE**) modified VEGF₁₆₅ to mutant (VEGF₁₆₅mut) that is insensitive to plasmin processing and can be covalently incorporated into a fibrin matrix for delivery. Further, bi-functional proteins comprising VEGF₁₆₅mut and fibronectin type III domain 10 (FNIII10) were generated, allowing for synergistic signalling via VEGFR-2 and integrin $\alpha v \beta 3$. The recombinant proteins were expressed in eukaryotic cells purified from cell supernatants and shown to promote phosphorylation of VEGFR-2 upon stimulation of HUVECs. In vivo experiments in diabetic mice revealed that wound closure kinetic is significantly increased in diabetic wounds treated with various VEGFmut/fibrin variants when compared to fibrin only treated wounds. There is currently a dialogue between Bayer Innovation AG and Kuros, regarding a potential patent overlap or exchange between the two companies; matter of interested is the TG bound VEGF-mut isoform.

5.2 Placenta Growth Factor (PIGF) belongs to the family of VEGF proteins and is a multifunctional cytokine, which is a key regulator in angiogenesis and tissue remodeling. To investigate the role of the heparin binding domain (HBD) for the PIGF mediated activity, last year we (**SE**) synthesized PIGF-1 and PIGF-2, the latter being a PIGF-2 is a target of the serine protease plasmin. HUVEC spheroids embedded in collagen type I gels responded with an significantly increased cumulative sprouting when stimulated with PIGF-2, compared to PIGF-1 or PIGFStop. Using db/db mice as a model for impaired wound healing, treatment with PIGF isoforms resulted in a significant increase of granulation tissue in PIGF-2 treated wounds compared to HBD lacking isoforms.

5.8 and 5.9. Due to difficulties with local authorities to obtain approval for the experimental protocols our studies (**HR**) were subjected to a delay.

Beneath we tabulate the progress towards our original objectives with details for each project that has been initiated & highlighting significant results:

No.	Title	Lead Scientists	Start Month	End Month
5.1	BVP related to Fibronectin fragments			
Checkpoint	No milestone associated with this task in this period	AZ, MS, JAH, SE	12	42
Deliverable	None in this reporting period			
Task update	The purpose of this task was to identify whether the PEGylated Fibrinogen hydrogel can be used as a morphogen slow release matrix for skin regeneration. Specifically VEGF ₁₆₅ was tested in view that an increased angiogenesis could be achieved with the growth factor immobilized inside the hydrogel. PEGylated			

Fibrinogen was tested either alone or with the addition of Fibronectin fragments (FN) with a growth factor binding domain developed in the Hubbell lab to increase the VEGF₁₆₅ immobilization and residence time in the matrix. To immobilize the FN in the hydrogels, a reaction between the FN cysteine and the PEG-DA 10kDa was first performed to get PEG-FN. PEG-FN was added to PEG-Fib solution before polymerization to enable the creation of a PEG-FIB-FN matrix with photopolymerization. To validate FN attachment to the matrix, FN was labeled with NHS-Fluoresceine. The release of labeled FN was measured in spectrophotometer and compared to the same amount of free, labeled FN in solution. As can be seen in Fig.1 there is a quick release of FN (after 30 min) and this amount stays stable for 18 hr. These experiments were made with PEG-Fib 8 mg/ml+1.5% PEG-DA addition. This result indicates the stable attachment of the FB to the PEG-Fib matrix.

In the next stage, VEGF₁₆₅ was added to the solution in a 100 nM concentration, when the PEG-FN concentration is 10 fold higher than VEGF₁₆₅ concentration. Concentration of released VEGF₁₆₅ was measured using an ELISA kit in PEG-FIB or PEG-FIB-FN hydrogels. After 6 days, there was a relatively stable value of the released VEGF₁₆₅ as can be seen in a representative graph of release [Fig.2]. Although no major different was seen in the release profiles with or without the FN addition, the amount of immobilized VEGF₁₆₅ in the hydrogels was significantly different with the FN fragments. It appears that the PEG-Fibrinogen alone has some enhanced affinity to the VEGF₁₆₅ owing to the fibrinogen constituent, and therefore a slow release is achieved without the use of PEG-Fibronectin. However, the FN fragments appear to immobilize more VEGF₁₆₅ in the matrix, which is important for many applications requiring on-demand, cell-mediated release of VEGF₁₆₅ by proteolysis of the encapsulating hydrogel.

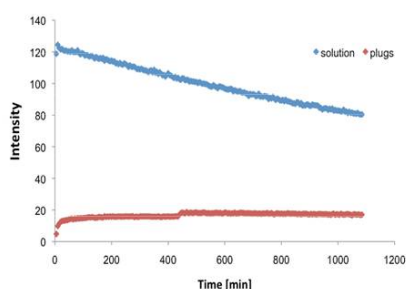


Figure 2: Representative release profiles of labelled FN from PF plugs compared to labelled FN free in solution (relative intensity over time).

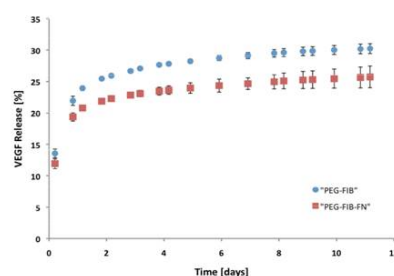


Figure 1: Representative VEGF₁₆₅ release profiles from PEG-FIB and PEG-FIB-FN hydrogels.

For the treatment of impaired skin regeneration, a VEGF₁₆₅ mutant (VEGF₁₆₅mut) rendered insensitive to plasmin processing was created, that can be covalently incorporated into a fibrin matrix for delivery. Further, bi-functional proteins comprising VEGF₁₆₅mut and the fibronectin type III domain 10 (FNIII10) were generated, allowing for synergistic signalling via VEGFR-2 and integrin α v β 3. Recombinant proteins expressed in *E. coli* proved to be biologically active, however, their endotoxin content was too high for *in vivo* investigations. Furthermore, proteins partially precipitate and agglomerate. FNIII10, TG-FNIII10, VEGF₁₆₅mut, TG-VEGF₁₆₅mut, FLV and TG-FLV therefore were expressed in eukaryotic cells, and purified from cell supernatants by a C-terminal polyhistidine tag. These proteins promoted phosphorylation of VEGFR-2 upon stimulation of HUVECs as detected by phospho-VEGFR-2 specific ELISA and western blotting. Furthermore, TG-VEGF₁₆₅mut and TG-FLV could be incorporated into fibrin matrices and were retained in the gel by more than 80% after two days of washing, whereas their soluble counterparts, VEGF₁₆₅mut and FLV, were released in a burst release during the first hours of washing. Subsequently, fibrin gels were formulated in full-thickness punch biopsy wounds created on the back of db/db mice containing 20 μ g/mL of either VEGF₁₆₅mut, TG-VEGF₁₆₅mut, TG-FLV or no

recombinant protein. When compared to fibrin only, wound closure was accelerated upon treatment with various VEGF-isoforms. Histological analysis at day 10 indicated a robust angiogenic response upon delivery of matrix-bound isoforms that was confirmed by immunohistochemical analysis. Both TG-isoforms proved to be significantly more potent in inducing blood vessel growth into the wound area, when compared with soluble isoforms. Major differences between the two TG-isoforms were observed in the maturity of neovessels as indicated by the recruitment of pericytes: pericyte recruitment was more efficient in fibrin/TG-VEGF treated wounds than in fibrin/TG-FLV treated wounds at day 10. At day 14 post injury, all treatment options revealed a reduced vascular network when compared to day 10 post injury wounds, indicating limited vascular growth and subsequent remodelling and regression following wound closure. Overall, our findings revealed that wound closure kinetic is significantly increased in diabetic wounds treated with various VEGFmut/fibrin variants when compared to fibrin only treated wounds.

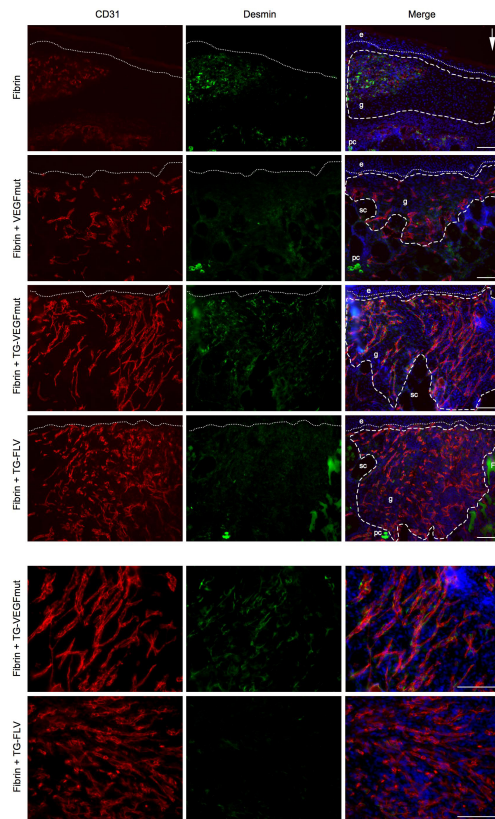


Figure 3: CD31/desmin stained cyrosections of day 10 wounds post injury treated as indicated. The CD31 stain (red) reveals an increased vascularization of the granulation tissue upon treatment with the matrix bound isoforms, TG-VEGFmut and TG-FLV as compared to wounds treated with fibrin only or with VEGFmut/fibrin. The desmin stain (green) indicates, that vascular structures in TG-FLV/fibrin treated wounds are less frequently associated with perivascular cells, when compared to treatment with other VEGFmut isoforms. Abbreviations used: e, epithelium; gr, granulation tissue; sc, subcutaneous fat tissue; pc, panniculus carnosus; F – fibrin gel; arrow indicates direction of wound edge; scale bar 100 mm.

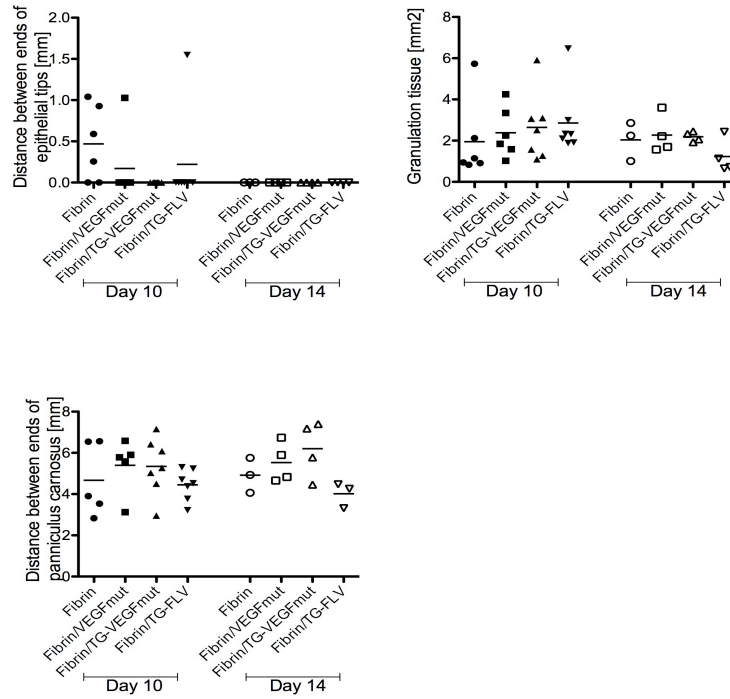


Figure 4: Morphometric analysis of wound healing CD31/desmin stained cryosections at day 10 and 14 post injury, treated with either fibrin alone, VEGFmut/fibrin, TG-VEGFmut/fibrin or TG-FLV/fibrin. Each data point represents the wound tissue of a different mouse.

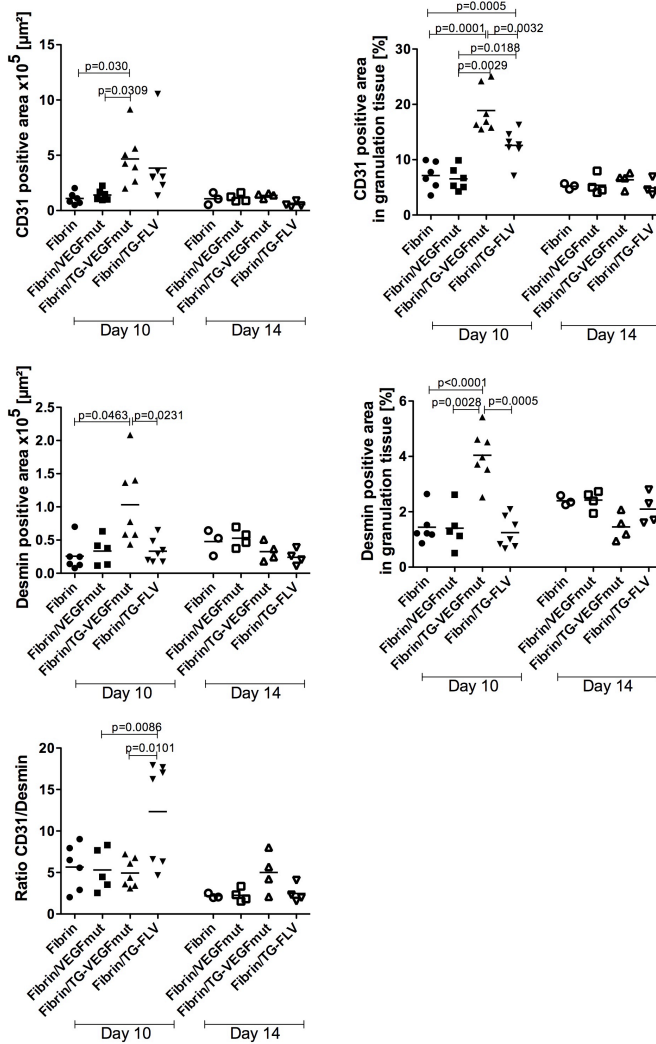


Figure 5: Quantification of CD31 and desmin positive stained areas within the granulation tissue of day 10 and day 14 wounds. Each data point represents the wound tissue of a different mouse.

Publications	None
Patents	There is currently a dialogue between Bayer Innovation AG and Kuros, regarding a potential patent overlap or exchange between the two companies; matter of interested is the TG bound VEGF-mut isoform.
Other	None
Work to be performed in year 3	Results on the use of VEGF-A and PDGF bound to the fibronectin fragments in skin repair validation models is very encouraging. This work will continue in skin healing validation models, including skin healing in diabetic mice, to the status of publication. Likewise, work on the engineered, protease-resistant mutants has been very encouraging, including the engineering of these novel molecules to impart other receptor binding characteristics. This work will also continue in Year 3 in skin healing validation models, including skin healing in diabetic mice.

No.	Title	Lead Scientists	Start Month	End Month
-----	-------	-----------------	-------------	-----------

5.2	BVP related to VEGF –A and -C			
Checkpoint	No milestone associated with this task in this period	SE	18	30
Deliverable	None in this reporting period			
Task update	<p>Placenta Growth Factor (PIGF) belongs to the family of VEGF proteins and is a multifunctional cytokine that is a key regulator in angiogenesis and tissue remodeling. As reported for VEGF, the PIGF gene gives rise to different protein isoforms by mRNA splicing, which differ primarily in the presence or absence of a c-terminal, highly basic heparin binding domain. Up to date little is known about the functional difference of PIGF splice variants in angiogenesis. The aim of this project is to investigate the role of the heparin binding domain (HBD) for the PIGF mediated activity. We synthesized rhPIGF-1 and rhPIGF-2 in HEK293 cells and performed differential structural and functional bioassays. Interestingly, analysis of protease sensitivity revealed that PIGF-2 is a target of the serine protease plasmin. Western-blot analysis and MALDI-TOF-mass-spectrometry of PIGF-2 fragments identified a specific plasmin cleavage site resulting in loss of the carboxyl-terminal domain comprising the HBD. Additionally, incubation of PIGF with exudate obtained from non-healing wounds revealed cleavage fragments that are consistent with plasmin cleavage. Due to this fact we generated a truncated form of PIGF, representing the plasmin processed fragment. Functional in vitro chemotaxis and endothelial cell sprouting analysis, revealed striking differences among the PIGF isoforms. Whereas PIGF-2 induced a robust chemotactic response on HUVE cells and on porcine endothelial cells (PAE) stably transfected with the coreceptor Neuropilin-1 (Nrp-1), PIGF-1, plasmin cleaved PIGF-2 and the PIGFStop mutant showed little effect. Similarly, HUVEC spheroids embedded in collagen type I gels responded with a significantly increased cumulative sprouting when stimulated with PIGF-2, compared to PIGF-1 or PIGFStop (Fig 1).</p> <p>Furthermore, unlike for the weak binding of PIGF-1, BIAcore analysis demonstrated a high affinity of PIGF-2 heparan-sulfate and chondroitinsulfate. The loss of the c-terminal part of the protein in the mutant form results in the complete loss of any tested binding capacity. To investigate the role of the HBD in PIGF mediated signalling, we compared the potential of PIGF-2 and PIGFStop to activate VEGFR-1 and the downstream targets Akt and Erk-1/-2 in HUVE cells and PAE/Nrp-1 cells. Preliminary results revealed no major difference in Flt-1, Akt and Erk-1/-2 phosphorylation among PIGF isoforms. Using db/db mice as a model for impaired wound healing, treatment with PIGF isoforms resulted in a significant increase of granulation tissue in PIGF-2 treated wounds compared to HBD lacking isoforms (Fig 2).</p> <p>Overall our results reveal novel functions of the carboxyl-terminal domain of PIGF and indicate that plasmin-mediated proteolysis is a major switch to control the activity of VEGF protein family members and might serve as an important mechanism during processes of angiogenic remodeling such as in tumor formation or tissue repair.</p>			

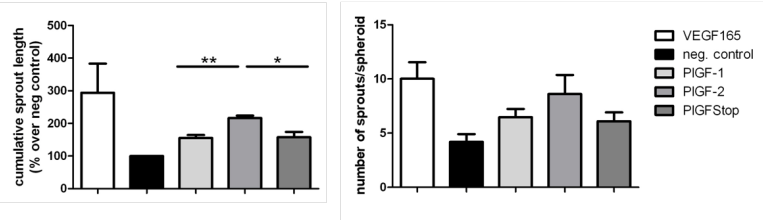
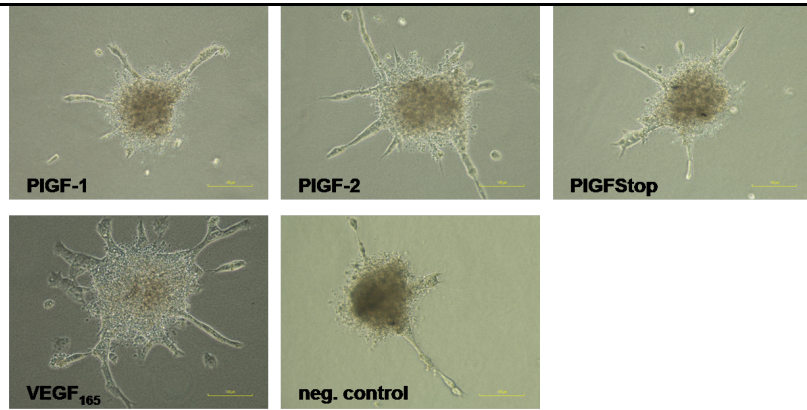


Figure 1: PIGF isoforms induce sprouting in a spheroid assay. 10^3 HUVE cells were seeded in $100\mu\text{L}$ /well (20% methylcellulose, 80% supplemented EGM-2; 96well, round bottom) to form spheroids (incubation for 24h, 37°C). Spheroids were harvested and seeded into $500\mu\text{L}$ collagen type I solution per well (24 well plate, 50 spheroids/well; 2mg/mL collagen I, 5% 10xDMEM, 10% FCS, 50% methylcellulose). Gel polymerisation was started by adding $0,2\text{ M}$ NaOH. After 20min of polymerisation $200\mu\text{L}$ EGM-2 (w/o supplements; 40ng/mL of PIGF or 5ng/mL VEGF165 as positive control, basal EGM-2 was used as negative control) were added onto the gel and incubated for 24h at 37°C . Analysis was performed by counting the sprouts and measurement of the cumulative sprout length (20x magnification; ImageJ software). Significance was calculated out of 3 independent experiments ($n=3$) using unpaired T-test (GraphPad Prism5 software).

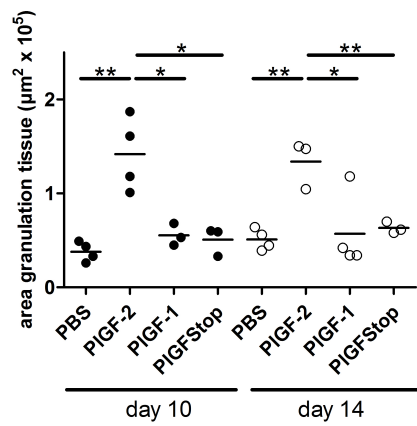
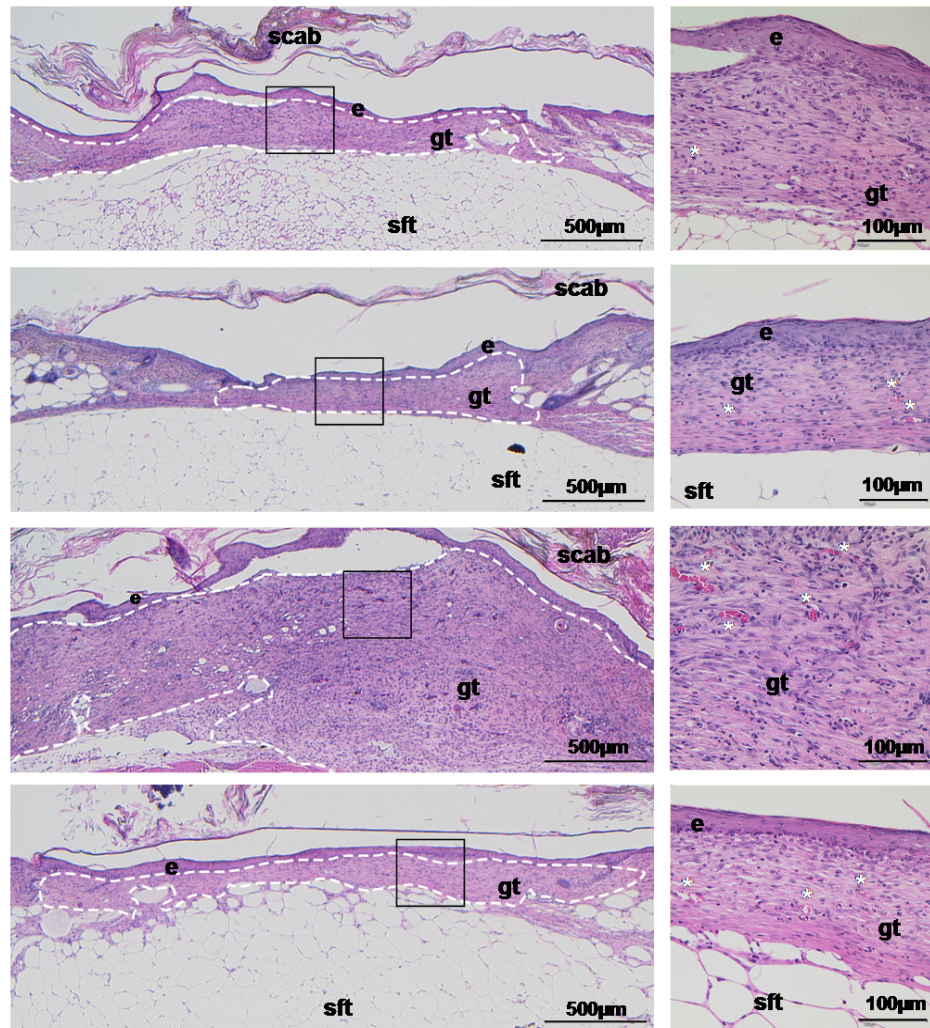


Figure 2: PIGF-2 induces a robust granulation tissue formation in LeptR KO mice. Homocygote LeptR KO mice were used as an *in vivo* model for impaired wound healing. 12 mice in total were wounded four times with a 6mm biopsy punch and treated with 1µg/5µL for each condition (PBS, PIGF-1, PIGF-2, PIGF-Stop) every day not exceeding day 7. At various time points (day 2 n=1, day 5 n=3, day 10 n=4, day 14 n=4) mice were killed and wounds were taken for parafine sections and H&E staining. Analysis was performed for day 10 and day 14 wounds at 2,5x magnification, using the discus software, boxed area in the left panel represents photograph at

	<i>higher magnification in the right panel (20x); statistics were performed using GraphPad Prism 5 software. Dashed line indicates granulation tissue, e epidermis, gt granulation tissue, sft subcutaneous fat tissue, white asterix indicate blood vessels; scale bar as indicated.</i>
Publications	D. Hoffmann, M. Koch, D. Zwolanek, A. Riese, P. Kurschat, T. Krieg and S. Eming. Identification of a novel mechanism that controls the activity of VEGF protein family members. <i>Exp Dermatol.</i> 19, 166–232, 2010
Patents	None
Other	None
Work to be performed in year 3	Work will continue in Year 3 on fibrin with VEGF isoforms, including PlGF isoforms, in skin healing validation models, including skin healing in diabetic mice. The results obtained in Years 1 and 2 are very encouraging, demonstrating to the management that such prioritization should continue.

No.	Title	Lead Scientists	Start Month	End Month
5.3	BVP related to VEGF Syndecan fusions			
Checkpoint	No milestone associated with this task in this period	NA	24	48
Deliverable	None in this reporting period			
Task update	No work was performed on this task in this period			
Publications	None			
Patents	None			
Other	None			
Work to be performed in year 3	Work on the VEGF-Syndecan fusion in Years 1 and 2 was focused on generation of the novel protein, which was not very straightforward. This work is now complete, and (as indicated above) work is now focused on angiogenesis validation models. If those are successful, work will also continue in Year 3 on skin healing validation models; but if those are negative then work will be stopped and skin healing validation models will not be undertaken.			

No.	Title	Lead Scientists	Start Month	End Month
5.4	BVP related to PDGF			
Checkpoint	No milestone associated with this task in this period	NA	12	24
Deliverable	None in this reporting period			
Task update	No work was performed on this task in this period			
Publications	None			

Patents	None
Other	None
Work to be performed in year 3	Work on the use of the fibronectin fragments in Year 3 includes work on PDGF, namely progressing the work in skin healing validation models with VEGF and PDGF delivered in fibrin using the fibronectin fragments to the status of publication. Planning for Year 3 is reported in the context of the fibronectin fragments. Work on PDGF <i>per se</i> and PDGF outside of the context of the fibronectin fragments will be stopped, prioritizing on the former fibronectin fragment approaches and the other morphogens.

No.	Title	Lead Scientists	Start Month	End Month
5.5	BVP related to TGFβ1/3			
Checkpoint	No milestone associated with this task in this period	NA	24	48
Deliverable	None in this reporting period			
Task update	No work was performed on this task in this period			
Publications	None			
Patents	None			
Other	None			
Work to be performed in year 3	Already in Year 2 a decision for prioritization toward other, more specific and less pleiotropic morphogens was reached. No work will be carried out in Year 3 on any TGF- β s in skin repair. (One should note that this decision is also consistent with the recent failure of TGF- β 3 in a large, Phase III skin repair trial.)			

No.	Title	Lead Scientists	Start Month	End Month
5.6	BVP related to gene delivered HIF1α			
Checkpoint	No milestone associated with this task in this period	NA	18	48
Deliverable	None in this reporting period			
Task update	No work was performed on this task in this period			
Publications	None			
Patents	None			
Other	None			
Work to be performed in year 3	Already in Year 2 a decision for prioritization toward protein morphogens in skin repair was reached. The rationale for gene delivery is to achieve a prolonged effect, and the delivery technologies were providing such prolonged morphogenetic effects that gene delivery in skin did not and does not seem to be necessary. No work will be carried out in Year 3 on HIF1 α gene delivery in skin repair.			

No.	Title	Lead Scientists	Start Month	End Month
5.7	BVP related to cell delivered VEGF			
Checkpoint	No milestone associated with this task in this period	NA	18	48
Deliverable	None in this reporting period			
Task update	No work was performed on this task in this period			
Publications	None			
Patents	None			
Other	None			
Work to be performed in year 3	Already in Year 2 a decision for prioritization toward protein morphogens in skin repair was reached, rather than delivery of protein morphogens via cells. The rationale for cell based delivery, like gene delivery, is to achieve a prolonged effect, and the delivery technologies were providing such prolonged morphogenetic effects that gene delivery in skin did not and does not seem to be necessary. No work will be carried out in Year 3 on cell-based VEGF delivery in skin repair.			

No.	Title	Lead Scientists	Start Month	End Month
5.8	Establishment of an ischemic excision model-Morphogens for skin regeneration			
Checkpoint	No milestone associated with this task in this period	HR	1	48
Deliverable	None in this reporting period			
Task update	<p>The aim of this work, which was reported in the first year, was to develop a delayed wound healing animal model based on regional ischemia which could better represent the clinical condition and facilitate translation of the work to the clinic. Therefore, an ischemic rodent epigastric flap model was modified. Two circular excision wounds (∅ 1.5 cm) are created in both the ischemic and the non-ischemic side of the flap. To obtain the optimal conditions for this ischemia induced delayed wound healing model several experiments with ascending degrees of invasiveness (=ischemia) were performed. Wounds are assessed preoperatively as baseline, postoperatively and after 1, 3, 7, 10 and 14 days using surface area morphometry. Laser Doppler imaging is performed to assess degree of ischemia and in case of subsequent therapy degree of superficial perfusion.</p> <p>The results from all three experimental setups performed so far showed insufficient ischemia in the follow- up without differences in wound healing between ischemic and non-ischemic wounds.</p> <p>Due to difficulties with local authorities to obtain approval for the experimental protocol the study was subjected to a delay. Meanwhile the study approval is available and further experiments are performed.</p>			
Publications	None			
Patents	None			
Other	None			

Work to be performed in year 3	In Year 3, model development will continue, to enable testing of the successful morphogen/material combinations in this more advanced model of skin repair, including fibrin with the fibronectin fragments, and with the VEGF/PIGF isoforms. The management believes that such data sets will be very valuable in industrial translation of the technologies for ultimate clinical impact.
---------------------------------------	---

No.	Title	Lead Scientists	Start Month	End Month
5.9	Establishment of an experimental decubitus model for therapeutic interventions – morphogen for skin regeneration			
Checkpoint	No milestone associated with this task in this period	HR	1	48
Deliverable	None in this reporting period			
Task update	<p>Clinical management of pressure ulcers is still challenging and therapeutic options often unsatisfying. Most of the experimental models used in the indication of pressure ulcers are limited to tissue damage in the skin and the subcutaneous layer only. The aim of task which was initiated in year 1 and previously reported was to develop a clinically more relevant deep pressure ulcer model in the rat involving all tissue layers. Therefore, an already established pressure ulcer model in the nude mouse will be modified.</p> <p>Due to difficulties with local authorities to obtain approval for the experimental protocol the study was subjected to a delay. Meanwhile the study approval is available and experiments will be performed in order to optimize the decubitus model.</p>			
Publications	None			
Patents	None			
Other	None			
Work to be performed in year 3	Prioritization toward other angiogenesis models, such as the diabetic skin model and the ischemic skin model of 5.8 above. Work in developing a decubitus ulcer model will be not be continued in Year 3.			

WP5 has produced 1 peer-reviewed publication in this period.

We have completed our tasks according to schedule as outlined in the original proposal. Task 5.8, which was due for completion at the end of this reporting period was delayed due to licence application for animal studies but is on schedule for delivery in year 3.

There were no changes to the original proposal with respect to collaborations and staff except that the effort of Ralph Muller and Jeronimo Blanco's teams which were specifically linked to the imaging aspect, for strategic reasons has been reallocated to the horizontal work package on imaging which is indicated at the end of this section. Additionally Martin Ehrbar's team are involved with some collaborations and will engage effort here.

Collaborations within the work package are as follows.

Exchanges of staff
None
Exchanges of reagents
C Werners lab sent starPEG-heparin to S Eming's lab J Hubbells lab sent fibronectin fragments to S Eming's lab

Work package number	6			Start date or starting event:					Month 1				
Work package title	Translation: Neuromuscular Repair												
Activity Type	RTD			Workpackage Leader					Thomas Eschenhagen				
Participant number	1	9	10	11	12	14	16	18	20	25	26	27	30
Principal Investigator	JAH	SD	M E	JB	RM	TE	GC	JF	AH	CD	MA	DF	GC
Planned Person-months for whole WP duration	32	12	0	24	12	52	48	48	4	16	24	1	54. 3
Actual Person-months so far	10.5	2	0	0	0	46	0	25	6.5	16	4	0	21

REPORT OVERVIEW: WP6 – Neuromuscular Repair

6.1 To study the influence of different matrix materials and growth factors on spontaneously occurring angiogenesis in engineered heart tissue (EHT) we (**TE, JAH**) continued our studies on rat engineered hearts and established two transgenic mouse lines in which endothelial cell-specific and tamoxifen-inducible expression of Cre-recombinase leads to Rosa26-driven β -galactosidase expression, thus making endothelial cells identifiable. EHTs from endothelial reporter mice show a dense network of LacZ-positive endothelial cells, which are oriented along force lines. The higher density of endothelial cell network indicates that the expression patterns observed in adult mice are preserved in EHT. The effect of soluble and immobilized angiogenic factors is currently analyzed. Fibrin appears superior to PEG-TG, HA and PEG-Fib.

Neonatal mouse cardiac cells, i.e. CMs, can be reprogrammed and grown in feeder-free conditions to generate iPS cells (**GCO**). CM-derived iPS cell populations, can be cultured and expanded in a photopolymerizable PEGylated-fibrinogen hydrogel, maintaining the expression of embryonic-specific markers and featuring gene expression profiles similar to embryonic stem cells, both possessing the capacity to re-differentiate into CMs. Furthermore, engraftment experiments, with or without hydrogel, in a mouse model of myocardial infarction established that CM-derived iPS cells survive, integrate, and differentiate in the host myocardium, significantly improving cardiac function. To evaluate the supporting function of the matrix in the ischemic area, the gel was injected alone as well. The data demonstrate that iPS cells methodology integrated with tissue engineering approach can ameliorate cardiac function when introduced into an infarcted myocardium.

6.2 We (**GC, JAH**) have tested engineered hydrogels such as PEG-Fib, TG-PEG and Heparin-STAR-PEG for cell based skeletal muscle reconstruction and regeneration. PEG-Fib was able to promote mature well-differentiated myofibers in vitro that are oriented, aligned and cylindrical like real skeletal muscle fibers. Moreover, they express skeletal muscle contraction proteins. PEG-Fib implant also showed well defined skeletal muscle organization and differentiation in vivo but without myofiber orientation. In mouse models of muscle injury TG-PEG and PEG-Fib caused increased survival of transplanted cells and an overall improvement in cell engraftment as measured by the newly regenerating myofibers formed; moreover PEG-Fib enhanced skeletal muscle differentiation of grafted cells.

6.3 The main challenges in peripheral nerve regeneration include overcoming the slow growth rate of the regenerating neurons, avoid misrouting during pathfinding and to secure a correct reconnection between central nervous system and its target. We (**JF, JAH**) have tested different fibrin gels and found out that FN-910-GBD gel gave superior support for the growth of dorsal root ganglia (DRG) neurites. Here, we continue this screening by determining the effect of hyaluronan scaffold on the outgrowth of DRG explants.

To study the effect of various PEGylated fibrinogen-or fibrinhydrogel in tubes on peripheral nerve regeneration we (**HR**) used a rat model in which the sciatic nerve is transected at two different levels midhigh creating a nerve gap. Tubes filled either with various PEGylated hydrogels or fibrin fine structure with laser fabricated channel structure did not support nerve regeneration. Potentially lower concentrations of hydrogels or more channels are needed.

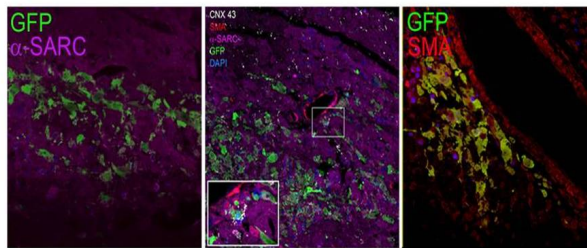
To deliver neurotrophic factors from a fibrin gel and enhance neurite extension, we (**JAH, Kuros-CD**) tested modified fibrin gels. Growth factor (BDNF) release rate was reduced by the GBD in the FN-9-10-GBD fragment. Neurite extension was significantly enhanced by the presence of BDNF in the gel and reached long distances into gels containing FN-9-10, FN-9-10-GBD and full-length fibronectin.

Using MACS[®] Cell Separation System from Miltenyi-Biotec, we (HR) are establishing a method to mobilize sufficient amounts of autologous Schwann cell-like cells from rat adipose tissue. Magnetic cell separation (positive selection for the p75 marker) and subsequent culture yielded superior frequency of cells positive for p75, compared to cells without selection, as well as undifferentiated cells (Adipose-derived stem cells, ASC). Autologous Schwann cell-like cells may be applied in grafts in order to direct, protect and enhance the growth of neuronal cells, thus accelerating nerve regeneration.

Beneath we tabulate the progress towards our original objectives with details for each project that has been initiated & highlighting significant results:

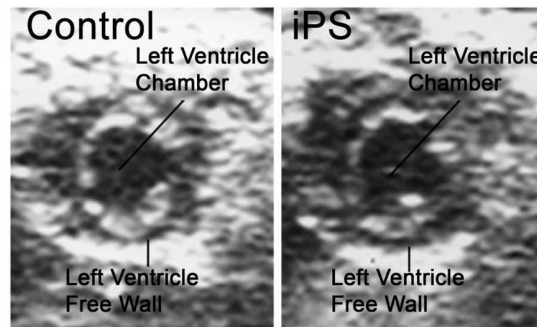
No.	Title	Lead Scientists	Start Month	End Month
6.1	BVP for cardiac muscle			
Checkpoint	6.6	TE, JAH, GCO	6	48
Deliverable	None in this reporting period			
Task update	<p>Cardiac validation projects took on a simultaneous in vitro and in vivo assessment.</p> <p>In vitro TE aimed to study the influence of different matrix materials and growth factors on spontaneously occurring angiogenesis in engineered heart tissue (EHT). Endothelial cell markers were investigated in EHT (day 20-25 of development) from neonatal rats by quantitative RT-PCR, Western blot and immunohistochemistry. Quantitative RT-PCR revealed that VEGF-R1 transcript is expressed in neonatal rat hearts but is absent in EHTs. This finding was supported by Western blot analyses: no band for VEGF-R1 was visualized in EHTs. CD31 transcripts were not differentially regulated in EHTs compared to neonatal rat hearts. In contrast, CD31 protein was upregulated in the presence of immobilized angiogenic factors, primarily in the presence of VEGF. Immunohistochemically, endothelial cells in fibrin matrix were stained with CD31, however signal to noise ratios were insufficient to evaluate these section quantitatively.</p> <p>Due to limited ability to evaluate endothelial cells in EHTs from neonatal rat hearts, two mouse lines with endothelial reporter genes were established. Therefore endothelial cell reporter mouse lines (BMX-mER-Cre-mER, VE-Cadherin-mER-Cre-mER) were crossed with a ROSA26-LacZ mouse line resulting in BMX-mER-Cre-mER/ROSA26-LacZ and VE-Cadherin-mER-Cre-mER/ROSA26-LacZ mouse lines. In both lines LacZ-gene expression (driven by ROSA26 promoter) is dependent on endothelial cell specific expression of Cre-recombinase after modified estrogen receptor (MER) activation. In the presence of 4-Hydroxytamoxifen arterial (BMX promoter) or arterial and venous (VE-Cadherin promoter) endothelial cells express β-galactosidase and can be identified via X-Gal-staining in adult mice. EHTs from endothelial reporter mice show a dense network of LacZ-positive endothelial cells which are oriented along force lines. The higher density of endothelial cell network in VE-Cadherin-EHTs indicates that the expression patterns observed in adult mice are preserved in EHT. The effect of soluble and immobilized angiogenic factors is currently analyzed.</p> <p>In comparison to fibrin three additional materials (PEG-TG, hyaluronic acid, PEG-Fibrinogen) were tested for their ability to promote EHT development. Due to low adhesion to silicone (hyaluronic acid, PEG-Fibrinogen) or high adhesion to agarose casting molds (PEG-TG) these materials could not be tested in standard strip-format EHTs, in alternative ring format EHTs no coherently contractile tissue formation was observed. These results suggest that neither of these materials is an alternative to fibrin in the EHT system.</p> <p>In vivo work by GCO focused on the integration between two of the newest technologies is opening great prospective in the field of regenerative medicine. Tissue engineering know-how and the development of induced pluripotent stem cells (iPS) technology, are obtaining significant improvements in the treatment of injured myocardium. Recently, the first generations of biomaterials, were substitute with new injectable polymers used, not only, as</p>			

cells carriers into the ischemic area, but to prevent associated cardiac remodelling and to improve cardiac mechanical properties as well. On the other hand, cell reprogramming technology has provided a new method for obtaining autologous differentiated cells, such as cardiomyocytes (CMs), directly from somatic tissue. Here we report that neonatal mouse cardiac cells, i.e. CMs, can be reprogrammed and grown in feeder-free conditions to generate iPS cells. CM-derived iPS cell populations, can be cultured and expanded in a photopolymerizable PEGylated-fibrinogen hydrogel, maintaining the expression of embryonic-specific markers and featuring gene expression profiles similar to embryonic stem cells, both possessing the capacity to re-differentiate into CMs. Furthermore, engraftment experiments, with or without hydrogel, in a mouse model of myocardial infarction established that CM-derived iPS cells survive, integrate, and differentiate in the host myocardium, significantly improving cardiac function. To evaluate the supporting function of the matrix in the ischemic area, the gel was injected alone as well. These data demonstrate that iPS cells methodology integrated with tissue engineering approach can ameliorate cardiac function when introduced into an infarcted myocardium.

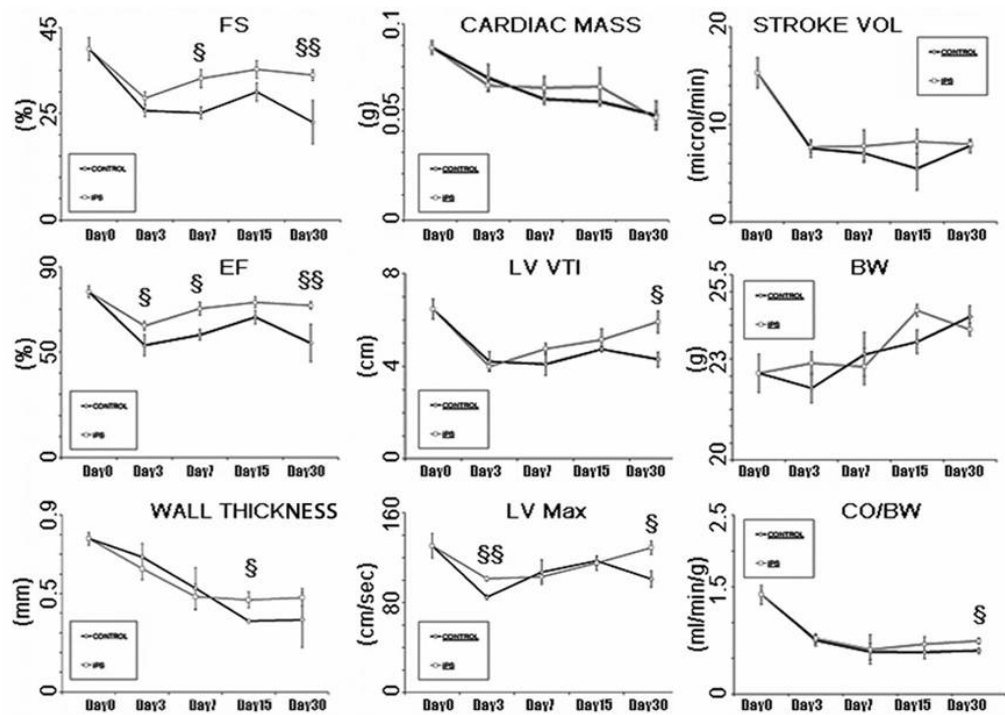


α -SARC-positive cells (magenta).

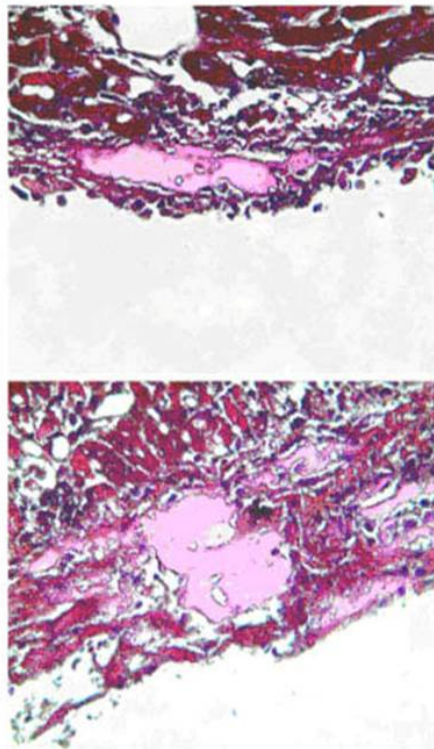
Representative immunofluorescence images of sections of myocardium 3 days after myocardial infarction and concomitant transplantation of GFP-expressing mouse CM-derived iPS cells. Functional integration of CM-derived iPS cells in the host myocardium is demonstrated by the expression of connexin 43 (white) among GFP-positive (green) cells and



Representative 2D views of hearts injected with PBS (control group, left panel) and CM-derived iPS cells (treated group, right panel) 7 days after coronary artery ligation.



Echo-doppler parameters: (black line is control, grey line is IPS, and for all conditions **n=5**) Fractional shortening (FS), percent ejection fraction (EF), left ventricular free wall thickness in diastole (LVFW) (left panels), cardiac mass, integral velocity/time (LV VT1), maximum velocity (LV max) (center panels), stroke volume (stroke vol), body weight (BW) and cardiac output normalized to body weight (CO/BW) (right panels) at 3, 7, 15, and 30 days after MI in mice engrafted with CM-derived iPS cells and the PBS-treated control group .

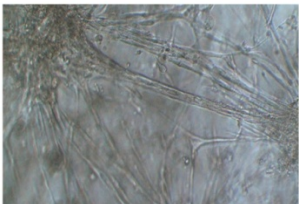


Examples of PEGylated fibrinogen hydrogel injected in the adult mouse heart and evaluated histologically by hematoxylin and eosin staining 7 days after infarction.

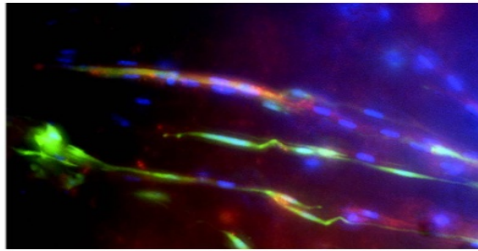
Publications

Development of a drug screening platform based on engineered heart tissue. Hansen A, Eder A, Bönstrup M, Flato M, Mewe M, Schaaf S, Aksehirlioglu B, Schwörer A, Uebeler J,

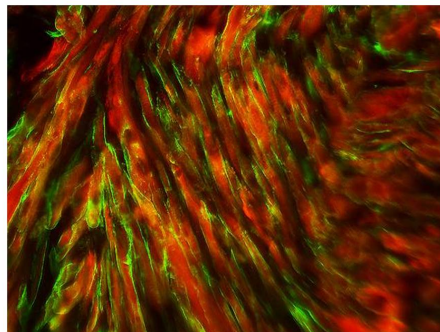
	Eschenhagen T. Circ Res. 2010;107:35-44.
Patents	None
Other	None
Work to be performed in year 3	Results from Years 1 and 2 are very encouraging about the use of IGF1 and VEGF in muscle repair indications, and work will continue on the exploration of these morphogens in fibrin or fibrinogen-polymer matrices in muscle repair validation models, focused on cardiac muscle repair.

No.	Title	Lead Scientists	Start Month	End Month
6.2	BVP related to skeletal muscle tissue Tasks: 6.3-1, 6.4-1, 6.5-1 and 6.7-1			
Checkpoint	6.6	GC	6	48
Deliverable	None in this reporting period			
Task update	<p>Tissue engineering consists of two main components: one biological (cell) and one chemical (biomaterial). In our experiments the biological component is represented by freshly isolated primary myoblast (Muscle Satellite Cells-MSC) and vessel associated progenitor cells (Mesoangioblast-Mabs), while the chemical component is represented by three different materials: two injectable PEG-Fibrinogen (PF) 8mg/ml and TG-PEG (TP) 2,5%, and one already polymerized Heparin-STAR-PEG (HSP) (we dropped Fibrin hydrogel because of the limited permanence in culture with our cell system). Our research follows two main directions: a) <i>in vitro</i> skeletal muscle tissue reconstruction and b) <i>in vivo</i> muscle regeneration. The first series of experiments have focused on identifying the optimal material which will then be combined with selected morphogens in the remaining two years.</p> <p>a) Biological and chemical component were combined and cultured for 24 hour in growth medium, then they were transferred into differentiation medium to promote muscle fiber formation. PF is able to promote mature well-differentiated myofibers, moreover using laser ablation for confining microchannel construction the myofibers start to be oriented, aligned and cylindrical likewise real skeletal muscle fibers. Microchannel plug immunofluorescence and western blot analysis reveal the expression of skeletal muscle contraction proteins such as Tropomyosin, Myosin heavy chain, Troponin, and others. TP and HSP are able as well to promote mature myofibers but they are batch sensible and less efficient than PF in promoting skeletal muscle differentiation.</p> <p>HSP and PF have been implanted subcutaneously, in Rag2/gammaChain^{-/-} immune compromise mice strain, in order to promote myofiber formation and the development of a well-differentiated, muscle like tissue. HSP did not improve muscle differentiation or maturation while PF implant showed well defined skeletal muscle organization and differentiation also if still without myofiber orientation.</p> <p>b) Biological and chemical component were combined, injected and polymerized <i>in vivo</i> into injured mouse Anterior Tibialis (AT) or for HSP (uninjectable material) was implanted into mouse Quadriceps (Quad). TP was injected with TG-IGF or without it in order to analyze the effect of this growth factor on promoting increased fiber size. HSP did not show remarkable result on cell engraftment and/or engrafted cell incorporation into host muscle tissue. TP and PF caused increased survival of transplanted cells and an overall improvement in cell engraftment as measured by the newly regenerating myofibers formed; moreover PF seems to enhance skeletal muscle differentiation of engrafted cells.</p>  <p><i>Disordered myofiber formation in presence of PF 8mg/ml into 96</i></p>			

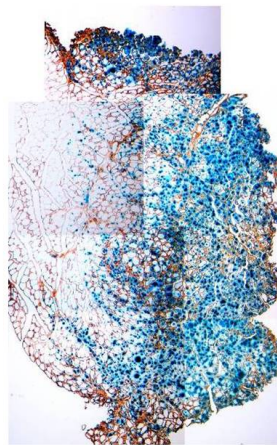
well plate.



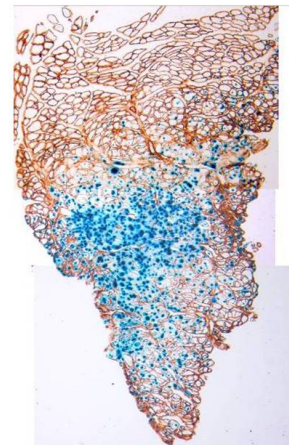
Staining of ASCs after 21 days of osteogenic differentiation with Xylenol Orange and Von Kossa.



Immunofluorescence revealing co-expression of Myosin Heavy Chain (red) and GFP (green) on PF 8mg/ml culture system.



a)



b)

Figure 7: In vivo injection of Mesoangioblast expressing LacZ with (a) or without (b) PF 8mg/ml indicating a remarkable amelioration on cell engraftment and retention into host Anterior Tibialis

Publications	None
Patents	None
Other	None
Work to be performed in year 3	Work is progressing well in the context of the fibrinogen-polymer matrices and of fibrin with IGF1 and VEGF, and this work will continue in Year 3 in the context of skeletal muscle repair.

No.	Title	Lead Scientists	Start Month	End Month												
6.3	BVP for neurological repair Tasks 6.2-1, 6.3-3, 6.4-3, 6.6-1, 6.8-1 and 6.9-1															
Checkpoint	No milestone associated with this task in this period	JF, JAH, HR, Kuros	12	48												
Deliverable	None in this reporting period															
Task update	<p>The main challenges in peripheral nerve regeneration include overcoming the slow growth rate of the regenerating neurons, avoid misrouting during pathfinding and to secure a correct reconnection between central nervous system and its target. Current surgical repair treatment provides a partial, but yet, not a full functional recovery. Stimulations of the lesion site using peripheral nerve electrode interfaces provide a possible way to re-establish the lost functional connectivity. However, encouraging neurons to go down the long and narrow channels remains a challenge. Incorporation of biomaterials to encourage axons going down these channels may therefore be helpful. JF has tested different fibrin gels and found out that FN-910-GBD gel gave superior support for the growth of DRG neurites. Here, we continue this screening by determining the effect of hyaluronan scaffold on the outgrowth of adult dorsal root ganglia (DRG) explants. DRG explants from adult GFP rats were cultured in a 3-D environment composed of either hyaluronan or collagen, which act as a positive control on coverslips. Three days after culture, neurons growing on the hyaluronan scaffold demonstrate significant outgrowth. The neurites showed more than 13% increase in length when compared with the positive collagen control. The average neurite length increases from 234 μm in collagen to 263 μm in the hyaluronan scaffolds ($P < 0.005$). For each condition 4 cover slips were analysed with over 20 neurons per coverslip measured. This suggested that hyaluronan scaffold may be a good biomaterial to be put into the channels. Further experiments will be performed in microchannel conduit to verify the effect of hyaluronan scaffold on the outgrowth of DRG explants.</p> <p style="text-align: center;"><u>Neurite outgrowth of adult rat DRG in 3-D scaffolds</u></p> <table border="1"> <caption>Data for Neurite outgrowth of adult rat DRG in 3-D scaffolds</caption> <thead> <tr> <th>Scaffold</th> <th>Length of neurites (μm)</th> </tr> </thead> <tbody> <tr> <td>Fibrin</td> <td>~210</td> </tr> <tr> <td>FN-GBD</td> <td>~190</td> </tr> <tr> <td>FN-910-GBD</td> <td>~240</td> </tr> <tr> <td>Hyaluronan</td> <td>263</td> </tr> <tr> <td>Collagen</td> <td>~234</td> </tr> </tbody> </table> <p>HR used male Sprague Dawley rats to study the effect of various PEGylated fibrinogen-or fibrinhydrogel in tubes on peripheral nerve regeneration after implantation in channels. In each animal, the right sciatic nerve is located mid thigh. The nerve and its branches are dissected microsurgically from the sciatic notch to the hollow of the knee and isolated atraumatically from the surrounding tissues with surgical microscope. Each sciatic is transected with a microsurgical scissor at two different levels of the mobilized segment:</p> <ul style="list-style-type: none"> • Standard gap model (8mm): • A standard gap model is used for evaluation of the best material. 				Scaffold	Length of neurites (μm)	Fibrin	~210	FN-GBD	~190	FN-910-GBD	~240	Hyaluronan	263	Collagen	~234
Scaffold	Length of neurites (μm)															
Fibrin	~210															
FN-GBD	~190															
FN-910-GBD	~240															
Hyaluronan	263															
Collagen	~234															

- The sciatic nerve is be transected at two different levels mid thigh creating a nerve gap of 8mm.
- The free nerve graft which was created by transection of the sciatic nerve at two different mid thigh levels is removed. Continuity of the sciatic nerve is reconstructed using:
- Group 1-x:
- Tubular nerve guidance: outer diameter 1.8-2.0mm, inner diameter 1.6-1.8mm. Coaptation of the proximal and distal nerve stump to the tubular nerve guidance structure will be carried out using 2 epineurial sutures at each site.

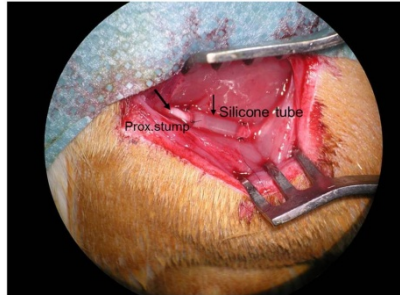


Figure 1

Evaluation was performed via histological Analysis of Axon regeneration. So far 12 animals (**n=12**) have been studied up to 3 months. Some times the Hydrogel was swollen and bulging out from the tube which caused problems.

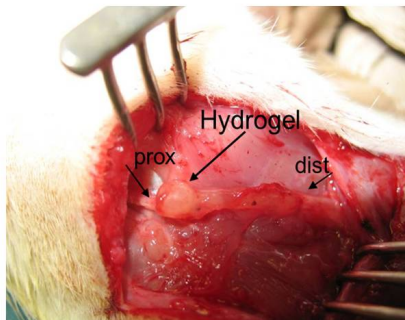


Figure 2: animal # 4; Fibrin 2.5 y PEG DA, tube with 1.5mm inner diameter; Hydrogel is swollen and bulging out from the tube.

Partly no regeneration was seen, the stumps were completely separated from each other.

In some tubes tube with 8mg/ml Fibrinogen+40mg/ml PEG-DA implantation, 3 months after operation; some nerve tissue was found between the nerve stumps.

In conclusion tubes filled either with various PEGylated hydrogels or fibrin fine structure with laser fabricated channel structure did not support nerve regeneration. Potentially lower concentrations of hydrogels or more channels are needed.

JAH and Kuros collaborated to deliver neurotrophic factors from a fibrin gel to enhance neurite extension. Fibrin gels modified with FN-9-10-GBD fragment (see WP3 FN project by Martino) and mixed with NT-3 and BDNF, led to reduced rate of release compared to gels modified with FN-9-10 without the GBD. In the case of NGF, both release profiles were similar. An in vitro chick 3D DRG culture inside the fibrin gels demonstrated that in the case of BDNF, neurite extension was significantly enhanced compared to no BDNF present in the gel. When BDNF was present in the gel without any fibronectin fragment, a high number of neurites started to grow close to the DRG cell body, but they were not able to extend to long distances into the gels. Neurite extension in the case of FN-9-10, FN-9-10-GBD, and full length fibronectin reached long distances into the gel and demonstrated similar results in all three cases, with FN-9-10-GBD and full length fibronectin resulting in a slightly higher number of neurites that extended at these far distances. To facilitate analysis, a microwell technique, developed in Matthias Lutolf's lab, will be tested to analyze neurite extension of individual neurons in fibrin wells containing growth factors with or without the GBD fragment.

Recently, glial cells have been implicated in essential mechanisms for neuroregeneration, such as guiding migration of neurons, forming the necessary scaffold for neurons and being critical participants in synaptic transmission and are indeed in clinical trials. However, although Schwann cell transplantation can promote nerve repair experimentally, it is difficult to generate sufficient amounts of Schwann cells rapidly for clinical application. Recent studies have demonstrated that differentiated Schwann-cell-like cells from bone marrow stromal cells or adipose-derived stem cells (ASC) may support nerve regeneration. ASC are highly capable for self-renewal and differentiation into several differentiation lineages. Furthermore, they are

easy and safe to obtain, and are available in large numbers.

It is becoming apparent that a combination therapy of materials and cells are likely to be necessary for effective regeneration, therefore it was considered essential that in tandem with the bioactive materials, effort be engaged to develop the potential therapeutic.

HR therefore investigated human and rat adipose-derived stem cells with regard to their ability of differentiation into Schwann cell-like cells that show specific characteristics including expression of Schwann cell marker.

Differentiation of ASCs, isolated from human and rat adipose tissue, to Schwann-cell-like cells, was induced by a combination of chemical compounds and growth factors, such as β -mercaptoethanol, all-trans-retinoic acid, forskolin, platelet-derived growth factor, fibroblast growth factor and heregulin. Subsequently, expression of an array of markers for Schwann cells was confirmed, such as S100, GFAP, p75, nestin and p0 using immunofluorescence staining.

Furthermore, we aimed to establish a method to mobilize sufficient amounts of autologous Schwann cell-like cells within a considerably short period of time. In our attempt to increase differentiation efficiency MACS[®] Cell Separation System from Miltenyi-Biotec was implemented. Cells positive for p75 were separated from the p75 negative cell population prior to differentiation procedure. The efficiency was compared to cells without selection and separation of p75 positive cells, as well as undifferentiated cells (ASC). After separation, the cells were seeded into 6-wells plates, differentiated according to the differentiation protocol and analysed by flow cytometry. The positive cells that were differentiated retained the p75 antigen. Only 17.6% of the cells lost the antigen and were probably dedifferentiated. (**Figure below**) In the future, autologous Schwann cell-like cells applied in grafts in order to direct, protect and enhance the growth of neuronal cells might accelerate the healing process of nerve regeneration.

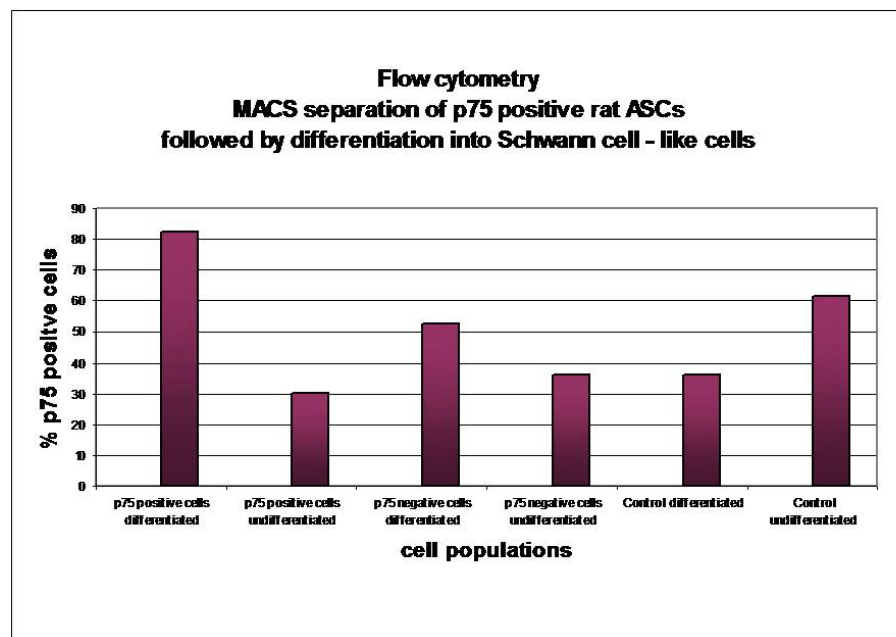


Figure 1: Flow cytometric analysis of cells separated with MACS Miltenyi Biotec cell separation system .

Publications	None
Patents	None
Other	None
Work to be performed in year 3	The fibronectin fragment technology demonstrated very surprising ability to bind and sequester the nerve morphogens NT3 and BDNF; work will continue in Year 3 on these combinations in nerve repair validation models. Work with the hyaluronic acid matrixes will

	also be continued in nerve repair validation models; if initial pilot results are positive, this work will be continued, and if initial pilot results are negative, the work will be stopped.
--	---

No.	Title	Lead Scientists	Start Month	End Month
6.4	Development and validation of bioassays for rhVEGF165 and rhPDGFBB			
Checkpoint	none	AH (Neuronova)	1	24
Deliverable	None in this reporting period			
Task update	<p>Several members of the Angioscaff consortium have an interest in applications of Platelet Derived Growth Factor (PDGF) and Vascular Endothelial Growth Factor (VEGF). While many of the investigations currently are at a preclinical level a long term goal is clinical application of e.g. scaffolds containing growth factors such as PDGF and VEGF. The aim of this project is to establish bioassays of GMP quality suitable for determining the bioactivity of PDGF and VEGF. This is a requirement for the release of drug products intended for clinical trials performed according to GCP and ICH guidelines. More specifically this sub-project focuses on recombinant human PDGF-BB (rhPDGFBB) and rhVEGF165, two isoforms of considerable clinical potential within the Angioscaff consortium. The identification, development and validation of these bioassays have been performed with the goal to set standards for consortium members and also to make possible a transfer of the bioassays to external GCP/GLP specialised contract research organisations, which represents a logical and necessary step during a clinical development. Initially, before the Angioscaff consortium was formed, reporter gene based assays were investigated for VEGF (eg the BaF3/Flt-EpoR and hKDR LepR 293-luc cell bioassays) with poor results in terms of reproducibility. We determined that in addition, a receptor binding assay, even if coupled to a second messenger system in e.g. isolated cell membranes, would not properly represent the drug activity for the above mentioned purposes. Hence, the initial work focussed on finding a suitable cell-line that could present a biological response on a “whole-cell” level.</p> <p>Multiple cell types and readouts were identified and screened for suitability, both from searching the available literature and by actual hands-on testing in the laboratory of NeuroNova. During this selection phase, special attention was paid to response amplitudes, inter- and intra-assay variability, cell-batch to cell-batch variability, response rates at different passages and freeze thaw cycles, reproducibility between different analysts and overall availability of the cell-line from the vendor over time. Both infinitely growing cell lines and freshly isolated cells in early stage cultures were tested. For PDGF the tested candidate cell lines were; Hs68, NHDF, MG63, ST-14. Baseline culture conditions and characteristics related to response amplitude and assay reproducibility was assessed for all these cell lines For VEGF, the tested candidate cell lines were; EA.hy926, HUVEC immortalised cell lines, HUVEC (non-immortalised), OVCA-3, ARPE-19. Baseline culture conditions and characteristics related to response amplitude and assay reproducibility was assessed for all these cell lines. Of these, non-immortalised HUVEC cells presented the best characteristics.</p> <p>PDGF: NHDFs showed the best characteristics and was selected for further development. VEGF bioassay: Normal, non-immortalised HUVECs were selected for further development. At present the work of validating these assays is still ongoing but nearing finalisation. For VEGF the assay is under transfer to an external company for the purpose of them setting up an identical assay to be used to perform bioactivity of VEGF-batches to be released for clinical use in the presently ongoing clinical trial related to VEGF as a treatment of ALS (sNN0029-001 and -002 studies). For PDGF, the assay has been used for determining the bioactivity of rhPDGFBB for its use in the clinical application of PDGF in Parkinson's Disease (sNN0031-001 study), but is still performed mainly in NeuroNova's lab. Angioscaff consortium members are being informed of the availability of these assays and encouraged to contact NeuroNova</p>			

	when in need to assess bioactivity of their products.
Publications	None
Patents	None
Other	None
Work to be performed in year 3	Based on the high quality production capabilities that have been developed for animal use, prioritization has moved away from production of human clinical grade proteins. The one path proceeded so well, that the other path is no longer necessary. No work on production of human clinical grade proteins will be carried out in Year 3.

WP6 has produced 1 peer-reviewed publication in this period.

We have completed our tasks according to schedule as outlined in the original proposal.

There were no changes to the original proposal with respect to collaborations and staff except that the effort of Ralph Muller and Jeronimo Blanco's teams which were specifically linked to the imaging aspect, for strategic reasons has been reallocated to the horizontal work package on imaging which is indicated at the end of this section. Furthermore, Heinz Redl's team has collaborated as part of this work package and their effort will also be recorded here.

Collaborations within the work package are as follows.

Exchanges of staff
None
Exchanges of reagents
T Eschenhagen received TG-IGF, TG-VEGF165, Factor XIII, FN 910 GBD, FN 9*10 GBD (Jeffery Hubbell lab), TG-VEGF form (M Ehrbars lab, Zürich), TG-PDGF (, Kuros, Zürich), PEG-fibrinogen (Dror Seliktar lab.), PEG-TG (Matthias Lutolf lab), hyaluronic acid (Jons Hilborn lab)
Giulio Cossu has received the following from D. Seliktar: PEG-Fibrinogen; J. Hubbell: Fibrin gel, FN-GBD and TG-IGF; M. Lutolf: TG-PEG; C. Werner: Star-PEG.
James Fawcett has received the following from: Dror Seliktar– PEG-fibrinogen Jöns Hilborn - hyaluronan
Gianluigi Condorelli received PEGylated fibrinogen from Dror Seliktar's Lab.

Horizontal Work Package - Imaging

During the kick off meeting it was decided that the imaging teams and their research projects should be extracted from the RTD work packages and collated to generate an independent work package. The rationale for this approach was that the tasks performed by these teams served as both independent research projects and as a platform with which all the RTD work packages would integrate. This restructuring enables us to better manage the development of the imaging approaches and the integration and collaboration of the imaging teams with the biomaterial development and biomaterial validation projects.

This was reported and approved in the first year report and the work presented below represents its continuation

Work package number	9	Start date or starting event:	Month 1
Work package title	Horizontal: Imaging		
Activity Type	RTD	Workpackage Leader	Ralph Muller
Participant number	11		12
Principal Investigator	JB		RM
Planned Person-months for whole WP duration	96		88
Actual Person-months so far	42.8		43.38

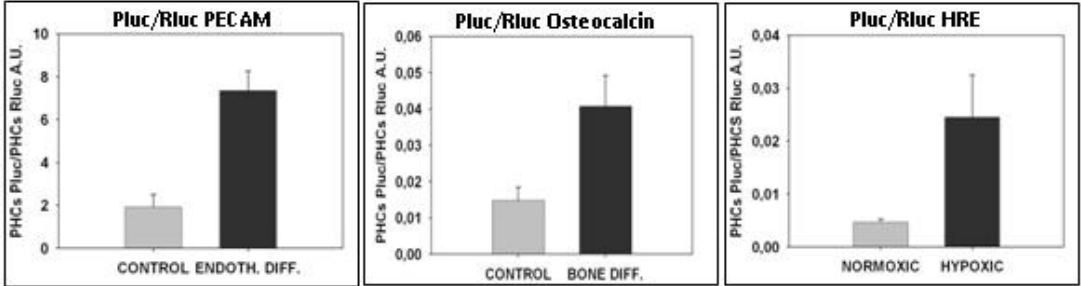
REPORT OVERVIEW: WP9 – Imaging

1. To assess the angiogenic capacity of AngioScaff materials we (**JB**) have established a non-invasive bioluminescence imaging (BLI) platform to quantify changes in gene expression and to analyze cell behavior in materials implanted in live animals. During year 2 we have developed and tested the BLI procedure to analyze angiogenic capacity of demineralized bone matrixes (DBM) during bone formation. The results show: *i*) correlation in vitro between expression luciferase and endothelial or osteoclast mRNA (*Pecam* and *Osteocalcin*, respectively); *ii*) dynamic luciferase expression in vivo in response to hypoxia; *iii*) optimization of a fluorescent angiography procedure to analyze by confocal microscopy vascular structures in implanted scaffolds and their structural relation with seeded stem cells. Moreover, we have found that PLA/CaP has better capacity to recruit endothelial-like cells than PLA only in vivo and that polymerization in subcutaneous Fibrin TG-Aprotinin implants works well and luciferin reaches the cells seeded in the material.

2a. To induce transgene expression in vivo and stimulate tissue regeneration we (**JB, JAH**) used PEG-PPS-PEI micelles complexed with reporter DNA constructs. Entrapping cells inside the gels resulted in transgene DNA expression up to a week, which is not attained with commercially available kits such as jet-PEI. Nevertheless, in vivo experiments require optimization to test the efficacy of micelles when delivered from fibrin gels.

2b. To develop new hyaluronan based siRNA/gene delivery agent we (**JB**) tested HA as an siRNA delivery vehicle to silence Renilla luciferase expression in vitro in comparison with polyethylenamine (PEI), which is considered as a gold standard for transfection experiment, and did not achieve satisfactory silencing. However we successfully showed gene delivery in vivo. Further optimization of gene/siRNA delivery vehicle is ongoing which will be tested in vitro and in vivo in near future.

3. To monitor vascular growth within biomaterials by micro-CT, we (**RM**) progressed in time-lapse imaging by performing analysis of Contrast stability in blood measured at the jugular vein using 3 different infusion protocols. Contrast stability in the M. tibialis anterior was also compared to that of the brain with a specific infusion rate. The dynamic imaging profile obtained for the muscle might be used to study tissue perfusion and the exchanges of solutes between vascular and tissue compartment. Corrosion cast imaging of the same animals will allow the calibration of our imaging method. Furthermore, we have submitted an application to use the Synchrotron beamtime at the Swiss Light Source (SLS), which is currently under review. It will deal with the detection of blood vessels in soft tissues and demineralized bone samples using SR phase-contrast imaging.

No.	Title	Lead Scientists	Start Month	End Month
IMG 1	Angiogenic capacity of AngioScaff materials			
Checkpoint	No milestone associated with this task in this period	JB	1	48
Deliverable	None in this reporting period			
Task update	<p>Due to the complementary nature of projects “Angiogenesis capacity of Angioscaff materials”, to analyze the capacity of materials to induce endothelial differentiation of stem cell seeded in them and “BLI of cell homing to materials”, directed to analyze the capacity of materials with or without stem cells to attract vascular structures from the host, both projects have been fused in a single one.</p> <p>The task is to produce a BLI analysis platform assess the capacity of a “material” for inducing <i>in vivo</i> endothelial differentiation of stem cells seeded in it; measure the capacity of a “material” for promoting invasion by host vascular structures and determine if stem cells and materials collaborate to promote invasion by host vascular structures?</p> <p>The strategy is based on non invasive bioluminescence imaging (BLI) of changes in gene expression, to analyze cell behavior in materials implanted in live animals, validated using standard <i>ex-vivo</i> analysis by RT-PCR, fluorescence angiography and isolectine binding. During this period we have developed and tested the BLI procedure to analyze angiogenic capacity using a reference biomaterial (demineralized bone matrixes (DBM)) during bone formation and have demonstrated the <i>in vitro</i> the dynamic range of reporter expression and its correlation with changes in mRNA expression (Fig. 1 below).</p> <div style="display: flex; justify-content: space-around;">  </div> <p>Fig 1: Induction of adipo-se mesenchymal stromal cells (hAMSCs) to differentiate to endothelial, osteogenic lineages or cultivation under hypoxia results in the increase of specific promoter regulated luciferase expression, relative to that of non induced cells (n=4), in correlation with changes in mRNA expression, as measured by RT-PCR</p> <p>We have also performed an <i>in vivo</i> BLI of gene expression using the DBM reference biomaterial (Fig. 2, 3).</p>			

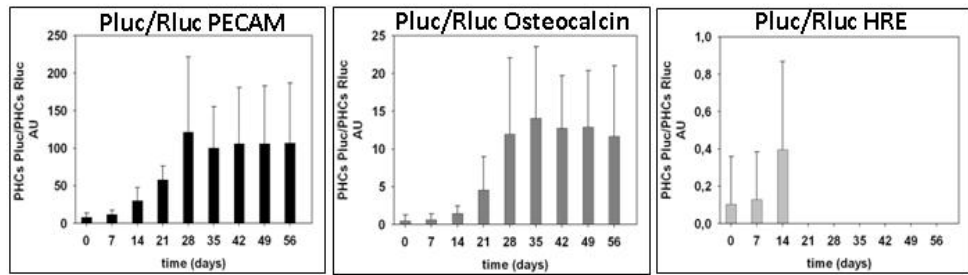
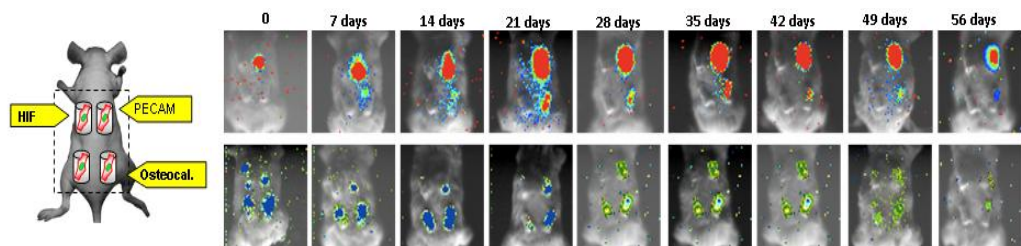


Fig. 2. hAMSCs expressing luciferases regulated by specific (upper row) and constitutive (lower row) promoters and seeded in DBMs implanted in SCID mice report changes in gene expression ($n=6$). Image data correlates with changes in mRNA expression

Figure 3



A fluorescent angiography procedure, based on the use of high molecular weight fluorescein-dextran and confocal microscopy (Fig. 4) has been optimized to analyze vascular structures in implanted scaffolds and their structural relation with seeded stem cells.

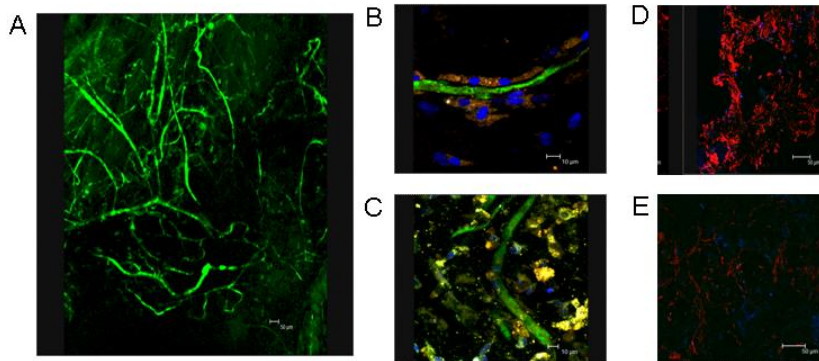


Figure 4 Application of the procedure to thick sections from 21 day scaffolds shows extensive (host derived) vascularization of DBMs (A). Higher magnification shows association of implanted hAMSCs expressing PCAM-luc-egfp with vascular structures (B), but no association of hAMSCs expressing Osteocalcin-luc-egfp with vascular structures (C). (yellow cells result from the expression of green fluorescence (regulated by either the PECAM or the Osteocalcin promoters) and red fluorescence (regulated by constitutive CMV promoter) in the same cell).

Analysis of the PLA and PLA/CaP composite materials (J. Planell) has been completed. PLA and PLA/CaP scaffolds were implanted without cells in mice and analyzed after 1 month for their capacity to induce endothelial differentiation of colonizing host cells by calculating areas of isolectine B4 binding in histological sections (Fig. 4, D, E). Table 1 shows that PLA/CaP has significantly ($p<0,001$) better capacity to recruit endothelial like cells than PLA only.

		N =	media	SD	T Student
	PLA	167	9.0	12.6	3,43504E-05
	PLA glass	97	15.6	11.8	p <0,001
Publications	None				
Patents	None				
Other	None				
Work to be performed in year 3	Work on methods development in imaging has been very successful. In Year 3, work as a collaborative platform will continue on angiogenic imaging in the materials/morphogen combinations that are being investigated above, focused on cell recruitment and angiogenesis. These powerful methods augment histological and morphological read-outs very effectively.				

No.	Title	Lead Scientists	Start Month	End Month
IMG 2a	Scaffold mediated reporter transfection project			
Checkpoint	No milestone associated with this task in this period	JB, JAH	1	48
Deliverable	None in this reporting period			
Task update	<p>The goal of this task is to measure DNA delivery from fibrin gels to induce transgene expression in vivo and stimulate tissue regeneration. PEG-PPS-PEI micelles were used to complex the DNA and enhance transgene expression. The DNA complexes did not release very slowly from the gel, with most of the DNA entrapped in the fibrin gel until gel degradation. Mixing cells inside the gels entrapped with DNA micelles led to transgene expression up to a week, with a peak at 3-4 days. This was in contrast with gels loaded with plasmid DNA or DNA complexed with commercially available jetPEI, which did not result in expression. Transfection was optimized for fibrin gels containing 40 mM Ca²⁺, 10 U/mL thrombin, and 4 U/mL Factor XIII. Modification of the gels with TG-aptin led to a delay of the max peak of transfection, and higher levels of expression at later time points (>1 week), this due to the retardation of gel degradation and the ability of the cells to migrate through the gel and take up the DNA. Similarly, in the case of a sandwich 3 layer gel with cells only in the middle layer and DNA micelles in the outer layers, the peak of expression was delayed until 7 days. At 10 days the gels were almost degraded but there was still a lower level of transfection left. In vivo experiments need to be optimized to test the efficacy of the micelles in vivo when delivered from a fibrin gel.</p> <p>Abbreviations: PEG, Polyethylene glycol; PEI, Polyethylenimine; PPS,</p>			
Publications	None			
Patents	None			
Other	This work was presented with an oral presentation at TERMIS 16 June 2010 in Galway			
Work to be performed in year 3	Work will continue in Year 3 on methods development in this approach, focused on achieving adequate transfection levels to reliably allow the imaging method to work. If that is achieved, then application of the imaging platform to the materials/morphogen combinations indicated above will be carried out.			

No.	Title	Lead Scientists	Start Month	End Month
-----	-------	-----------------	-------------	-----------

IMG 2b	Development of tools for measuring in vivo nucleic acid delivery																					
Checkpoint	No milestone associated with this task in this period	JB, JH	1	48																		
Deliverable	None in this reporting period																					
Task update	<p>New hyaluronan modified hydrogels with covalently linked guanidinium residues have been developed for gene/siRNA delivery applications. These modifications form stable polyelectrolyte complexes with DNA and their complex formation with siRNA/DNA and in vitro/in vivo cellular uptake has been performed.</p> <p>In vitro gene silencing experiment was performed in renilla luciferase expressing PC-3 cells. Different partially cationised HA was tested as an siRNA delivery vehicle and compared with polyethylenamine (PEI) which is considered as a gold standard for transfection experiment. As shown in Figure 1, PEI complex was the best unlike the HA based transfection agents.</p> <div data-bbox="395 734 1184 1182"> <table border="1"> <caption>Data for Figure 1: siRNA INHIBITION 48H</caption> <thead> <tr> <th>Condition</th> <th>Ratio: Firefly/Renilla</th> </tr> </thead> <tbody> <tr><td>1. HA-siRNA conjugate</td><td>~1.55</td></tr> <tr><td>2. HA-siRNA conjugate+Hase</td><td>~1.63</td></tr> <tr><td>3. HA-Guanidine</td><td>~1.51</td></tr> <tr><td>4. HA-amine1</td><td>~1.43</td></tr> <tr><td>5. HA-amine2</td><td>~1.52</td></tr> <tr><td>6. PEI</td><td>~1.22</td></tr> <tr><td>7. HA-Gua+PEI</td><td>~1.60</td></tr> <tr><td>8. Cells+Hase</td><td>~1.28</td></tr> </tbody> </table> </div> <p>100 nM siRNA concentration in PC3 cells</p> <p>Figure 1. In vitro siRNA transfection experiment showing suppression of renilla luciferase gene expression in PC-3 cells (n=3 per transfection condition).</p> <p>Preliminary in vivo experiments were also performed. HA gels with and without guanidinium groups were complexed with plasmid DNA that express <i>firefly</i> luciferase and injected in mice muscle. At different time points (days) mice were analysed using luminescence camera and showed gene delivery in guanidinium groups (Figure 2). Though this result is promising we did not observe efficient gene delivery in all groups which could be due to improper distribution of DNA in the gel. Further optimization of gel formation and in vivo injection has to be optimized.</p> <p>As a control experiment we have also performed a comparison with polyethylenamine (PEI). In vitro experiment showed PEI to be more efficient; however, in vivo it was a completely different scenario. We did not observe any gene transfection when PEI-DNA complex were added to the gel (Figure 3).</p>				Condition	Ratio: Firefly/Renilla	1. HA-siRNA conjugate	~1.55	2. HA-siRNA conjugate+Hase	~1.63	3. HA-Guanidine	~1.51	4. HA-amine1	~1.43	5. HA-amine2	~1.52	6. PEI	~1.22	7. HA-Gua+PEI	~1.60	8. Cells+Hase	~1.28
Condition	Ratio: Firefly/Renilla																					
1. HA-siRNA conjugate	~1.55																					
2. HA-siRNA conjugate+Hase	~1.63																					
3. HA-Guanidine	~1.51																					
4. HA-amine1	~1.43																					
5. HA-amine2	~1.52																					
6. PEI	~1.22																					
7. HA-Gua+PEI	~1.60																					
8. Cells+Hase	~1.28																					

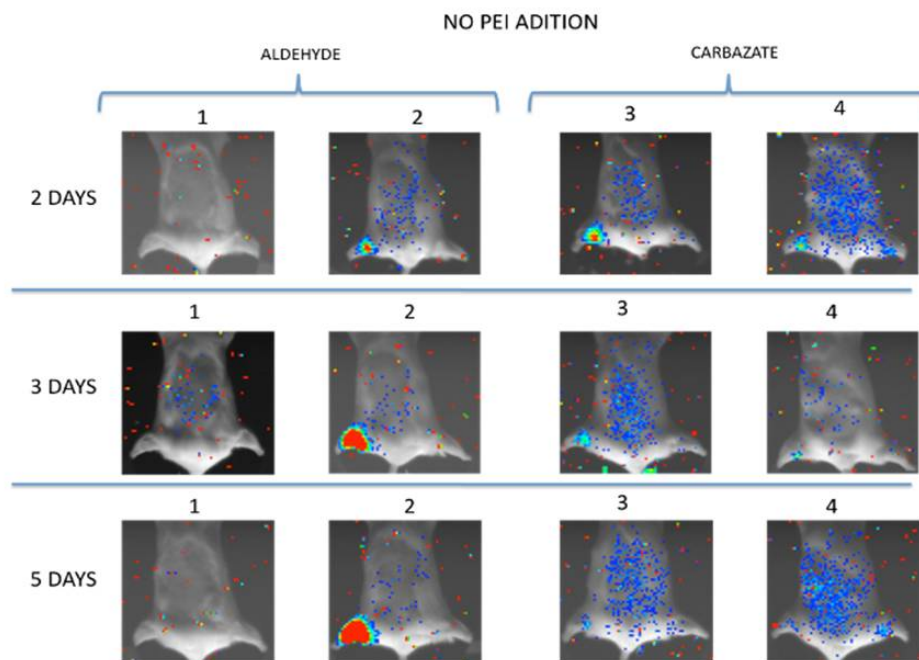


Figure 2: *In vivo* experiment of firefly luciferase gene delivery with gels (1, 2) having guanidinium groups and (3, 4) having no guanidinium groups. The plasmid DNA was added to HA-guanidinium/HA-carbazate groups before gel formation.

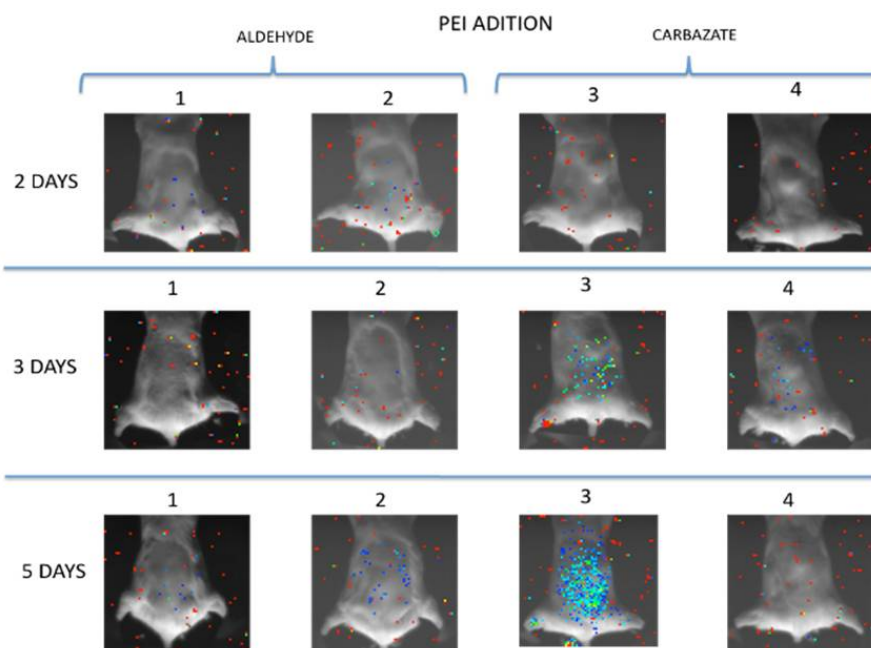


Figure 3: *In vivo* experiment of firefly luciferase gene delivery with gels (1, 2) having guanidinium groups and (3, 4) having no guanidinium groups. The plasmid DNA was complexed with PEI before mixing with the gel component.

We have successfully showed gene delivery *in vivo*, though we could not get similar results *in vitro*. Further optimization of the delivery vehicle is necessary which will be tested *in vitro* and *in vivo* in near future which will be tested both in normal mice and tumor models.

Publications

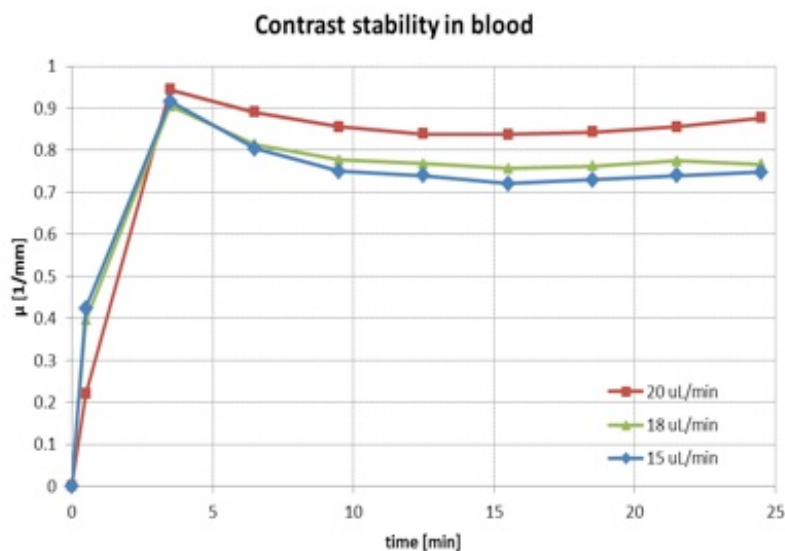
Macromol. Rapid Commun. **2010**, 31, 1175–1180

Patents	None
Other	None
Work to be performed in year 3	Work will continue on validation for the hyaluronic acid composite materials as a nucleic acid delivery vehicle will continue in Year 3. If that shows feasibility, then the platform will be used to characterize angiogenesis with the materials/morphogen combinations of the consortium.

No.	Title	Lead Scientists	Start Month	End Month
IMG 3	Time lapsed in vivo and corrosion cast imaging			
Checkpoint	No milestone associated with this task in this period	RM	1	48
Deliverable	None in this reporting period			

Contrast-enhanced micro-CT has shown potential in detecting the vascular space *in vivo*. A water-based X-ray contrast agent containing Iodine (*Iomeron 400* – Bracco, Switzerland) allows repeated measurements in a time-lapsed fashion. The major blood vessels of the network can be visualized *in vivo* at different locations (abdominal aorta, femoral vein, jugular vein). Smaller vessels (namely capillaries) are below the resolution of the micro-CT scanner; therefore, their vascular volume can be estimated by quantifying the grey level changes in the corresponding tissue. Micro-CT measurements require a scanning time up to 20 minutes, depending on the resolution used. Therefore, it is important that blood and tissue X-ray attenuation remains stable over time. Thus, it is necessary to reach a balance between the amount of contrast agent infused intravenously and the quantity which is filtrated through the kidneys. Different infusion protocols were tested regarding the contrast stability provided to blood (figure 1a). In all protocols a bolus injection of 200 $\mu\text{L}/\text{min}/30\text{g}$ mouse is followed by a constant infusion rate during the scanning time (20, 18 and 15 $\mu\text{L}/\text{min}/30\text{g}$ mouse).

Fig 1a:



Task update

Fig 1b

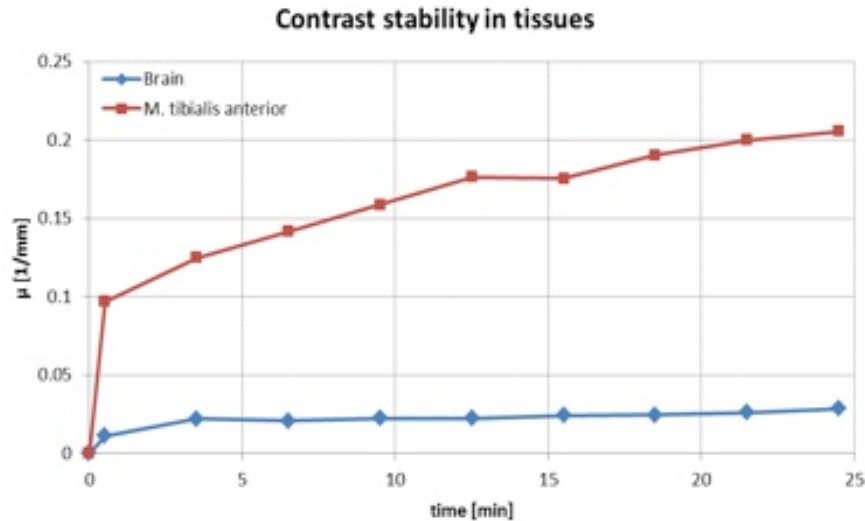


Figure 1 – a) Contrast stability in blood measured at the jugular vein using 3 different infusion protocols. b) Contrast stability in the *M. tibialis anterior* and in the brain with an infusion rate of 18 $\mu\text{L}/\text{min}$. The values of μ are corrected with respect to the pre-contrast images. Micro-CT settings: $E = 55\text{kVp}$; integration time = 200 ms; number of projections/180 degrees = 250; resolution = 70 μm . **N=5 for each group.**

The protocol with infusion rate of 18 $\mu\text{L}/\text{min}/30\text{g}$ mouse gave the lowest contrast variation over time (1.01%). Thus, it was applied for dynamic measurements in a region of interest (ROI), the *M. tibialis anterior*. Figure 1b shows the results of contrast stability in the ROI and in the brain. While in blood and brain the X-ray absorption (μ) is stable, it is continuously increasing in the muscle. In this case the permeability of the tissue capillaries allows the diffusion of the water-soluble contrast agent from the vascular compartment to the interstitial spaces. In brain instead, the *blood-brain barrier* prevents any passage of contrast agent from the cerebral capillaries to the neural tissue.

The vascular density can be estimated in brain, as here the contrast is provided only by enhanced blood vessels. Pre- and post-contrast micro-CT measurements were performed in the cerebral tissue with a resolution of 17.5 μm . The vascular density, defined as vessel volume on tissue volume (VV/TV), can be calculated as the percentage ratio between the tissue contrast (μ_{TV}) and the contrast of the reference vessel (μ_{VV}). Taking the left jugular vein as a reference, μ_{TV} and μ_{VV} were estimated to be 0.042 mm^{-1} and 0.895 mm^{-1} respectively, which resulted in a VV/TV of 4.72%. This value is in accordance with the vascular density of the brain that can be found in literature.

The water-soluble contrast agent cannot be used to estimate the level of vascularization in tissues other than brain, due to the aforementioned diffusion at the capillary level. Newly formed vessels might also be strongly affected by leakage. Nevertheless, the dynamic profile obtained in figure 1b for the muscle might be used to study tissue perfusion and the exchanges of solutes between vascular and tissue compartment. Furthermore, a new vascular contrast agent based on gold nanoparticles (*AuroVistTM* – Nanoprobes) that is known not to permeate the endothelium of healthy capillaries has been ordered and will be tested soon. This contrast agent will enhance the vascular volume alone and will hopefully allow the quantification of the vascular density in different kinds of tissues.

Corrosion cast imaging of the same animals will allow the calibration of our imaging method. Sample preparation of vascular corrosion casts will be optimized for ultra-high resolution scanning with our new micro-CT ($\mu\text{CT 50}$ – Scanco Medical AG, Brüttisellen, Switzerland). Furthermore, a proposal to apply for Synchrotron beamtime at the Swiss Light Source (SLS) has been submitted and it is currently under review. It will deal with the detection of blood vessels in soft tissues and demineralized bone samples using SR phase-contrast imaging.

	Superficial meshes of ultra-high resolution scans of the vascular volume are produced in different formats (STL, VTK) and sent to Damien Lacroix's group (Institute for Bioengineering of Catalonia – Barcelona, Spain). Fluid dynamic analysis allows the assessment of the functionality of the vascular network.
Publications	None
Patents	None
Other	<p>L. Nebuloni, G. Kuhn and R. Müller. <i>In vivo visualization and quantification of the vascular network in angiogenesis and tissue regeneration using micro-computed tomography</i>. Proc. Gemeinsame Jahrestagung der Deutschen, Österreichischen und Schweizerischen Gesellschaft für Biomedizinische Technik, Rostock, Germany, October 5-8 2010.</p> <p>L. Nebuloni, G. Kuhn and R. Müller. <i>In vivo micro-computed tomography of the vascular network for quantification of angiogenesis in tissue regeneration</i>. TOPEA Meeting, Barcelona, June 30-July 2 2010.</p>
Work to be performed in year 3	Work on methods development in imaging has been very successful. In Year 3, work as a collaborative platform will continue on angiogenic and morphogenetic imaging in the materials/morphogen combinations that are being investigated above, focused on angiogenesis and on the morphogenetic results of angiogenesis that result, including for example bone repair.

This work package has produced 1 peer-reviewed publication in this period.

Collaborations within the work package exist and are as follows.

Exchanges of staff
<p>Vascular corrosion cast trainings were organized in Zurich in June 2010 for four partners (Andrea Banfi – Basel University Hospital, Switzerland; Jeronimo Blanco – Cardiovascular Research Center, CSIC, Barcelona, Spain; Ranieri Cancedda – Università degli Studi di Genova, Italy; Heinz Redl, Ludwig Boltzmann Institute for Experimental and Clinical Traumatology, Vienna).</p> <p>In July 2010 Laura Nebuloni visited Damien Lacroix's group (Institute for Bioengineering of Catalonia – Barcelona, Spain).</p>
Exchanges of reagents
<p>J. Planell provided PLA and PLA/CaP material for testing of angiogenic capacity in vivo</p> <p>D. Seliktar provided PEG-fibrinogen (u.v. and temp. crosslinkable) material for in vivo analysis of angiogenic capacity.</p> <p>J. Hilborn provided hyaluronic acid based material for testing of angiogenic capacity.</p> <p>J. Hubbell provided fibrin TG-Aprotinin material for testing angiogenic capacity in vivo.</p> <p>H. Riedl provided transgenic VEGFR mice for BLI analysis of host derived angiogenesis of scaffolds.</p>